UNIVERSITY OF MILAN-BICOCCA

Department of Biotechnology and Biosciences

PhD program in Convergent Technology for Biomolecular Sciences – XXXIII cycle

The cadmium altered oxidative homeostasis leads to energetic metabolism rearrangement, Nrf2 activation with increased GSH production and reduced SOD1 activity in neural cells

BOVIO FEDERICA

Registration number: 752903

Supervisor: PAOLA ALESSANDRA FUSI

Tutor: MARINA LOTTI

Coordinator: PAOLA BRANDUARDI

ACADEMIC YEAR 2019/2020

Summary

Abstract 7

Chapter 1 – Introduction 10

Part I – Cadmium: a non-essential element with toxic effects on the nervous system 11

I.1 Introduction 11

I.2 Sources of cadmium exposure 12

I.3 Cadmium uptake in humans 14

I.4 Cadmium toxic effects 16

I.5 Cadmium and the nervous system 18

I.5.1 Cadmium uptake in the nervous system 19

I.5.1 Cadmium toxicity in the nervous system 21

Part II – Focusing on human superoxide dismutase 1: what to know about it 24

II.1 Introduction 24

II.2 From an euxinic world to an oxygenic one 25

II.3 The evolution of SOD 26

II.4 SOD1 gene structure and regulation 27

II.5 SOD1 protein structure 29

II.6 SOD1 protein activation 31

II.7 SOD1 catalytic function 33

II.8 SOD1 in amyotrophic lateral sclerosis 34

References 37

Chapter 2 – Aim of the thesis 50

Chapter 3 – Cadmium promotes glycolysis upregulation and glutamine dependency in human neuronal cells....53

Abstract....54

3.1 Introduction....55

3.2 Materials and methods....57

3.2.1 Mammalian cell culture....57

3.2.2 Cell viability assay....57

3.2.3 Oxygen consumption rate and extra-cellular acidification rate measurements....58

3.2.4 Lipid peroxidation assay....60

3.2.5 Glutathione detection....61

3.2.6 Glutathione S-transferase and glutathione reductase enzyme activity assays....62

3.2.7 Statistical analysis....62

3.3 Results....62

3.3.1 Exposure to $CdCl_2$ affects neural cells viability....62

3.3.2 Evaluation of SH-SY5Y energy phenotype shows that cadmium treated cells increase basal glycolysis....63

3.3.3 $CdCl_2$ administration increases both glycolytic capacity and glycolytic reserve....65

3.3.4 $CdCl_2$ administration induces a higher ATP production rate through glycolysis....68

3.3.5 $CdCl_2$ administration leads to a decrease in mitochondrial respiration....69

3.3.6 Mitochondrial fuel oxidation pattern changes when neuronal cells are treated with cadmium....71

3.3.7 Cadmium exposure increases oxidative stress....73

3.4 Discussion....74

3.5 Conclusions 78

References 79

Chapter 4 – The study of cadmium toxicity on LUHMES cell line showed the activation of Nrf2 signalling pathway and the protective role of GSH 83

4.1 Introduction 84

4.2 Materials and methods 86

4.2.1 Cell cultures 86

4.2.2 Viability assay 87

4.2.3 GSH assay 88

4.2.4 ATP assay 89

4.2.5 SDS-PAGE and Western blotting 89

4.2.6 Real-time quantitative PCR analysis 90

4.2.7 Statistical analysis 91

4.3 Results 91

4.3.1 Cadmium exposure reduces LUHMES cells viability and ATP and GSH intracellular content 91

4.3.2 Cadmium induces Nrf2 protein activation through p21 and P-Akt 91

4.3.3 Glutathione rescues LUHMES cells loss of viability induced by cadmium 94

4.3.4 Evaluation of cadmium toxicity on viability in a LUHMES-BV2 co-culture model and in astrocytes CM 96

4.4 Discussion 98

References 102

Chapter 5 – Superoxide dismutase 1 (SOD1) and cadmium: a three models approach to the comprehension of its neurotoxic effects 107

Abstract 108

5.1 Introduction 109

5.2 Materials and methods 112
5.2.1 Human SOD1 cloning and bacterial strains 112
5.2.2 Recombinant protein expression optimization 112
5.2.3 *E. coli* BL21 growth curves, hSOD1 expression and activity analysis in the presence of different metals mixtures 113
5.2.4 SOD1 activity assay 114
5.2.5 Mammalian cell culture 115
5.2.6 Neuronal cell viability assay 115
5.2.7 SDS-PAGE and Western blotting of SOD1 from SH-SY5Y human neuroblastoma cells 116
5.2.8 *C. elegans* strain maintenance and handing procedures 117
5.2.9 *C. elegans* acute toxicity assay 117
5.2.10 *C. elegans* protein extraction and quantification 118
5.2.11 Statistical analysis 119
5.3 Results 119
5.3.1 Recombinant hSOD1 expression optimization 119
5.3.2 Single metals administration effects on *E. coli* BL21 growth and recombinant hSOD1 activity 120
5.3.3 Metal mixture effects on recombinant GST-SOD1 122
5.3.4 Cadmium effect on endogenous SOD1 in SH-SY5Y cell line 125
5.3.5 SOD1 analysis in the presence of cadmium in the in vivo *Caenorhabditis elegans* model 127
5.4 Discussion 128
5.5 Conclusions 132
5.6 Supplementary figures 133
References 136

Chapter 6 –Discussion 145

References 153

Pubblications 158

Acknowledgement 159

Abstract

The heavy metal cadmium is a widespread toxic pollutant, released into the environment mainly by anthropogenic activities. Human exposure can occur through different sources: occupationally or environmentally, with its uptake through inhalation of polluted air, cigarette smoking or ingestion of contaminated food and water. It mainly enters the human body through the respiratory and the gastrointestinal tract and it accumulates in liver and kidneys. Brain is also a target of cadmium toxicity, since this toxicant may enter the central nervous system by increasing blood brain barrier permeability or through the olfactory nerves. In fact, cadmium exposure has been related to impaired functions of the nervous system and to neurodegenerative diseases, like amyotrophic lateral sclerosis (ALS). ALS is a fatal motor neuron pathology with the 90-95% of ALS cases being sporadic (sALS), while the remaining 5-10% of familial onset (fALS); among fALS, the 15-20% is attributed to mutations in superoxide dismutase 1 (SOD1). SOD1 is an antioxidant protein responsible for superoxide anions disruption and it is a homodimeric metalloenzyme of 32 kDa mainly located in the cytoplasm, with each monomer binding one catalytic copper ion and one structural zinc ion within a disulfide bonded conformer.

Since oxidative stress is one of the major mechanisms of cadmium induced toxicity and an alteration of oxidative homeostasis, through depletion of antioxidant defences, it is responsible for a plethora of adverse outcoming mainly leading to cell death; we focused on cadmium effect (1) on the energy metabolism in human neuroblastoma SH-SY5Y cell line, (2) on the oxidative defence responses in differentiated human LUHMES neural cell line and (3) on the function of human SOD1 in a three models approach (recombinant protein in *E. coli*, in SH-SY5Y cell line and in the nematode *Caenorhabditis elegans*).

The evaluation of energetic metabolism of SH-SY5Y neural cells treated with sub-lethal $CdCl_2$ doses for 24 hours, showed an increase in glycolysis compared to control. This shift to anaerobic metabolism has been confirmed by both glycolytic parameters and greater ATP production from glycolysis than oxidative phosphorylation, index of lower mitochondrial functionality in cadmium treated cells. Regarding the fuel oxidation, cadmium caused an increase in glutamine dependency and a specular reduction in the fatty acids one, without altering glucose dependency. Moreover, we observed an increase in total GSH, as well as in the GSSG/GSH ratio and in lipid

peroxidation, all indexes of an altered oxidative homeostasis better investigated in LUHMES cells. In this model, a 24 hours cadmium administration enhanced total GSH content at the lowest doses, at which it also activates Nrf2 through a better protein stabilization via p21 and P-Akt. The metal adverse effects on cell viability could be rescued by GSH addition and by cadmium administration in astrocytes- or microglia-conditioned medium. In the latter cases the total GSH level remained comparable to untreated cells even at higher $CdCl_2$ concentrations. Finally, SOD1 catalytic activity was investigated in the presence of cadmium. The first evaluation of this metal combined with fixed copper and/or zinc concentrations on the recombinant GST-SOD1, expressed in *E. coli* BL21, showed a dose-dependent reduction in SOD1 activity only when copper was added to cellular medium, while the expression remained always constant. Similar results were obtained in SH-SY5Y cell line, in which SOD1 enzymatic activity decreased in a dose- and time-dependent way after cadmium treatment for 24 and 48 hours, without altering its expression; as well as in the *Caenorhabditis elegans* model, where a 16 hour cadmium treatment caused a 25% reduction only in SOD1 activity.

In conclusion, cadmium caused a shift to anaerobiosis, Nrf2 activation, with increased GSH production, and a reduction in SOD1 activity.

Chapter 1

Introduction

Part I

Cadmium: a non-essential element with toxic effects on the nervous system

I.1 Introduction

The chemical elements cadmium (Cd) belongs to the group IIB of the periodic table. It is a soft, silvery-white metal, with chemical and physical properties similar to zinc (Zn) and mercury (Hg). Resistant to corrosion, it is a rare element usually present in nature as a compound with zinc sulphide and in the majority of its compounds it is found at the oxidation state of 2+. Cadmium, possessing a specific density of more than 5 g/cm^3, is classified as a heavy metal and it is found in air, water and sediment with a concentration of 0.15 mg/kg in the Earth crust and of 1.1×10^{-4} mg/L in the sea (Zhang and Reynolds, 2019).

This element was first discovered in 1817 by German chemist Friedrich Strohmier, as an impurity of zinc carbonate, and it has been extensively used in the middle of the 19^{th} and all over the 20^{th} century in industry and agriculture. In fact, cadmium compounds are used as stabilizers in PVC products, colour pigment, in re-chargeable Ni–Cd batteries, as anticorrosion agent (cadmiation) and this metal is also present as a pollutant in phosphate fertilizers, with about 22,000 tons produced yearly worldwide (IARC, 2012; Rani et al., 2014). The wide use of cadmium compounds by anthropogenic activities, together with the absence of its biodegradation, caused a widespread distribution of this element in the environment, with a rapid increase in the period 1800-1960 (Sarkar et al., 2013). The widespread use of this element led the scientific community to study its adverse effect since 1858 and, from this date on, several studies on cadmium toxicity, both on animals and humans, have been reported: the first experimental toxicological studies are from 1919, while the first report on cadmium chronic effects on humans was published in the late 1930s-1940s (Nordberg, 2009; Rani et al., 2014). The most famous one is the study on the *Itai-Itai* disease, a skeletal disease observed in Fuchu, Toyama prefecture, Japan in the 1950s (Nordberg, 2009). Cadmium exposure can provoke damage to several organs, such as kidney,

liver, lungs, brain, testes and heart. Moreover, it can cause osteoporosis, anaemia, non-hypertrophic emphysema, eosinophilia, anosmia and chronic rhinitis, representing a risk factor for humans' and other animals' health and leading this toxic heavy metal to be part of the group of main environmental and occupational chemical pollutants, since not only the high prolonged exposure, but also the moderate and low one can be a risk factor (Mezynska and Brzóska, 2018). However, after 1960 we have assisted to a decrease in cadmium emissions caused by the improvement in technologies and the application of restrictions. This reduction correlates with a progressive decrease of the average cadmium intakes (Sarkar et al., 2013). In fact investigations around the world have shown that, for general population, the average cadmium intakes in 1960 were about 15 μg/kg body weight per month, while in 2000 were 5 μg/kg body weight per month, well below the current WHO JECFA (Joint FAO/WHO Expert Committee on Food Additives) standard established in 2010 (25 μg/kg body weight per month) (Sarkar et al., 2013).

Moreover in 1993, the International Agency for Research on Cancer (IARC), on the basis of sufficient evidence for carcinogenicity in both humans and experimental animals, has classified cadmium as a human carcinogen (group I); while the European Commission has classified some cadmium compounds as possibly carcinogenic (Carcinogen Category 2) (IARC, 2012).

I.2 Sources of cadmium exposure

In humans cadmium has an extremely long half-life of about 20-30 years and its content at 50 years of age is about 15-30 mg and increases with age (Sarkar et al., 2013). Human exposure to cadmium occurs by occupational sources, through ingestion of contaminated food and/or water and by inhalation of polluted air or cigarette smoking. Considering the fact that cadmium and its compounds enter the body mainly through the respiratory tract (10-40%) and that about the 30-64% of inhaled cadmium is absorbed by the body, people occupationally exposed and smokers show high cadmium levels in blood and urine placing them in the categories at risk (Sarkar et al., 2013). In fact, one cigarette contains from 0.5 to 2 μg cadmium and about the 10% of the cadmium content is inhaled and absorbed by the lungs when the cigarette is smoked, giving to smokers a 4-5 times higher cadmium level in the

blood (Järup, 2003; Nawrot et al., 2010). In particular workers exposed to cadmium show average levels of 6.23 μg Cd/g of creatinine and 6.54 μg Cd/L of blood; while smokers have values of 3.32 μg Cd/L of blood and 1.20 μg Cd/L of urine, compared to non-smokers levels of 1.0 μg Cd/L of blood and 0.8 μg Cd/L of urine, as evaluated by the German Commission on Human Biological Monitoring (Reyes-Hinojosa et al., 2019).

Regarding the non-smoking population the main source of chronic cadmium exposure (95%) is represented by the consumption of contaminated food. Virtually cadmium is present in all food since its compounds are readily taken up by plants, due to their highly soluble nature, resulting in their storage in crops for food and feed production and in a high soil-to-plant transfer (Sarwar et al., 2010). However, the metal concentrations vary in function of the type of food and the level of environmental contamination. Elevated cadmium concentrations can be found in food from plants, in particular from cereals like rice and wheat, green leafy vegetables, potato and root vegetables such as carrot and celeriac; as well as in molluscs, crustaceans, offal products, oil seeds, cocoa beans and in certain wild mushrooms (Järup and Åkesson, 2009). More than 80% of this element derives from cereals, vegetables and potato, with a regular cadmium intake rates around 2-25 μg/day among children and range from 10 to 50 μg/day in adults (Bhattacharyya, 2009). The average cadmium intake from food generally varies between 8 and 25 μg per day of which approximately 0.5 to 1.0 μg is actually retained in the body (Berglund et al., 1994; Olsson et al., 2002). This mode of uptake can be influenced by several factors, like dose and exposure time, chemical components of the diet, the body's nutritional status, age and gender; having subgroups of the population (vegetarians, women in the reproductive phase of life and people living in highly contaminated areas) with an exceed in the tolerably weekly intake of about 2-fold (Nawrot et al., 2010). A less than a few percentage of cadmium intake is represented by drinking water and inhalation of contaminated air (Olsson et al., 2002; Vahter et al., 1991). In details, the exposure references for cadmium in food is set at 10 mg/kg of dry weigh, in drinking water at 3 μg/L and at 5 ng/m^3 for the air (Reyes-Hinojosa et al., 2019).

Currently the risk assessment of environmental exposure to cadmium is conducted based on dietary cadmium intake and its concentration in the urine. The Agency for

Toxic Substances and Disease Registry (ATSDR), basing on studies in animals, has determined the minimum risk levels for acute and chronic inhalation of 0.03 μg Cd/m^3 and 0.01 μg Cd/m^3, respectively (Faroon et al., 2012). A safe intake limit of 7 μg Cd/week/kg body weight or 25 μg Cd/kg body weight per month (mg/kg bw-mo) or 0.4-0.5 mg /week and the maximum dose of 60-70 μg per day were set based on the critical renal cadmium concentration of between 100 and 200 μg/g wet weight that corresponds to a urinary threshold limit of 5–10 μg/g creatinine (Sarkar et al., 2013).

I.3 Cadmium uptake in humans

The main entry pathways for cadmium in humans are lungs and the gastrointestinal tract, with the skin playing a minor role (Nordberg, 2009).

First the metal needs to enter the cells and, since it does not possess any biological function, the use of transport systems for other essential elements has been suggested for its cellular uptake. Ion channels and transporters present on the plasma membrane, normally involved in the physiological cellular trafficking, are used by cadmium for entering the cells. Among ion channels, the voltage gated calcium (Ca) channels (VGCC) and transient receptor potential (TRP) channels, are involved in cadmium uptake. In particular, the not high selectivity for calcium of T-type VGCC, together with their smallest selectivity filter formed by two aspartate and two glutamate (EEDD motif), instead of four glutamate (EEEE motif), like the other VGCC, allows cadmium permeation in cells (Shuba, 2014). The non-selective cation channels TRP, which can be permeated by sodium (Na), calcium and magnesium (Mg), also plays a role in cellular cadmium uptake, with TRPA1, TRPV5, TRPV6 and TRPML1 permeated by cadmium (Thévenod et al., 2019).

Solute carriers (SLC) for essential metals are responsible for cadmium entrance in cell too. The human divalent metal transporter 1 (DMT1) transports a broad range of divalent metal ions; it is ubiquitously expressed on cell plasma membrane and in epithelial cells it also localized on endosomes, lysosomes and mitochondria (Shawki et al., 2012). DMT1 has a cadmium transport efficiency similar to the iron (Fe) one and represents a valid route for cadmium uptake from water and food in the duodenum, as well as being a key mediator of vesicle-to-cytosol transfer of cadmium in various cell type (Thévenod et al., 2019). It is important to note that if the iron

stores in the body decrease or if there is an iron deficiency, the intestinal cadmium absorption increases; this condition is more prevalent in women at fertile age than among men (Akesson et al., 2002). Generally, women show higher cadmium concentrations in blood, urine and kidney compared to men and this difference could be explained by the close correlation between cadmium absorption and the expression of DMT1, which transports cadmium and iron into the mucosa cell in a competitive manner. This situation is exacerbated during pregnancy when enterocytes have an increased DMT1 density at the apical surface to optimize micronutrients absorption (Akesson et al., 2002; Vahter et al., 2007).

The zinc transporters, Zrt-, Irt-related proteins (ZIP) are valid candidates for cadmium entrance in cells, due to the similarity between cadmium and zinc. Among them, ZIP8 and ZIP14 can be permeated by cadmium, with ZIP8, highly expressed in lungs, liver, kidneys and testis, involved in cadmium accumulation and ZIP14 responsible for cadmium transport at high affinity (Thévenod et al., 2019).

Following absorption in the lungs and/or intestine, it is assumed that cadmium in the blood primarily binds to albumin and other thiol-containing reactive biomolecules in the plasma, as well as on red blood cell membranes, making the blood stream responsible for its transport inside the organism (Genchi et al., 2020). Cadmium accumulate mainly in the liver and kidneys due to their ability to express metallothioneins (MTs), which are the precursor of cadmium detoxification. MTs are low molecular weight proteins of 6-7 kDa, rich in sulfhydryl groups (-SH), responsible for the maintenance of essential metal ions homeostasis and involved in the scavenging of toxic metals and free radicals produced in oxidative stress. Under physiological conditions, they bind zinc and copper; however, MTs show affinity for other metals, like cadmium, lead (Pb), mercury, nickel (Ni) and silver (Ag). In mammals MTs are ubiquitously expressed, with highest concentration in liver, kidneys, pancreas and testis, and localized in the cytoplasm, in lysosome, mitochondria and nuclei (Sabolić et al., 2010). They are made of 61-68 amino acid residues, of which 18-23 are cysteines, and four different isoforms are expressed: MT1 and MT2 are present in several tissues, while the other two are tissue-specific, with MT3 present in brain and renal tissue and MT4 in keratinocytes (Nordberg, 2009). The -SH groups of these metal proteins (apoproteins) can complex seven

divalent cations, such as zinc and cadmium, or 12 monovalent metal ions (Nielsen et al., 2007).

Inside the hepatocytes MTs bind cadmium in order to protect the cells from metal ions toxicity, with consequent accumulation of Cd-MT complexes. The majority of these complexes is stored in the liver; however a small amounts is released into blood plasma and then filtered by the renal glomeruli, where the renal tubular cells reabsorb Cd-MT complexes through ZIP8-mediated endocytosis (Nordberg, 2009; Wang et al., 2007). Inside the lysosomes of renal tubular cells, the acidic pH promotes the dissociation of cadmium from Cd-MT complex, with the release of free cadmium ions, eliminated through urine. Cd-MT complexes can be taken up by other organs and they show a short half-life, in contrast to the half-life of free cadmium ions (25-30 years) (Genchi et al., 2020). However, when almost all binding sites in MT are occupied by cadmium, no further binding of cadmium is possible, leading to the end of this protective process and to the spread of cadmium toxicity in the cell, that arise at concentrations smaller than almost any commonly found mineral, with a multifactorial toxicity mechanism (Nordberg, 2009).

I.4 Cadmium toxic effects

Cadmium can exert a plethora of toxic effects. The free cadmium ions possess not only a high affinity for biological structures containing -SH, amino, carboxyl, imidazolyl and disulfide groups causing disturbances of their function; but they can also interfere with essential bio-elements, such as zinc, calcium, iron, altering their homeostasis and biological functions (Mezynska and Brzóska, 2018; Sabolić et al., 2010). This xenobiotic can stimulate the indirect production of reactive oxygen species (ROS), mainly by weakening the enzymatic and non-enzymatic defence systems, resulting in the damage of key macromolecules, intracellular organelles and cellular membranes. It can also lower the mitochondrial membrane potential, disrupting cellular respiration and ATP production (Nair et al., 2013). Moreover cadmium provoke oxidative damage on the DNA structure, which leads to the induction of cellular proliferation, the inhibition of the apoptotic mechanisms and the blocking of the DNA repair mechanisms (Mezynska and Brzóska, 2018; Rani et al., 2014). Different modes of cell death have been associated with cadmium toxicity in a

dose-dependent correlation: sub-micromolar concentrations of cadmium lead to proliferation or delayed apoptosis, intermediate concentrations of 10 μM cadmium cause various types of apoptotic cell death, and very high concentrations (>50 μM) lead to necrosis (Templeton and Liu, 2010).

Among the toxic effects, oxidative stress is assumed to be the principal molecular basis underlying cadmium-induced cytotoxicity, although this element is a redox-inactive metal. Even though this xenobiotic in unable to directly generate ROS; cadmium exposure resulted in an increase in ROS production. In fact, cadmium indirectly induces oxidative stress by a displacement of redox-active metals, depletion of redox scavengers, inhibition of anti-oxidant enzymes and inhibition of the electron transport chain (ETC) resulting in mitochondrial damage (Nair et al., 2013).

Cadmium can replace redox-active metals, such as iron and copper, from cytoplasmic and membrane proteins, thereby increasing the ability of free redox-active ions in cells, that can cause the production of ROS via Fenton reaction (Cuypers et al., 2010; Rani et al., 2014). It has been demonstrated in rat Leydig cells that cadmium induced iron displacement from its binding sites and consecutively iron redistribution in these cells caused oxidative stress (Nair et al., 2013). Moreover, cadmium interference with iron leads to lipid peroxidation, as shown in male Wistar rats exposed to $CdCl_2$ in which it was absent in liposomes in iron-free conditions, showing the inability of cadmium to directly induce lipid peroxidation (Casalino et al., 1997).

Cadmium can also reduce antioxidant defence mechanisms. Among ROS scavengers, glutathione (GSH), being implicated in transition metals' chelation, is considered the first line of defence against cadmium toxicity. Due to its high affinity for -SH groups, cadmium binds GSH causing the depletion of the GSH pools and the alteration of the cellular redox balance with consequent increase in oxidative stress. The importance of GSH in cadmium detoxification has been reported by Dudley and Klaassen, who showed how its depletion results in enhanced metal hepatotoxicity (Dudley and Klaassen, 1984). Cadmium also affects the function of antioxidant enzymes, with the activities of superoxide dismutase (SOD), catalase (CAT), glutathione peroxidase (GPx), and glutathione reductase (GR) altered in the presence of the metal (Nair et al., 2013). Cadmium atoms also combine with selenium ones and they are excreted via

the bile system, causing a depletion in the amount of selenium from the body, which leads to less selenium for GPx formation (Rani et al., 2014).

The mitochondrial ETC is one of cadmium main cellular targets. In a study performed on isolated mitochondria from liver, brain and heart of male Dunkin-Hartley guinea pigs, complex II and complex III are more sensitive to cadmium than complexes I, IV, and V, in all three tissues tested, with a cadmium strong inhibitory effect of 60% on complex II and 77% on complex III (Wang et al., 2004). This elevated sensibility of complex II and III could be related to the presence, in these complexes, of Fe-S clusters, potential cadmium targets (Branca et al., 2020). Cadmium binding to complex III causes the impairment of electron transfer through these complex and the accumulation of unstable semiubiquinones, which then transfer an electron to molecular oxygen, resulting in the formation of superoxide (Nair et al., 2013). Moreover, cadmium induces the opening of mitochondrial transition pore, which resulted in an increased membrane permeability responsible for cytochrome c release and ETC disruption, causing more ROS production (Branca et al., 2020). This mitochondrial damage via ROS production causes a significant inhibition of the mitochondrial respiratory chain, with a reduced ATP production and oxygen consumption, that lead to a shift to anaerobic metabolism and increased production of lactate (Al-Ghafari et al., 2019; Monteiro et al., 2018).

I.5 Cadmium and the nervous system

The function of the nervous system is severely affected by cadmium exposure. Cadmium administration in experimental animals causes behavioural defects, changes in nervous system biochemistry and brain lesions; in humans acute cadmium poisoning produced parkinsonism symptoms, while chronic cadmium exposure can generate neuro-behavioural disturbances, such as altered attention, psychomotor speed, memory, reduced visuomotor functioning and increase in the risk of polineuropathy disease (Méndez-Armenta and Ríos, 2007; Okuda et al., 1997).

Experimental studies on animals show cadmium ability in inducing neurotoxicity, with a wide spectrum of clinical entities, such as neurological disturbance and neurochemistry changes (Méndez-Armenta and Ríos, 2007). Newborn rats exposed to low cadmium doses exhibit damage in the central nervous system (CNS): the brain

cortex, cerebellum, caudate nuclei and putamen showed extensive necrosis and haemorrhage, with the endothelium of some blood vessel in the necrotic areas slightly damaged (Wong and Klaassen, 1982).

The symptoms of cadmium toxicity on nervous system in humans are headache, vertigo, olfactory dysfunction, parkinsonian-like symptoms, slowing of vasomotor functioning, peripheral neuropathy, decreased equilibrium, decreased ability to concentrate and learning disabilities (Wang and Du, 2013). However, the exact mechanism through which this metal elicits its neurotoxic effects is still unresolved. Effects of this xenobiotic on neurotransmitter, oxidative damage, interaction with other metals, estrogen-like effect, and epigenetic modification could be involved.

I.5.1 Cadmium uptake in the nervous system

The blood brain barrier (BBB) is a selective permeable layer composed by endothelial cells characterized by tight junctions between the cells, involved in brain and spinal cord protection from toxic substances. The BBB supplies the CNS with nutrients, regulates the molecular traffic in and out and, being a physical separation between the systemic circulation and the brain's microenvironment, is responsible for the maintenance of CNS integrity.

Under normal conditions cadmium can barely reach the BBB; however, if present in the blood stream, it may enter the brain by crossing the BBB and the choroid plexus (CP), entering the cerebrospinal fluid (CSF), through which it can reach a specific part of the CNS (Yokel, 2006). Cadmium accumulation in the BBB and in the CSF has been reported, showing a weak integrity of the blood-cerebrospinal fluid barrier, despite the presence of several efflux mechanisms responsible for traffic's control in and out the brain (Karri et al., 2016). Cadmium can enter the cells exploiting the physiological ionic channels, transporters and receptors present on the luminal surface of the BBB endothelial cells (Thévenod et al., 2019). In case of an acute cadmium exposure the BBB protects the majority of the CNS; while in chronic and prolonged ones, cadmium is responsible for the weakening of cellular antioxidant defences and increasing ROS formation, with the consequent activation of matrix metalloproteinase (MMP) that disrupts the BBB tight junctions and enhances its permeability (Branca et al., 2020; Yang et al., 2007). MMP expression is linked to pericytes, responsible

for the maintenance of vascular structure and function during cerebrovascular maturation, homeostasis and disease, and in ischemic brain regions activated MMP colocalized with ROS at the level of capillary walls, assuming a key role of pericytes in BBB permeability regulation in both physiological and pathological mechanisms (Gasche et al., 2001; Underly et al., 2017).

An *in vivo* study on adult rats showed how a small amount of cadmium reach the brain, due to selective permeability of BBB, while it might diffuse across the barrier with the help of a vehicle such as ethanol (Pal et al., 1993). Wong and Klassen also reported a higher cadmium toxicity in newborns than in adult rats, probably due to differences in BBB maturation (Wong and Klaassen, 1982).

Another route of cadmium uptake can be represented by the nasal mucosa or olfactory pathways, with the metal, transported along the primary olfactory neurons, able to reach the termination in the olfactory bulbs bypassing the intact BBB. It has been reported how occupational inhalation of cadmium can be toxic to olfactory sense, with intranasal exposure related to olfactory disfunction in humans and nasal epithelial damage as altered odorant-guide behaviour in rodent models (Wang and Du, 2013). Moreover, Kumar and colleagues suggested that the effect of cadmium in brain is region-specific and most pronounced in olfactory bulb; in fact they observed a decrease in membrane fluidity, phosphatidylcholine and phosphatidylethanolamine content, as well as an increase in intracellular calcium level and TBA reactivity in olfactory bulb of rats after cadmium exposure (Kumar et al., 1996).

Once in the brain, cadmium accumulates in the CP in much greater concentrations, about 2-3 times higher than the one found in the brain cortex, as revealed by a post-mortem study on humans (Wang and Du, 2013). This accumulation is mainly due to both an abundant pool of metal binding ligands, responsible for metal ions binding, and the presence of a highly active antioxidant defence system (Zheng et al., 1991). However, none of the cellular defence mechanisms is unlimited causing direct damage to CP ultrastructure.

Even in the nervous system, cadmium ions in cells bind MT. Astrocytes, endothelial cells, ependymal cells and oligodendroglia have MT1 and MT2, while in neurons there is MT3 (Méndez-Armenta and Ríos, 2007). Cadmium induces the expression of MT1 and MT3 mRNA, in relationship to the metal concentration and distribution, as

well as the stage of brain development (Choudhuri et al., 1996). Hence the differential constitutive expression of brain MTs in newborns and adults might be important in cadmium induced neurotoxicity.

I.5.2 Cadmium toxicity in the nervous system

Exposure to cadmium affects both neurons and glial cells. Morphological changes of the cells of the nervous systems have been reported: in mesencephalic trigeminal (Me5) neurons from adult rat destruction of the cytoplasmic organelles, swelling and vacuolization of the cell body, with consequent cell lysis have been seen (Yoshida, 2001). The neural extension, axons and dendrites, are the mostly affected and apoptotic morphological changes have been identified in cerebral cortical neurons treated with cadmium (Wang and Du, 2013). Moreover, cadmium administration at the embryonic level caused impaired neurogenesis, resulting in reduced neuronal differentiation with fewer differentiated neurons and glia in the facial sensory ganglia (Chow et al., 2008).

In various brain regions the metal administration determined a decrease in total thiols and GSH pool as well as an increase in the oxidized glutathione (GSSG) level; while the activities of antioxidant enzymes, like SOD, CAT, GST, GR and GPx were reduced (Nair et al., 2013). GSH depletion has been reported in primary oligodendrocytes, in mouse neuronal cell lines and in rat primary mesencephalic cultures (Branca et al., 2020). Moreover, this decrease in antioxidant defence, together with the disruption of mitochondrial potential and ETC, determined an enhanced ROS level, which results in the activation signalling pathways such as JNK, Erk1/2, p38 MAPK and their upstream kinases like ASK1, MKK4, MEK1/2, and MEK3/6 responsible for the activation of apoptosis both caspase-dependent and independent (Branca et al., 2020; Nair et al., 2013).

This increase in free radicals' production affects the membranes by altering not only their fluidity, due to a decrease in cholesterol content, but also the phospholipid composition, with an increase in phosphatidylethanolamine and a decrease in phosphatidylcholine, phosphatidylinositol, phosphatidylserine and sphingomyelin (Gupta and Shukla, 1996; Kumar et al., 1996). However, the major consequence of cadmium-induced oxidative stress on membranes is represented by lipid peroxidation,

due to the high susceptibility of lipid to be oxidized by superoxide anions and hydroxyl radicals. A significantly enhanced lipid peroxidation has been found in parietal cortex, striatum and cerebellum in the brain of developing rats exposed to cadmium (Méndez-Armenta and Ríos, 2007). Moreover, the level of lipid peroxidation corresponds to the level of cadmium exposure (Valko et al., 2006). Lipid peroxidation produces a progressive loss of membrane fluidity, that reduces the membrane potential and increases membrane permeability to calcium ions, altering the intracellular calcium concentration (Simonian and Coyle, 1996).

Cadmium is responsible for the inhibition of calcium influx, through membrane channels, into the nerve terminal following the action potential by acting as a competitive ion to VGCC, leading to altered neurotransmitters release (Wang and Du, 2013). In the amygdala of cadmium-exposed animals the levels of the excitatory neurotransmitters glutamate and aspartate were found decreased, while the ones of inhibitory neurotransmitters glycine and GABA were increased, suggesting a cadmium effect on the balance excitation/inhibition of the synaptic neurotransmission (Minami et al., 2001). Together with neurotransmission, other neuronal functions may be affected by cadmium, leading to apoptosis in primary murine neurons (Wang and Du, 2013). A dose-dependent increase in intracellular calcium concentration has been observed in cadmium exposed neurons and this sustained increase could be a mediator of cadmium induced apoptosis via activation of the calcium-mitochondria apoptotic signalling pathway (Yuan et al., 2013).

This xenobiotic accumulation at the fetal stage or at birth might cause irreversible changes in the brain; in fact neurogenesis is affected by cadmium with a marked reduction in neuronal differentiation and axonogenesis, due to a metal-induced altered gene expression (Wang and Du, 2013). Cadmium effect on genes could be explained by its action as a co-genotoxic chemical agent, due to its ability in causing genomic instability through inhibition of DNA repair mechanisms and altered DNA methylation (Rani et al., 2014). In fact, by interacting with the methyltransferase DNA binding domain, might interfere with the enzyme-DNA interaction leading to alterations in methylation metabolism responsible for gene-specific DNA hypo- or hyper-methylation (Wang et al., 2012). Failure of DNA methylation systems in the brain leads to clinical syndromes such as mental retardation and autistic-like

behaviours (Shahbazian and Zoghbi, 2002). Moreover, cadmium can disrupt the endocrine induction by affecting the hypothalamic-pituitary-gonadal axis and/or the Leydig cells (Wang and Du, 2013).

In conclusion cadmium neurotoxicity is a multifactorial process, mainly characterized by increased oxidative stress, mitochondrial dysfunction and interference with other divalent ions homeostasis, that interests all the cellular types present in the CNS. These pathophysiological mechanisms, together with axonal transport impairment, excitotoxicity, protein aggregation, neuroinflammation, endoplasmic reticulum stress and abnormal RNA processing, are present in the amyotrophic lateral sclerosis (ALS), a fatal adult neurodegenerative disease characterized by progressive loss of motor neurons (Mancuso and Navarro, 2015). Epidemiological studies on cadmium involvement in ALS etiology have been carried out; however the data presented if on one side cannot state a direct involvement of this metal in ALS, on the other side cannot be excluded (Oggiano et al., 2020).

Part II

Focusing on human Superoxide dismutase 1: what to know about it

II.1 Introduction

Superoxide dismutase (SOD) proteins show themselves to the world as a defense mechanism against reactive oxygen species (ROS) toxicity. In fact, they represent a family of antioxidant enzymes responsible for the dismutation of superoxide anions derived either from extracellular stimuli or as a byproduct of mitochondrial respiration. This family is ubiquitous and widely distributed among aerobic organisms, aerotolerant anaerobes and some obligate anaerobes too (Scandalios, 1993). It is also highly conserved among eukaryotes and, to date, three isoforms of SOD have been identified in mammals: a cytosolic copper-zinc superoxide dismutase (CuZnSOD or SOD1), a mitochondrial manganese superoxide dismutase (MnSOD or SOD2) and an extracellular superoxide dismutase (ECSOD or SOD3). These forms of SODs elicit similar functions, but differ in protein structures, chromosome localizations, metal cofactor requirements, gene distributions and cellular compartmentalization (Miao and St. Clair, 2009; Parge et al., 1992).

The scientific history of SOD (EC 1.15.1.1) started in 1938 when Mann and Keilin isolated from bovine blood a copper green protein, named erythrocuprein, with a believed biological function in copper storage and it followed by the discovery that this erythrocuprein showed a superoxide dismutase activity, by Fridovich and McCord in 1969 (McCord and Fridovich, 1969; Scandalios, 1993). Subsequently, the presence of zinc in addition with copper was reported, leading to name that protein copper-zinc superoxide dismutase (Carrico and Deutsch, 1970). However the first appearance of SOD to the world is much older and it was triggered by the proliferation of photosynthetic organisms that began to produce oxygen over 2 billion years ago (Zelko et al., 2002).

II.2 From a euxinic world to an oxygenic one

When the earth was born the composition of the atmosphere and the ocean was different from the one we know today and over the 4.5 billion years history of the planet has evolved significantly from reducing to oxidizing (Case, 2017). The early biosphere was composed by hydrogen (H_2), carbon dioxide and monoxide (CO_2 and CO), hydrogen sulfide (H_2S) and methane (CH_4) and was lacking in any significant concentration of dioxygen (O_2) (Holland, 2002; Sheng et al., 2014). Oxygen atmospheric level started to increase between 3.0 and 2.0 billion years ago, during the so called Great Oxidation Event (GOE), which led to an increase of oxygen of about 0.1-15% driven by cyanobacteria as a product of oxygen photosynthesis (Holland, 2006; Sheng et al., 2014). After the GOE, from 1.9 to 0.9 billion years ago there was the "boring billion", during which the rate of oxygen remained constant, followed by the Neoproterozoic Oxidation Event (NOE), 0.8-0.5 billion years ago, the second major oxidation incident that elevated the level of atmospheric oxygen to nowadays level (Case, 2017; Holland, 2006; Och and Shields-Zhou, 2012).

The organisms learned how to use oxygen to create energy and new biochemical pathways became possible (Smith and Doolittle, 1992). However the use of this molecule in biological systems with high electron fluxes comes at the potential threat of generating ROS, which, at elevated concentrations, not only can lead to cellular damage and cell death, but also may contribute to the development of various diseases, like cancer, hypertension, diabetes, atherosclerosis, inflammation and premature aging (Case, 2017; Zelko et al., 2002). In fact, oxygen reduction to water (reaction 1) in his intermediate steps (reactions 2-5) can lead to the formation of the tree major ROS, that are superoxide anion ($O_2^{\bullet-}$), hydrogen peroxide (H_2O_2) and hydroxyl radical ($HO^{\bullet}$).

(1) $O_2 + 4H^+ + 4e^- \rightarrow 2H_2O$

(2) First step: $O_2 + e^- \rightarrow O_2^{\bullet-}$

(3) Second step: $O_2^{\bullet-} + 2H^+ + e^- \rightarrow H_2O_2$

(4) Third step: $H_2O_2 + H^+ + e^- \rightarrow H_2O + HO^{\bullet}$

(5) Fourth step: $HO^{\bullet} + H^+ + e^- \rightarrow H_2O$

In order to avoid ROS toxic effects, aerobic organisms developed defense mechanisms both non-enzymatic, such as glutathione, cysteine or flavonoids, and

enzymatic, capable of removal, neutralization or scavenging of free radicals. Among the enzymatic defenses, SOD together with catalase (CAT) is the major mechanism involved in superoxide anion detoxification: SOD converts superoxide anion into hydrogen peroxide, which is then scavenged to H_2O by catalase, avoiding the formation of the hydroxyl radical ($HO^{\bullet}$), which can react with all the macromolecules causing several damages (Scandalios, 1993).

In all living organisms superoxide anion is formed and it can behave as a signal molecule ("redox signaling" event), as a harmless intermediate that degrades spontaneously or as a toxic agent ("oxidative stress" event); it has been estimated that it exists in the biological systems at concentrations ranging from 10 to 200 pM and to date SOD is the only family of enzymes able to autonomously eliminate superoxide anions in biological systems (Cadenas and Davies, 2000; Murphy, 2009).

Even if the oxidation of the atmosphere and the ocean brings us to think that antioxidants defenses originated in this period for counteracting the oxygen oxidative pressure, sequencing analysis of ancient species revealed that the antioxidants originated long before the GOE, due to local localization of oxygen from either abiotic source, like photolysis of H_2O by UV light, or cohabitation in close proximity to an oxidative photosynthesizing organism (Case, 2017).

II.3 The evolution of SOD

SODs are metalloproteins and the metals uptake seems to be related to the time of appearance of transition metals in the atmosphere: iron (Fe) first, then manganese (Mn) and in the end copper (Cu) and zinc (Zn) (Bannister et al., 1991).

When life arose, the oceans were euxinic, so iron was highly bioavailable making the primitive SOD using this metal for its catalytic center. In fact the most primitive form of this enzyme is the FeSOD and it is found in aerobic and anaerobic bacteria, in Archea, in Protists and in the chloroplasts of some eukaryotic plants (Smith and Doolittle, 1992). This form of SOD shares the 50% similarity with the other one that originated in the very early primitive lifeforms, the MnSOD, suggesting that these two have evolved from a close common ancestor (Case, 2017).

MnSOD can be found in all species ranging from Archea to Eukarya, even if in eukaryotes is present only in mitochondria. The mitochondrial MnSOD and the

prokaryotic MnSOD are structurally related with a high degree of sequence similarity, leading to the hypothesis that they have evolved from a common ancestral protein. It seems unlikely that mitochondrial and bacterial MnSOD originated from a process of convergent evolution, because it should imply the fact that mitochondria and bacteria had been subjected to similar selective pressure for a considerable period of time (Bridgen et al., 1975).

The most modern family of the lineage is represented by the CuZnSOD. This protein is ubiquitous among plants and animal species and it is localized in the nucleus, cytoplasm, mitochondrial intermembrane space, chloroplasts and in the extracellular matrix (ECSOD). CuZnSOD can also be found in the periplasmic space of selected gram-negative bacteria (Case, 2017). In the higher-level eukaryotes, the ECSOD and the intracellular CuZnSOD diverged at an early stage of evolution, before the differentiation of fungi, plants and metazoan (Bordo et al., 1994). The higher similarity of ECSOD to the fungal one than to the intracellular form, suggests either that the extracellular one represents a more primitive version from which the intracellular form divergently evolved or that both enzymes converged on the same enzymatic reaction and metals used for catalysis and stability (Case, 2017).

The CuZnSOD developed at a much later time than the Fe/MnSOD and it evolved during or after the GOE, due to the increasing copper and zinc bioavailability when the level of the atmospheric and oceans oxygen enhanced (Bannister et al., 1991). There is minimal structure homology between CuZnSOD and Fe/MnSOD, signifying that these two families of SOD derived independently of one another and underwent convergent evolution to perform identical reaction (Zelko et al., 2002). Another example of convergent evolution upon the same need of superoxide anion removal is represented by the most recently discovered family of SOD, the NiSOD; which is found in marine bacteria and algae and it´s not related to the other families (Case, 2017; Youn et al., 1996).

II.4 SOD1 gene structure and regulation

The human CuZnSOD is encoded by the *SOD1* gene (Entrez Gene ID 6647) located on chromosome 21q22.11 with a genomic size of 9307 bp, according to UCSC Genome Browser. The five exons, interspersed by four introns, code for a 153 bp

polypeptide of 16 kDa and several polymorphisms have been identified, mainly in the regulatory regions. Two functional species of *SOD1* mRNA have been identified: one of about 0.7 kb and the other of 0.9kb, both transcribed from the same gene, but with different length in their 3'UTR caused by multiple polyadenylation sites (Milani et al., 2011).

This gene is often considered as a "housekeeping gene" because it is mostly constitutively expressed and not as easily inducible as the other superoxide dismutase genes; however several transcription factors (TFs) are involved in *SOD1* regulations in response to intracellular and extracellular events (Miao and St. Clair, 2009).

The constitutive expression is regulated in the proximal promoter region by the C/EBP-related factors (CCAAT/Enhancer Binding Proteins), a family of TFs, all containing a highly conserved, basic leucine zipper (bZIP) domain at the C-terminus, and Sp1 (Specificity protein 1), a ubiquitously expressed C2H2-type zinc finger-containing DNA binding protein. Both C/EBPα and C/EBPβ can interact with the CAAT box located at position -64 to -55 from transcription start site, while Sp1 binds in the GC-rich domain between positions -104 to -89 and, when it binds to a noncanonical binding-site located between nucleotide -59 and -49, can also upregulated *SOD1* as a response to exogenous stress (Minc et al., 1999; Seo et al., 1996). Other TFs responsible for *SOD1* upregulation under stress conditions are Egr-1, AP-2, AHR, Nrf2 and NF-kB.

The DNA binding site for nuclear phosphoprotein Egr-1 (Early Growth Response-1) is located between nucleotide -59 and -49 in which there is also the noncanonical consensus recognition sequences for Sp1 (Minc et al., 1999). Two AP-2 (Activate protein 2, a family of closed TFs) sites, located at positions -134 to -127 and -118 to -111, are involved in the promoter response to *Panax ginseng* extracts; while in the 5' flanking region between positions -255 and -238 Cho and coworkers have identified a xenobiotic responsive element, recognized by the Aryl Hydrocarbon Receptor (AHR), a ligand-activated TF belonging to the helix-loop-helix (bHLH) family (Kim et al., 1996; Seo et al., 1996). An antioxidant responsive element (ARE) is located between -356 and -330 from the transcription start site in the *SOD1* gene promoter and it is recognized by the Nrf-2 (Nuclear factor E2) protein (Milani et al., 2011). NF-kB (Nuclear Factor-kappa B), a family of five TFs (p50, p52, RelA/p65, c-Rel, and

RelB), all containing the Rel homology domain (RHD) at the N-terminus and acting as homo- and heterodimeric DNA binding complexes, is also responsible for the upregulation of *SOD1* expression through the PI3K/Akt pathway (Miao and St. Clair, 2009).

The AP-1 (Activate protein 1, a homo- or heterodimeric TF made by proteins from Jun, Fos, and Maf subfamilies) and TRs (Thyroid Hormone Receptors) proteins are instead responsible for the downregulation of this gene. AP-1 repression of gene transcription occurs by sequestering essential coactivators, such as Sp1, rather than interacting directly with *SOD1* gene promoter; while the direct interaction between TRs and the thyroid hormone inhibitory element at position -157 to +17 of the *SOD1* gene promoter is responsible for the downregulation (Milani et al., 2011).

II.5 SOD1 protein structure

Human SOD1 is a 32-kDa homodimeric enzyme in which each subunit holds one copper and one zinc binding site in close proximity and an intramolecular disulfide bond between Cys57 and Cys146 that further stabilizes the enzyme (Figure 1). SOD1 monomer is made by eight stranded anti-parallel Greek-key β-barrel, with a hydrophobic inner core that constitutes half of the protein backbone and seven connecting loops, with loop IV (residues 49−83) and loop VII (residues 121−142) being functionally important (Sheng et al., 2014; Wright et al., 2019).

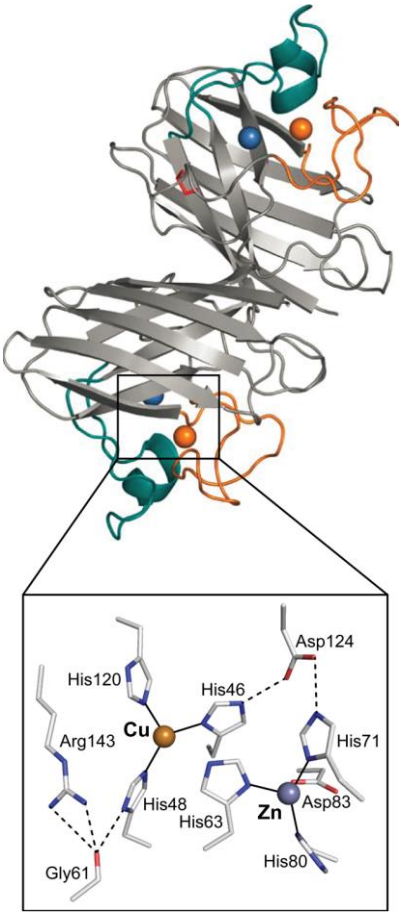

Figure 1. *SOD1 structure, focus on the metal binding sites (from Sheng et al., 2014).*

Loop IV or zinc loop contains all four zinc-binding residues and Cys57, while the loop VII or electrostatic loop holds most of the second-sphere active site residues including the catalytically important Arg143. These two loops create both the active site and the electrostatic forces in and beyond the active site channel that speed diffusion of superoxide towards the positively charged copper, zinc and Arg143 in the correct orientation to maximize productive interactions (Getzoff et al., 1983).

The zinc site is tetrahedrally coordinated via three histidine ligands (His63, His71, His80) and one aspartate residue (Asp83); while the copper coordination environment varies upon copper oxidation state in the active site. In its reduced form it is ligated by His46, His48 and His120 in a nearly trigonal planar geometry; upon oxidation the imidazolate side chain of His63 bridges the oxidized copper and zinc ions. In addition to His63, the copper ion also binds a water molecule and becomes five-coordinate in

a distorted square pyramidal geometry, while the zinc ion retains the tetrahedral coordination geometry as in the reduced form of the enzyme (M. Fetherolf et al., 2017; Sheng et al., 2014).

Asp124 and Arg143 are other two key residues: the first links the two metal-binding sites via hydrogen bonds with His46 and His71; while the second not only is linked to copper ligand His48 through hydrogen bonds with Gly61, but also forms a hydrogen bond with Cys57, involved in the disulfide intramonomer bridge (Sheng et al., 2014).

The fully metallated, disulfide oxidized SOD1 is an extraordinary stable enzyme with a melting temperature of 92 °C and it remains folded in denaturating circumstances, like 8M urea or 1% SDS (Roe et al., 1988; Valentine et al., 2005). Metal ions removal (apoprotein) drastically reduces the melting temperature to 54 °C and the disulfide reduced apo-protein results in a less stable form, that melts at 42 °C (Sheng et al., 2014).

The disulfide reduced apo-protein is predominantly found in the monomeric state, while zinc addition or disulfide bond formation favors the dimerization, underlying the importance of both metallation state and intrasubunit disulfide bond (M. Fetherolf et al., 2017). These post-translational modifications strongly influenced SOD1 monomer-dimer equilibrium, making copper and zinc acquisition together with disulfide bond formation the key events for SOD1 maturation.

II.6 SOD1 protein activation

Human SOD1 requires several post-translational modifications for its activation, that are called maturation reactions and include acetylation of the N-terminus, insertion of copper and zinc ions, intramolecular disulfide formation and dimerization.

The non-redox active metal zinc is the second most abundant trace metal and it is widely used as a cofactor in proteins. The total intracellular zinc concentrations are 10^5-10^8 molecules per cell, but the “free” zinc pool may be quite low due to the high abundance of zinc metalloproteins (M. Fetherolf et al., 2017). Its uptake occurs without the need of a chaperone and may be the first SOD1 maturation event (Banci et al., 2013).

In unfolded SOD1 most of the His residues, and not only the ligands in the two metal-binding sites, are sensitive to addition of zinc ions. The initial binding of zinc to the protein occurs via a diffuse coordination, which in turn suggests that the ligands need to be rearranged during the course of the folding process to reach the native metal-bound state. In fact, zinc catalyses protein folding by binding transiently to the SOD1 $Cu^{2+}/^{1+}$ ligands and, once folding is completed, the zinc ion is transferred to the thermodynamically favourable position in the zinc site (Szpryngiel et al., 2015).

The other metal cofactor, copper, enters the cells via copper transporters with low affinity or high affinity, like Ctr1, and its incorporation into SOD1 occurs via a copper chaperon for SOD1 (CCS) dependent pathway and a CCS independent one.

CCS is a 27 kDa protein primarily localized in the cytoplasm and in the mitochondrial intermembrane space and it consists of three distinct domains. The N-terminal domain or domain 1 (D1) harboring the copper-binding motif MXCXXC is responsible for metal binding, delivery and transfer to SOD1 (Banci et al., 2013). The SOD1-like domain or domain 2 (D2) is made of an eight-stranded anti-parallel β-barrel domain homologous to SOD1 and is critical for SOD1-CCS interaction (Furukawa and O'Halloran, 2006; Lamb et al., 1999). Domain 3 (D3) is a short polypeptide with a conserved CXC motif and it is also called activation domain, since its deletion or mutation impairs SOD1 activation (M. Fetherolf et al., 2017). CCS complexes with SOD1 through D2 and it transfers copper via D1, with D3 involved in disulfide bond formation in an oxygen-dependent manner, evidencing that only disulfide-reduced SOD1 monomer are able to interact with CCS (Sheng et al., 2014). CCS is able to activate the disulfide-reduced, apoprotein; however the already zinc-bound form acquires copper rapidly from CCS, suggesting that the zinc binding is a necessary step prior to copper incorporation (Banci et al., 2012).

Human SOD1 can acquire copper also through a CCS-independent pathway, involving reduced glutathione (GSH), having copper delivered into SOD1 by Cu^{1+}-GSH complexes (Carroll et al., 2004). In fact, deletion of γ-glutamyl cysteine synthase 1 results in impaired SOD1 activation in the absence of CCS (M. Fetherolf et al., 2017).

The SOD1 intramonomer disulfide bond is critical for its enzymatic activity, since SOD1 mutants lacking one of the disulfide cysteine possess limited catalytical activity

(Sea et al., 2015). Disulfide bonds are often present in proteins to confer them stability, but it is rare to find them in such reducing environment like cytosol. For SOD1, predominantly a cytosolic protein, copper, CCS and oxygen are required for an efficient disulfide bond formation as seen by Banci and colleagues on *in vivo* NMR analysis (Banci et al., 2013). In details co-expression of human CCS with human SOD1 in HEK293T cells in zinc-supplemented media resulted in a copper deficient SOD1, bound to zinc and with ~50% oxidized disulfide bond; the complete disulfide formation was observed after the cells were incubated with copper (Banci et al., 2013). It is important to underline the role of oxygen in SOD1 maturation, since copper transfer and disulfide formation are facilitated in the presence of oxygen and a prolonged incubation of wild-type SOD1 under anaerobic conditions led to a loss of enzymatic activity (Leitch et al., 2009; M. Fetherolf et al., 2017).

II.7 SOD1 catalytic function

The antioxidant SOD1 enzyme, like the other isoforms of this family, is responsible for the superoxide anion dismutation, a process linked to the redox properties of the copper ion located in the active site. The dismutation mechanism takes place in two steps: first one molecule of superoxide anion binds to Cu(II)-SOD1, reducing the Cu^{2+} center and forming oxygen (step 1); then a second superoxide anion equivalent reacts with Cu(I)-SOD1, resulting in oxidation of Cu^{+} ion and formation of hydrogen peroxide (step 2).

Step 1: $Cu^{2+}ZnSOD + O_2^{\bullet -} \rightarrow Cu^{+}ZnSOD + O_2$

Step 2: $Cu^{+}ZnSOD + O_2^{\bullet -} + 2H^{+} \rightarrow Cu^{2+}ZnSOD + H_2O_2$

The first half-reaction is not affected by pH independently from the presence or the absence of a metal ion in the zinc site; while step 2 is strongly pH dependent, with a strong reduction in activity at pH > 6 in the absence of a metal in the zinc site (Sheng et al., 2014).

Superoxide anion is electrostatically guided into the active site by Arg143 that sits on the active site lid, as demonstrated by an order of magnitude drop in the rate constant upon the Arg143 positive charge neutralization (Fisher et al., 1994). Moreover, two protons are required for the disproportionation process and the structural change upon

reduction of Cu^{2+} to Cu^{+} demonstrates delivery of the first proton to the active site in this process (Sheng et al., 2014).

The rates of the two half reactions are both nearly diffusion-controlled, with an overall constant rate of about 2×10^9 M^{-1} s^{-1} and the catalysis is largely unaffected by pH changes in the range 5-9.5 (Klug et al., 1972; Valentine et al., 2005).

This enzyme has been traditionally characterized as a reactive oxygen scavenging mechanism, however only a small fraction of cellular SOD1 is necessary for this role, leading to possible alternatives functions considering the fact that this protein is one of the most abundant in eukaryotic cell.

II.8 SOD1 in amyotrophic lateral sclerosis

SOD1 has been the first gene found mutated in amyotrophic lateral sclerosis (ALS), a fatal progressive neurodegenerative disease firstly described by the French scientist and physician Jean-Martin Charcot in 1869 (Rosen et al., 1993).

ALS is characterized by the loss of both upper and lower motor neurons in the brain and in the spinal cord, causing progressive muscle atrophy, paralysis and eventually death. The primary symptoms are associated with motor dysfunction, like muscle weakness, atrophy, spasticity and dysphagia, even if they can vary among the patients: some present spinal-onset disease (weakness in the muscle of the limbs), while one-third of patients shows bulbar-onset disease, characterized by dysarthria (difficulty with speech) and dysphagia (difficulty swallowing). Up to 50% of patients develops cognitive and/or behavioural impairment during the course of disease, and 13% of patients presents concomitant behavioural variant frontotemporal dementia (FTD) (Hardiman et al., 2017). ALS worldwide incidence is between 0.6 and 3.8 per 100,000 individuals and differs based on ancestral origin, with populations of European origin showing the higher incidence (2.1 to 3.8 per 100,000 individuals) (Benjaminsen et al., 2018; Chiò et al., 2013; Logroscino et al., 2010; Longinetti and Fang, 2019; Marin et al., 2014; Palese et al., 2019). Moreover, areas having different ancestral populations living in close proximity, such as North America, possess a lower ALS incidence (0.63 cases per 100,000 individuals) compared to regions characterised by a quite homogeneous population, like Faroe Islands or Scotland (2.6 to 3.8 cases per 100,000 individuals) (Gordon et al., 2013; Joensen, 2012; Leighton et al., 2019).

The age of onset is between 51 and 66 years, a quite wide range since patients in Europe have a later age of onset compared to China, Cuba and Uruguay; while the mean survival time from symptoms onset to death or invasive respiratory support is 24 to 50 months, with a male-to-female ratio between 1 and 2 (Longinetti and Fang, 2019). Although its classification depends on the criteria used, ALS can be divided into two groups depending on whether or not there is a family history of the disease: about 10% of all ALS cases are considered familial (fALS), due to genetic mutations inherited from a family member, while the remaining 90% are considered sporadic (sALS), probably caused by a combination of environmental and genetic risk factors. 20% of fALS and the 3% of sALS cases are associated with mutations in *SOD1* gene, with over 180 different mutations throughout the five exons; the majority of which are missense point mutations resulting in a dominant mode of inheritance causing more than 160 disease associated variations spread over the entire 154 amino acid sequence (Huai and Zhang, 2019; Kaur et al., 2016). Among SOD1 mutations, the most common is the D90A (aspartic acid 90 to alanine), inherited both as a dominant and a recessive trait, though the recessive one happens in the majority of cases. The A4V (alanine 4 to valine) mutation is only found in the USA and it is the most common, being present in 50% of SOD1 linked fALS; while the most famous one is the G93A (glycine 93 to alanine), a relatively rare pseudo-wild-type mutation, with the enzymatic activity undamaged and the first SOD1 mutated transgenic mouse model (Kaur et al., 2016).

SOD1 mutations in ALS are predominantly single amino acid substitutions, although deletions, insertions, and C-terminal truncations can also occur; SOD1 mutants can be classified into two groups based on their position in the protein: the "wild-type like" and the "metal binding region" mutants (Hayward et al., 2002). The "wild-type like" mutants present mutations scattered throughout the β-barrel structure and zinc levels similar to wild-type SOD1; while the "metal binding region" mutants possess a very low zinc and copper content since the mutations affect the metal binding ligands themselves or elements intimately associated with metal binding (Sirangelo and Iannuzzi, 2017).

Independently form the type of mutation, experimental studies on SOD1 mutants have shown an accumulation of SOD1-rich proteinaceous aggregates in the spinal cord,

suggesting a toxic mechanism exerted through a gain of function rather than to a loss of function, even if the enzymatic activity decreases of about 50-80% compared to wild type protein (Borchelt et al., 1994; Kaur et al., 2016). In fact, most ALS-associated mutations have the greatest effect on the immature form of SOD1, destabilizing the metal-free and disulfide-reduced polypeptide to the point that it becomes unfolded at physiological temperatures (Furukawa and O'Halloran, 2005). An improper protein maturation can make the two aggregation prone segments in the C terminus (residues 101-107 and 147-153) available for interaction and alterations in the surface hydrophobicity, with increased exposure of the hydrophobic surfaces, induce the formation of high molecular weight SOD1 species with lowered solubility (Ivanova et al., 2014; Lin et al., 2013). Additionally, demetallation and aberrant metal binding promote misfolding and aggregation in SOD1, suggesting a possible key role of metal binding in SOD1 pathological aggregation (Sirangelo and Iannuzzi, 2017). Heterodimerization seems also to increase the stability of SOD1 mutants, since different studies in mice have shown that co-expression of wild-type and mutants accelerates the progress of the disease; moreover, the more stable the heterodimer, the shorter is the survival time of patients with fALS (Araujo Eleutherio et al., 2020).

It is important to note that SOD1 aggregates occur not only in neurons, but also in the glial cells surrounding the motor neuron; misfolded SOD1 mutant protein within microglial cells and astrocytes, together with their activation in response to neuronal damage, can cause inflammation and this causes an increased release of toxic factors, causing a more rapid disease progression (Kaur et al., 2016). In addition, Urushitani and collaborators have shown the interaction between mutant SOD1 and chromogranins, components of neurosecretory vesicles and neuroendocrine system, that may act as chaperone-like proteins helping mutant SOD1 secretion by motor neurons and astrocytes (Urushitani et al., 2006). Finally, several studies have demonstrated that SOD1 participates in cell-to-cell propagation of aggregates, suggesting a "prion-like behaviour" as a key mechanism underlying the aggregation and spreading of misfolded proteins (Pansarasa et al., 2018).

References

Akesson, A., Berglund, M., Schütz, A., Bjellerup, P., Bremme, K., Vahter, M., 2002. Cadmium exposure in pregnancy and lactation in relation to iron status. Am. J. Public Health 92, 284–287. https://doi.org/10.2105/ajph.92.2.284

Al-Ghafari, A., Elmorsy, E., Fikry, E., Alrowaili, M., Carter, W.G., 2019. The heavy metals lead and cadmium are cytotoxic to human bone osteoblasts via induction of redox stress. PLoS One 14, e0225341. https://doi.org/10.1371/journal.pone.0225341

Araujo Eleutherio, E.C., Silva Magalhães, R.S., de Araújo Brasil, A., Monteiro Neto, J.R., de Holanda Paranhos, L., 2020. SOD1, more than just an antioxidant. Arch. Biochem. Biophys. 697, 108701. https://doi.org/10.1016/j.abb.2020.108701

Banci, L., Barbieri, L., Bertini, I., Luchinat, E., Secci, E., Zhao, Y., Aricescu, A.R., 2013. Atomic-resolution monitoring of protein maturation in live human cells by NMR. Nat. Chem. Biol. 9, 297–299. https://doi.org/10.1038/nchembio.1202

Banci, L., Bertini, I., Cantini, F., Kozyreva, T., Massagni, C., Palumaa, P., Rubino, J.T., Zovo, K., 2012. Human superoxide dismutase 1 (hSOD1) maturation through interaction with human copper chaperone for SOD1 (hCCS). Proc. Natl. Acad. Sci. 109, 13555–13560. https://doi.org/10.1073/pnas.1207493109

Bannister, W.H., Bannister, J. V., Barra, D., Bond, J., Bossa, F., 1991. Evolutionary aspects of superoxide dismutase: The copper/zinc enzyme. Free Radic. Res. 12, 349–361. https://doi.org/10.3109/10715769109145804

Benjaminsen, E., Alstadhaug, K.B., Gulsvik, M., Baloch, F.K., Odeh, F., 2018. Amyotrophic lateral sclerosis in Nordland county, Norway, 2000-2015: prevalence, incidence, and clinical features. Amyotroph. Lateral Scler. Frontotemporal Degener. 19, 522–527. https://doi.org/10.1080/21678421.2018.1513534

Berglund, M., Akesson, A., Nermell, B., Vahter, M., 1994. Intestinal absorption of dietary cadmium in women depends on body iron stores and fiber intake. Environ. Health Perspect. 102, 1058–1066. https://doi.org/10.1289/ehp.941021058

Bhattacharyya, M.H., 2009. Cadmium osteotoxicity in experimental animals: mechanisms and relationship to human exposures. Toxicol. Appl. Pharmacol.

238, 258–265. https://doi.org/10.1016/j.taap.2009.05.015

Borchelt, D.R., Lee, M.K., Slunt, H.S., Guarnieri, M., Xu, Z.S., Wong, P.C., Brown, R.H.J., Price, D.L., Sisodia, S.S., Cleveland, D.W., 1994. Superoxide dismutase 1 with mutations linked to familial amyotrophic lateral sclerosis possesses significant activity. Proc. Natl. Acad. Sci. U. S. A. 91, 8292–8296. https://doi.org/10.1073/pnas.91.17.8292

Bordo, D., Djinovic, K., Bolognesi, M., 1994. Conserved Patterns in the Cu,Zn Superoxide Dismutase Family. J. Mol. Biol. 238, 366–386. https://doi.org/10.1006/JMBI.1994.1298

Branca, J.J.V., Fiorillo, C., Carrino, D., Paternostro, F., Taddei, N., Gulisano, M., Pacini, A., Becatti, M., 2020. Cadmium-induced oxidative stress: Focus on the central nervous system. Antioxidants 9, 1–21. https://doi.org/10.3390/antiox9060492

Bridgen, J., Harris, J.I., Northrop, F., 1975. Evolutionary relationships in superoxide dismutase. FEBS Lett. 49, 392–395.

Cadenas, E., Davies, K.J.A., 2000. Mitochondrial free radical generation, oxidative stress, and aging. Free Radic. Biol. Med. 29, 222–230. https://doi.org/10.1016/S0891-5849(00)00317-8

Carrico, R.J., Deutsch, H.F., 1970. The presence of zinc in human cytocuprein and some properties of the apoprotein. J. Biol. Chem. 245, 723–727.

Carroll, M.C., Girouard, J.B., Ulloa, J.L., Subramaniam, J.R., Wong, P.C., Valentine, J.S., Culotta, V.C., 2004. Mechanisms for activating Cu- and Zn-containing superoxide dismutase in the absence of the CCS Cu chaperone. Proc. Natl. Acad. Sci. U. S. A. 101, 5964–5969. https://doi.org/10.1073/pnas.0308298101

Casalino, E., Sblano, C., Landriscina, C., 1997. Enzyme activity alteration by cadmium administration to rats: the possibility of iron involvement in lipid peroxidation. Arch. Biochem. Biophys. 346, 171–179. https://doi.org/10.1006/abbi.1997.0197

Case, A.J., 2017. On the origin of superoxide dismutase: An evolutionary perspective of superoxide-mediated redox signaling. Antioxidants 6. https://doi.org/10.3390/antiox6040082

Chiò, A., Logroscino, G., Traynor, B.J., Collins, J., Simeone, J.C., Goldstein, L.A.,

White, L.A., 2013. Global epidemiology of amyotrophic lateral sclerosis: a systematic review of the published literature. Neuroepidemiology 41, 118–130. https://doi.org/10.1159/000351153

Choudhuri, S., Liu, W.L., Berman, N.E., Klaassen, C.D., 1996. Cadmium accumulation and metallothionein expression in brain of mice at different stages of development. Toxicol. Lett. 84, 127–133. https://doi.org/10.1016/0378-4274(95)03444-7

Chow, E.S.H., Hui, M.N.Y., Lin, C.C., Cheng, S.H., 2008. Cadmium inhibits neurogenesis in zebrafish embryonic brain development. Aquat. Toxicol. 87, 157–169. https://doi.org/https://doi.org/10.1016/j.aquatox.2008.01.019

Cuypers, A., Plusquin, M., Remans, T., Jozefczak, M., Keunen, E., Gielen, H., Opdenakker, K., Nair, A.R., Munters, E., Artois, T.J., Nawrot, T., Vangronsveld, J., Smeets, K., 2010. Cadmium stress: an oxidative challenge. Biometals an Int. J. role Met. ions Biol. Biochem. Med. 23, 927–940. https://doi.org/10.1007/s10534-010-9329-x

Dudley, R.E., Klaassen, C.D., 1984. Changes in hepatic glutathione concentration modify cadmium-induced hepatotoxicity. Toxicol. Appl. Pharmacol. 72, 530–538. https://doi.org/10.1016/0041-008x(84)90130-3

Faroon, O., Ashizawa, A., Wright, S., Tucker, P., Jenkins, K., Ingerman, L., Rudisill, C., 2012. Toxicological Profile for Cadmium, Agency for Toxic Substances and Disease Registry (ATSDR) Toxicological Profiles. Agency for Toxic Substances and Disease Registry (US), Atlanta (GA).

Fisher, C.L., Cabelli, D.E., Tainer, J.A., Hallewell, R.A., Getzoff, E.D., 1994. The role of arginine 143 in the electrostatics and mechanism of Cu,Zn superoxide dismutase: computational and experimental evaluation by mutational analysis. Proteins 19, 24–34. https://doi.org/10.1002/prot.340190105

Furukawa, Y., O'Halloran, T. V, 2006. Posttranslational modifications in Cu,Zn-superoxide dismutase and mutations associated with amyotrophic lateral sclerosis. Antioxid. Redox Signal. 8, 847–867. https://doi.org/10.1089/ars.2006.8.847

Furukawa, Y., O'Halloran, T. V, 2005. Amyotrophic lateral sclerosis mutations have the greatest destabilizing effect on the apo- and reduced form of SOD1, leading

to unfolding and oxidative aggregation. J. Biol. Chem. 280, 17266–17274. https://doi.org/10.1074/jbc.M500482200

Gasche, Y., Copin, J.C., Sugawara, T., Fujimura, M., Chan, P.H., 2001. Matrix metalloproteinase inhibition prevents oxidative stress-associated blood-brain barrier disruption after transient focal cerebral ischemia. J. Cereb. blood flow Metab. Off. J. Int. Soc. Cereb. Blood Flow Metab. 21, 1393–1400. https://doi.org/10.1097/00004647-200112000-00003

Genchi, G., Sinicropi, M.S., Lauria, G., Carocci, A., Catalano, A., 2020. The Effects of Cadmium Toxicity. Int. J. Environ. Res. Public Health 17. https://doi.org/10.3390/ijerph17113782

Getzoff, E.D., Tainer, J.A., Weiner, P.K., Kollman, P.A., Richardson, J.S., Richardson, D.C., 1983. Electrostatic recognition between superoxide and copper, zinc superoxide dismutase. Nature 306, 287–290. https://doi.org/10.1038/306287a0

Gordon, P.H., Mehal, J.M., Holman, R.C., Rowland, L.P., Rowland, A.S., Cheek, J.E., 2013. Incidence of amyotrophic lateral sclerosis among American Indians and Alaska natives. JAMA Neurol. 70, 476–480. https://doi.org/10.1001/jamaneurol.2013.929

Gupta, A., Shukla, G.S., 1996. Ontogenic profile of brain lipids following perinatal exposure to cadmium. J. Appl. Toxicol. 16, 227–233. https://doi.org/10.1002/(SICI)1099-1263(199605)16:3<227::AID-JAT337>3.0.CO;2-5

Hardiman, O., Al-Chalabi, A., Chio, A., Corr, E.M., Logroscino, G., Robberecht, W., Shaw, P.J., Simmons, Z., Van Den Berg, L.H., 2017. Amyotrophic lateral sclerosis. Nat. Rev. Dis. Prim. 3. https://doi.org/10.1038/nrdp.2017.71

Hayward, L.J., Rodriguez, J.A., Kim, J.W., Tiwari, A., Goto, J.J., Cabelli, D.E., Valentine, J.S., Brown, R.H.J., 2002. Decreased metallation and activity in subsets of mutant superoxide dismutases associated with familial amyotrophic lateral sclerosis. J. Biol. Chem. 277, 15923–15931. https://doi.org/10.1074/jbc.M112087200

Holland, H.D., 2006. The oxygenation of the atmosphere and oceans. Philos. Trans. R. Soc. B Biol. Sci. 361, 903–915. https://doi.org/10.1098/rstb.2006.1838

Holland, H.D., 2002. Volcanic gases, black smokers, and the great oxidation event. Geochim. Cosmochim. Acta 66, 3811–3826. https://doi.org/10.1016/S0016-7037(02)00950-X

Huai, J., Zhang, Z., 2019. Structural properties and interaction partners of familial ALS-associated SOD1 mutants. Front. Neurol. 10, 1–5. https://doi.org/10.3389/fneur.2019.00527

IARC, 2012. TOXICOLOGICAL PROFILE FOR CADMIUM. U.S. Dep. Heal. Hum. Serv. Public Heal. Serv. Agency ToxicSubstances Dis. Regist.

Ivanova, M.I., Sievers, S.A., Guenther, E.L., Johnson, L.M., Winkler, D.D., Galaleldeen, A., Sawaya, M.R., Hart, P.J., Eisenberg, D.S., 2014. Aggregation-triggering segments of SOD1 fibril formation support a common pathway for familial and sporadic ALS. Proc. Natl. Acad. Sci. U. S. A. 111, 197–201. https://doi.org/10.1073/pnas.1320786110

Järup, L., 2003. Hazards of heavy metal contamination. Br. Med. Bull. 68, 167–182. https://doi.org/10.1093/bmb/ldg032

Järup, L., Åkesson, A., 2009. Current status of cadmium as an environmental health problem. Toxicol. Appl. Pharmacol. 238, 201–208. https://doi.org/10.1016/j.taap.2009.04.020

Joensen, P., 2012. Incidence of amyotrophic lateral sclerosis in the Faroe Islands. Acta Neurol. Scand. 126, 62–66. https://doi.org/10.1111/j.1600-0404.2011.01611.x

Karri, V., Schuhmacher, M., Kumar, V., 2016. Heavy metals (Pb, Cd, As and MeHg) as risk factors for cognitive dysfunction: A general review of metal mixture mechanism in brain. Environ. Toxicol. Pharmacol. 48, 203–213. https://doi.org/10.1016/j.etap.2016.09.016

Kaur, S.J., McKeown, S.R., Rashid, S., 2016. Mutant SOD1 mediated pathogenesis of Amyotrophic Lateral Sclerosis. Gene 577, 109–118. https://doi.org/10.1016/j.gene.2015.11.049

Kim, Y.H., Park, K.H., Rho, H.M., 1996. Transcriptional activation of the Cu,Zn-superoxide dismutase gene through the AP2 site by ginsenoside Rb2 extracted from a medicinal plant, Panax ginseng. J. Biol. Chem. 271, 24539–24543. https://doi.org/10.1074/jbc.271.40.24539

Klug, D., Rabani, J., Fridovich, I., 1972. A direct demonstration of the catalytic action

of superoxide dismutase through the use of pulse radiolysis. J. Biol. Chem. 247, 4839–4842.

Kumar, R., Agarwal, A.K., Seth, P.K., 1996. Oxidative stress-mediated neurotoxicity of cadmium. Toxicol. Lett. 89, 65–69. https://doi.org/10.1016/s0378-4274(96)03780-0

Lamb, A.L., Wernimont, A.K., Pufahl, R.A., Culotta, V.C., O'Halloran, T. V, Rosenzweig, A.C., 1999. Crystal structure of the copper chaperone for superoxide dismutase. Nat. Struct. Biol. 6, 724–729. https://doi.org/10.1038/11489

Leighton, D.J., Newton, J., Stephenson, L.J., Colville, S., Davenport, R., Gorrie, G., Morrison, I., Swingler, R., Chandran, S., Pal, S., 2019. Changing epidemiology of motor neurone disease in Scotland. J. Neurol. 266, 817–825. https://doi.org/10.1007/s00415-019-09190-7

Leitch, J.M., Jensen, L.T., Bouldin, S.D., Outten, C.E., Hart, P.J., Culotta, V.C., 2009. Activation of Cu,Zn-superoxide dismutase in the absence of oxygen and the copper chaperone CCS. J. Biol. Chem. 284, 21863–21871. https://doi.org/10.1074/jbc.M109.000489

Lin, P.-Y., Simon, S.M., Koh, W.K., Folorunso, O., Umbaugh, C.S., Pierce, A., 2013. Heat shock factor 1 over-expression protects against exposure of hydrophobic residues on mutant SOD1 and early mortality in a mouse model of amyotrophic lateral sclerosis. Mol. Neurodegener. 8, 43. https://doi.org/10.1186/1750-1326-8-43

Logroscino, G., Traynor, B.J., Hardiman, O., Chiò, A., Mitchell, D., Swingler, R.J., Millul, A., Benn, E., Beghi, E., 2010. Incidence of amyotrophic lateral sclerosis in Europe. J. Neurol. Neurosurg. Psychiatry 81, 385–390. https://doi.org/10.1136/jnnp.2009.183525

Longinetti, E., Fang, F., 2019. Epidemiology of amyotrophic lateral sclerosis: An update of recent literature. Curr. Opin. Neurol. 32, 771–776. https://doi.org/10.1097/WCO.0000000000000730

M. Fetherolf, M., Boyd, S.D., Winkler, D.D., Winge, D.R., 2017. Oxygen-dependent activation of Cu,Zn-superoxide dismutase-1. Metallomics 9, 1047–1059. https://doi.org/10.1039/C6MT00298F

Mancuso, R., Navarro, X., 2015. Amyotrophic lateral sclerosis: Current perspectives from basic research to the clinic. Prog. Neurobiol. 133, 1–26. https://doi.org/10.1016/j.pneurobio.2015.07.004

Marin, B., Hamidou, B., Couratier, P., Nicol, M., Delzor, A., Raymondeau, M., Druet-Cabanac, M., Lautrette, G., Boumediene, F., Preux, P.M., 2014. Population-based epidemiology of amyotrophic lateral sclerosis (ALS) in an ageing Europe--the French register of ALS in Limousin (FRALim register). Eur. J. Neurol. 21, 1292–300, e78-9. https://doi.org/10.1111/ene.12474

McCord, J.M., Fridovich, I., 1969. Superoxide Dismutase. J. Biol. Chem. 244, 6049–6055.

Méndez-Armenta, M., Ríos, C., 2007. Cadmium neurotoxicity. Environ. Toxicol. Pharmacol. 23, 350–358. https://doi.org/10.1016/j.etap.2006.11.009

Mezynska, M., Brzóska, M.M., 2018. Environmental exposure to cadmium—a risk for health of the general population in industrialized countries and preventive strategies. Environ. Sci. Pollut. Res. 25, 3211–3232. https://doi.org/10.1007/s11356-017-0827-z

Miao, L., St. Clair, D.K., 2009. Regulation of superoxide dismutase genes: Implications in disease. Free Radic. Biol. Med. 47, 344–356. https://doi.org/10.1016/j.freeradbiomed.2009.05.018

Milani, P., Gagliardi, S., Cova, E., Cereda, C., 2011. SOD1 transcriptional and posttranscriptional regulation and its potential implications in ALS. Neurol. Res. Int. 2011. https://doi.org/10.1155/2011/458427

Minami, A., Takeda, A., Nishibaba, D., Takefuta, S., Oku, N., 2001. Cadmium toxicity in synaptic neurotransmission in the brain. Brain Res. 894, 336–339. https://doi.org/10.1016/s0006-8993(01)02022-4

Minc, E., De Coppet, P., Masson, P., Thiery, L., Dutertre, S., Amor-Guéret, M., Jaulin, C., 1999. The human copper-zinc superoxide dismutase gene (SOD1) proximal promoter is regulated by Sp1, Egr-1, and WT1 via non-canonical binding sites. J. Biol. Chem. 274, 503–509. https://doi.org/10.1074/jbc.274.1.503

Monteiro, C., Ferreira de Oliveira, J.M.P., Pinho, F., Bastos, V., Oliveira, H., Peixoto, F., Santos, C., 2018. Biochemical and transcriptional analyses of cadmium-

induced mitochondrial dysfunction and oxidative stress in human osteoblasts. J. Toxicol. Environ. Heal. Part A 81, 705–717. https://doi.org/10.1080/15287394.2018.1485122

Murphy, M.P., 2009. How mitochondria produce reactive oxygen species. Biochem. J. 417, 1–13. https://doi.org/10.1042/BJ20081386

Nair, A.R., DeGheselle, O., Smeets, K., Van Kerkhove, E., Cuypers, A., 2013. Cadmium-induced pathologies: Where is the oxidative balance lost (or not)? Int. J. Mol. Sci. 14, 6116–6143. https://doi.org/10.3390/ijms14036116

Nawrot, T.S., Staessen, J.A., Roels, H.A., Munters, E., Cuypers, A., Richart, T., Ruttens, A., Smeets, K., Clijsters, H., Vangronsveld, J., 2010. Cadmium exposure in the population: From health risks to strategies of prevention. BioMetals 23, 769–782. https://doi.org/10.1007/s10534-010-9343-z

Nielsen, A.E., Bohr, A., Penkowa, M., 2007. The Balance between Life and Death of Cells: Roles of Metallothioneins. Biomark. Insights 1, 99–111.

Nordberg, G.F., 2009. Historical perspectives on cadmium toxicology. Toxicol. Appl. Pharmacol. 238, 192–200. https://doi.org/10.1016/j.taap.2009.03.015

Och, L.M., Shields-Zhou, G.A., 2012. The Neoproterozoic oxygenation event: Environmental perturbations and biogeochemical cycling. Earth-Science Rev. 110, 26–57. https://doi.org/10.1016/j.earscirev.2011.09.004

Oggiano, R., Pisano, A., Sabalic, A., Farace, C., Fenu, G., Lintas, S., Forte, G., Bocca, B., Madeddu, R., 2020. An overview on amyotrophic lateral sclerosis and cadmium. Neurol. Sci. https://doi.org/10.1007/s10072-020-04957-7

Okuda, B., Iwamoto, Y., Tachibana, H., Sugita, M., 1997. Parkinsonism after acute cadmium poisoning. Clin. Neurol. Neurosurg. 99, 263–265. https://doi.org/10.1016/s0303-8467(97)00090-5

Olsson, I.-M., Bensryd, I., Lundh, T., Ottosson, H., Skerfving, S., Oskarsson, A., 2002. Cadmium in blood and urine--impact of sex, age, dietary intake, iron status, and former smoking--association of renal effects. Environ. Health Perspect. 110, 1185–1190. https://doi.org/10.1289/ehp.021101185

Pal, R., Nath, R., Gill, K.D., 1993. Influence of ethanol on cadmium accumulation and its impact on lipid peroxidation and membrane bound functional enzymes (Na+, K(+)-ATPase and acetylcholinesterase) in various regions of adult rat

brain. Neurochem. Int. 23, 451–458. https://doi.org/10.1016/0197-0186(93)90129-s

Palese, F., Sartori, A., Verriello, L., Ros, S., Passadore, P., Manganotti, P., Barbone, F., Pisa, F.E., 2019. Epidemiology of amyotrophic lateral sclerosis in Friuli-Venezia Giulia, North-Eastern Italy, 2002-2014: a retrospective population-based study. Amyotroph. Lateral Scler. Frontotemporal Degener. 20, 90–99. https://doi.org/10.1080/21678421.2018.1511732

Pansarasa, O., Bordoni, M., Diamanti, L., Sproviero, D., Gagliardi, S., Cereda, C., 2018. Sod1 in amyotrophic lateral sclerosis: "ambivalent" behavior connected to the disease. Int. J. Mol. Sci. 19, 1–13. https://doi.org/10.3390/ijms19051345

Parge, H.E., Hallewellt, R.A., Tainer, J.A., 1992. Atomic structures of wild-type and thermostable mutant recombinant human Cu,Zn superoxide dismutase (hydrogen bonds/protein design/helix dipole/metafloenzyme/protein conformation). Proc. Natl. Acad. Sci. USA 89, 6109–6113.

Rani, A., Kumar, A., Lal, A., Pant, M., 2014. Cellular mechanisms of cadmium-induced toxicity: A review. Int. J. Environ. Health Res. 24, 378–399. https://doi.org/10.1080/09603123.2013.835032

Reyes-Hinojosa, D., Lozada-Pérez, C.A., Zamudio Cuevas, Y., López-Reyes, A., Martínez-Nava, G., Fernández-Torres, J., Olivos-Meza, A., Landa-Solis, C., Gutiérrez-Ruiz, M.C., Rojas del Castillo, E., Martínez-Flores, K., 2019. Toxicity of cadmium in musculoskeletal diseases. Environ. Toxicol. Pharmacol. 72, 103219. https://doi.org/10.1016/j.etap.2019.103219

Roe, J.A., Butler, A., Scholler, D.M., Valentine, J.S., Marky, L., Breslauer, K.J., 1988. Differential scanning calorimetry of Cu,Zn-superoxide dismutase, the apoprotein, and its zinc-substituted derivatives. Biochemistry 27, 950–958. https://doi.org/10.1021/bi00403a017

Rosen, D.R., Siddique, T., Patterson, D., Figlewicz, D.A., Sapp, P., Hentati, A., Donaldson, D., Goto, J., O'Regan, J.P., Deng, H.X., 1993. Mutations in Cu/Zn superoxide dismutase gene are associated with familial amyotrophic lateral sclerosis. Nature 362, 59–62. https://doi.org/10.1038/362059a0

Sabolić, I., Breljak, D., Škarica, M., Herak-Kramberger, C.M., 2010. Role of metallothionein in cadmium traffic and toxicity in kidneys and other mammalian

organs. BioMetals 23, 897–926. https://doi.org/10.1007/s10534-010-9351-z

Sarkar, A., Ravindran, G., Krishnamurthy, V., 2013. a Brief Review on the Effect of Cadmium Toxicity: From Cellular To Organ Level. Int. J. Bio-Technology Res. 3, 2249–6858.

Sarwar, N., Saifullah, Malhi, S.S., Zia, M.H., Naeem, A., Bibi, S., Farid, G., 2010. Role of mineral nutrition in minimizing cadmium accumulation by plants. J. Sci. Food Agric. 90, 925–937. https://doi.org/https://doi.org/10.1002/jsfa.3916

Scandalios, J.G., 1993. Oxygen stress and superoxide dismutases. Plant Physiol. 101, 7–12. https://doi.org/10.1104/pp.101.1.7

Sea, K., Sohn, S.H., Durazo, A., Sheng, Y., Shaw, B.F., Cao, X., Taylor, A.B., Whitson, L.J., Holloway, S.P., Hart, P.J., Cabelli, D.E., Gralla, E.B., Valentine, J.S., 2015. Insights into the role of the unusual disulfide bond in copper-zinc superoxide dismutase. J. Biol. Chem. 290, 2405–2418. https://doi.org/10.1074/jbc.M114.588798

Seo, S.J., Kim, H.T., Cho, G., Rho, H.M., Jung, G., 1996. Spl and C/EBP-related factor regulate the transcription of human Cu/Zn SOD gene. Gene 178, 177–185. https://doi.org/10.1016/0378-1119(96)00383-6

Shahbazian, M.D., Zoghbi, H.Y., 2002. Rett syndrome and MeCP2: linking epigenetics and neuronal function. Am. J. Hum. Genet. 71, 1259–1272. https://doi.org/10.1086/345360

Shawki, A., Knight, P.B., Maliken, B.D., Niespodzany, E.J., Mackenzie, B., 2012. H(+)-coupled divalent metal-ion transporter-1: functional properties, physiological roles and therapeutics. Curr. Top. Membr. 70, 169–214. https://doi.org/10.1016/B978-0-12-394316-3.00005-3

Sheng, Y., Abreu, I.A., Cabelli, D.E., Maroney, M.J., Miller, A.F., Teixeira, M., Valentine, J.S., 2014. Superoxide dismutases and superoxide reductases. Chem. Rev. 114, 3854–3918. https://doi.org/10.1021/cr4005296

Shuba, Y.M., 2014. Models of calcium permeation through T-type channels. Pflügers Arch. - Eur. J. Physiol. 466, 635–644. https://doi.org/10.1007/s00424-013-1437-3

Simonian, N.A., Coyle, J.T., 1996. Oxidative stress in neurodegenerative diseases. Annu. Rev. Pharmacol. Toxicol. 36, 83–106.

https://doi.org/10.1146/annurev.pa.36.040196.000503

Sirangelo, I., Iannuzzi, C., 2017. The role of metal binding in the amyotrophic lateral sclerosis-related aggregation of copper-zinc superoxide dismutase. Molecules 22, 1–13. https://doi.org/10.3390/molecules22091429

Smith, M.W., Doolittle, R.F., 1992. A comparison of evolutionary rates of the two major kinds of superoxide dismutase. J. Mol. Evol. 34, 175–184. https://doi.org/10.1007/BF00182394

Szpryngiel, S., Oliveberg, M., Mäler, L., 2015. Diffuse binding of Zn2+ to the denatured ensemble of Cu/Zn superoxide dismutase 1. FEBS Open Bio 5, 56–63. https://doi.org/10.1016/j.fob.2014.12.003

Templeton, D.M., Liu, Y., 2010. Multiple roles of cadmium in cell death and survival. Chem. Biol. Interact. 188, 267–275. https://doi.org/10.1016/j.cbi.2010.03.040

Thévenod, F., Fels, J., Lee, W.K., Zarbock, R., 2019. Channels, transporters and receptors for cadmium and cadmium complexes in eukaryotic cells: myths and facts. BioMetals 32, 469–489. https://doi.org/10.1007/s10534-019-00176-6

Underly, R.G., Levy, M., Hartmann, D.A., Grant, R.I., Watson, A.N., Shih, A.Y., 2017. Pericytes as Inducers of Rapid, Matrix Metalloproteinase-9-Dependent Capillary Damage during Ischemia. J. Neurosci. 37, 129–140. https://doi.org/10.1523/JNEUROSCI.2891-16.2016

Urushitani, M., Sik, A., Sakurai, T., Nukina, N., Takahashi, R., Julien, J.-P., 2006. Chromogranin-mediated secretion of mutant superoxide dismutase proteins linked to amyotrophic lateral sclerosis. Nat. Neurosci. 9, 108–118. https://doi.org/10.1038/nn1603

Vahter, M., Akesson, A., Lidén, C., Ceccatelli, S., Berglund, M., 2007. Gender differences in the disposition and toxicity of metals. Environ. Res. 104, 85–95. https://doi.org/10.1016/j.envres.2006.08.003

Vahter, M., Berglund, M., Slorach, S., Friberg, L., Sarić, M., Zheng, X., Fujita, M., 1991. Methods for integrated exposure monitoring of lead and cadmium. Environ. Res. 56, 78–89. https://doi.org/https://doi.org/10.1016/S0013-9351(05)80111-2

Valentine, J.S., Doucette, P.A., Zittin Potter, S., 2005. Copper-zinc superoxide dismutase and amyotrophic lateral sclerosis. Annu. Rev. Biochem. 74, 563–593.

https://doi.org/10.1146/annurev.biochem.72.121801.161647

Valko, M., Rhodes, C.J., Moncol, J., Izakovic, M., Mazur, M., 2006. Free radicals, metals and antioxidants in oxidative stress-induced cancer. Chem. Biol. Interact. 160, 1–40. https://doi.org/10.1016/j.cbi.2005.12.009

Wang, B., Du, Y., 2013. Cadmium and its neurotoxic effects. Oxid. Med. Cell. Longev. 2013. https://doi.org/10.1155/2013/898034

Wang, B., Li, Y., Tan, Y., Miao, X., Liu, X.-D., Shao, C., Yang, X.-H., Turdi, S., Ma, L.-J., Ren, J., Cai, L., 2012. Low-dose Cd induces hepatic gene hypermethylation, along with the persistent reduction of cell death and increase of cell proliferation in rats and mice. PLoS One 7, e33853. https://doi.org/10.1371/journal.pone.0033853

Wang, B., Schneider, S.N., Dragin, N., Girijashanker, K., Dalton, T.P., He, L., Miller, M.L., Stringer, K.F., Soleimani, M., Richardson, D.D., Nebert, D.W., 2007. Enhanced cadmium-induced testicular necrosis and renal proximal tubule damage caused by gene-dose increase in a Slc39a8-transgenic mouse line. Am. J. Physiol. Physiol. 292, C1523–C1535. https://doi.org/10.1152/ajpcell.00409.2006

Wang, Y., Fang, J., Leonard, S.S., Rao, K.M.K., 2004. Cadmium inhibits the electron transfer chain and induces reactive oxygen species. Free Radic. Biol. Med. 36, 1434–1443. https://doi.org/10.1016/j.freeradbiomed.2004.03.010

Wong, K.L., Klaassen, C.D., 1982. Neurotoxic effects of cadmium in young rats. Toxicol. Appl. Pharmacol. 63, 330–337. https://doi.org/10.1016/0041-008x(82)90261-7

Wright, G.S.A., Antonyuk, S. V., Hasnain, S.S., 2019. The biophysics of superoxide dismutase-1 and amyotrophic lateral sclerosis. Q. Rev. Biophys. 52, e12. https://doi.org/10.1017/S003358351900012X

Yang, Y., Estrada, E.Y., Thompson, J.F., Liu, W., Rosenberg, G.A., 2007. Matrix metalloproteinase-mediated disruption of tight junction proteins in cerebral vessels is reversed by synthetic matrix metalloproteinase inhibitor in focal ischemia in rat. J. Cereb. blood flow Metab. Off. J. Int. Soc. Cereb. Blood Flow Metab. 27, 697–709. https://doi.org/10.1038/sj.jcbfm.9600375

Yokel, R.A., 2006. Blood-brain barrier flux of aluminum, manganese, iron and other

metals suspected to contribute to metal-induced neurodegeneration. J. Alzheimers. Dis. 10, 223–253. https://doi.org/10.3233/jad-2006-102-309

Yoshida, S., 2001. Re-evaluation of acute neurotoxic effects of Cd2+ on mesencephalic trigeminal neurons of the adult rat. Brain Res. 892, 102–110. https://doi.org/10.1016/s0006-8993(00)03240-6

Youn, H.D., Kim, E.J., Roe, J.H., Hah, Y.C., Kang, S.O., 1996. A novel nickel-containing superoxide dismutase from Streptomyces spp. Biochem. J. 318, 889–896. https://doi.org/10.1042/bj3180889

Yuan, Y., Jiang, C., Xu, H., Sun, Y., Hu, F., Bian, J., Liu, X., Gu, J., Liu, Z., 2013. Cadmium-induced apoptosis in primary rat cerebral cortical neurons culture is mediated by a calcium signaling pathway. PLoS One 8, e64330. https://doi.org/10.1371/journal.pone.0064330

Zelko, I.N., Mariani, T.J., Folz, R.J., 2002. Superoxide dismutase multigene family: a comparison of the CuZn-SOD (SOD1), Mn-SOD (SOD2), and EC-SOD (SOD3) gene structure, evolution and expression. Free Radic. Biol. Med. 33, 337–349. https://doi.org/10.1177/1461444810365020

Zhang, H., Reynolds, M., 2019. Cadmium exposure in living organisms: A short review. Sci. Total Environ. 678, 761–767. https://doi.org/10.1016/j.scitotenv.2019.04.395

Zheng, W., Perry, D.F., Nelson, D.L., Aposhian, H.V., 1991. Choroid plexus protects cerebrospinal fluid against toxic metals. FASEB J. 5, 2188–2193. https://doi.org/10.1096/fasebj.5.8.1850706

Chapter 2

Aim of the thesis

The heavy metal cadmium is a widespread toxic pollutant, released into the environment mainly by anthropogenic activities. Human exposure can occur through different sources and once absorbed it accumulates throughout a lifetime (biological half-life of 20-30 years). Brain is also a target of cadmium toxicity, since this toxicant may enter the central nervous system by increasing blood brain barrier permeability or through the olfactory nerves. Inside the nervous system this heavy metal spreads its toxicity in several ways, such as interfering with essential metal ions homeostasis, depleting cell's antioxidant defence systems or damaging mitochondria with a consequent alteration of energetic metabolism.

Cadmium exposure has been related to impaired functions of the nervous system and to neurodegenerative diseases, like amyotrophic lateral sclerosis (ALS) in which genetic, environmental and lifestyle factors play a role in the pathology onset, with the 90-95% of cases being sporadic (sALS) and the remaining 5-10% of familial origin (fALS). Among fALS, the 15-20% is attributed to mutations in superoxide dismutase 1 (SOD1) gene, that encodes for the homonym antioxidant protein responsible for superoxide anions dismutation. SOD1 is a homodimeric metalloenzyme of 32 kDa mainly located in the cytoplasm, with each monomer binding one copper and zinc ions within a disulfide bonded conformer. Zinc is involved in structure stability, while the copper ion is responsible for the catalytic activity.

Oxidative stress is one of the major mechanisms of cadmium induced toxicity and an alteration of oxidative homeostasis, through depletion of antioxidant defences, is responsible for a plethora of adverse outcoming mainly leading to cell death. Since the main goal of this thesis was a better understanding of the consequences of cadmium-induced oxidative stress, we focused on:

i. the investigation of energy metabolism following cadmium exposure in human neural cell line SH-SY5Y
ii. the evaluation of cadmium toxicity in LUHMES cell line, as a model of differentiated neurons, underlining the role of glutathione and the importance of more complex experimental models

iii. the analysis of cadmium effect on the function and expression of human SOD1 in three models: expressed as a recombinant protein in *E. coli*, in human neural SH-SY5Y cell line and in the nematode *Caenorhabditis elegans*

Chapter 3

Cadmium promotes glycolysis upregulation and glutamine dependency in human neuronal cells

Federica Bovio, Pasquale Melchioretto, Matilde Forcella, Paola Fusi and Chiara Urani

This chapter is an extract of the submitted paper in Neurochemistry International, NEUROCHEMINT-S-21-00049

Abstract

Cadmium is a widespread pollutant, which easily accumulates inside the human body with an estimated half-life of 25-30 years. Many data strongly suggest that it may play a role in neurodegenerative diseases pathogenesis. In this paper we investigated cadmium effect on human SH-SY5Y neuroblastoma cells metabolism. Results showed that, although SH-SY5Y cells already showed hyperactivated glycolysis, cadmium further increased basal glycolytic rate. Both glycolytic capacity and reserve were also increased, following cadmium administration, endowing the cells with a higher compensatory glycolysis when oxidative phosphorylation was inhibited. Cadmium administration also led to an increase in glycolytic ATP production rate, paralleled by a decrease in ATP production by oxidative phosphorylation, due to an impairment of mitochondrial respiration. Moreover, following cadmium administration, mitochondria increased their dependency on glutamine, while decreasing lipids oxidation. On the whole, our data show that cadmium exacerbates the Warburg effect and promotes the use of glutamine as a substrate for lipid biosynthesis. Although increased glutamine consumption leads to an increase in glutathione level, this cannot efficiently counteract cadmium-induced oxidative stress, leading to membrane lipid peroxidation. Oxidative stress represents a serious threat for neuronal cells and our data confirm glutathione as a key defense mechanism.

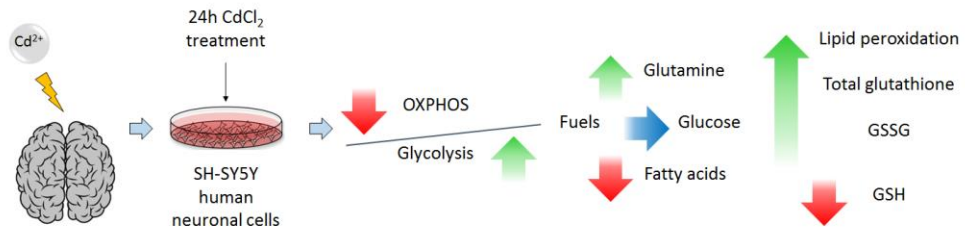

3.1 Introduction

The rare heavy metal cadmium (Cd), found in air, water and sediment with a concentration of 0.15 mg/kg in the Earth crust and of 1.1×10^{-4} mg/L in the sea, is widely used in both industry and agriculture, leading to its widespread diffusion into the environment (Zhang and Reynolds, 2019). The absence of a biodegradation system united to its toxicity and accumulation in organisms, with an estimated half-life of 25-30 years in humans, led the scientific community to classify this metal as part of the group of main environmental and occupational chemical pollutants in industrialized countries (Mezynska and Brzóska, 2018).

Since cadmium uptake can occur through inhalation of polluted air, cigarette smoking or ingestion of contaminated food and water, the main routes of its entry into human body are the respiratory and the gastrointestinal tract, accounting respectively for the 10-40% and 5-8% of the load, with the skin playing a minor role (Nordberg, 2009; Sabolić et al., 2010; Sarkar et al., 2013). Once inside, the majority of cadmium is stored in the liver and kidneys, which help spreading its toxicity; however, this metal can affect also lungs, testis, cardiovascular and nervous systems.

Under normal conditions, cadmium can barely cross the blood brain barrier (BBB), reaching the central nervous system (CNS); however, if present in the blood stream, it can enter the cells through channels, transporters and receptors placed on the luminal surface of the BBB endothelial cells (Thévenod et al., 2019). In case of acute cadmium exposure, the BBB protects the majority of the CNS; while in chronic and prolonged exposures, cadmium is responsible for weakening the cellular antioxidant defences and increasing reactive oxygen species (ROS) formation, with the consequent activation of matrix metalloproteinases that disrupt BBB tight junctions and enhance its permeability (Branca et al., 2020; Yang et al., 2007). Another route of cadmium uptake in the CNS is represented by the nasal mucosa or olfactory pathways, with the metal, transported along primary olfactory neurons, reaching the terminations in the olfactory bulbs and bypassing the intact BBB (Tjälve and Henriksson, 1999).

Once in the brain, this metal accumulates in the choroid plexus in concentrations much greater than those found in the cerebrospinal fluid (Wang and Du, 2013). Having an abundant pool of metal binding ligands responsible for metal ions binding, such as metallothioneins, and a highly active antioxidant defence system, like the antioxidant

enzymes superoxide dismutase and catalase, makes the choroid plexus the first line of defence against cadmium toxicity in the CNS (Zheng et al., 1991). However, none of the cellular defence mechanisms is perfectly efficient and the consequences of cadmium exposure act on several molecular pathways.

Even though the exact mechanisms through which cadmium exerts its neurotoxicity are still unresolved, one of its main targets is the mitochondrion, which can suffer several damages triggered by this metal. Cadmium can act on complex II (succinate dehydrogenase) and complex III (cytochrome bc1 complex) inducing the inhibition of the electron transport chain (ETC) and ATP production, which results in the formation of ROS favoured by the high $NADH/NAD^+$ ratio present in the matrix (Brand, 2016). In particular the principal site of ROS production seems to reside in complex III, and ROS accumulation disrupts the mitochondrial membrane potential, activating a sequence of events (Genchi et al., 2020). This altered membrane potential leads to an increase in mitochondrial membrane permeability, followed by the release of cytochrome *c* through the opening of transition pore with consequent activation of the caspase pathway (Oh and Lim, 2006). Additionally, cadmium has been reported to inhibit ATPase, to enhance the level of lipid peroxidation and to alter the cellular redox status by reacting with exogenous and endogenous antioxidants, such as reduced glutathione (Cannino et al., 2009; Cuypers et al., 2010).

Al-Ghafari and colleagues showed a loss in the ETC of cadmium-exposed osteoblasts together with a reduced ATP production and oxygen consumption, that correlate with an increase in lactate production, suggesting a shift to anaerobic metabolism (Al-Ghafari et al., 2019). Moreover, a metabolomic study on neuronal PC-12 cells confirmed the increase in lactic acid content, which could be a reflection of enhanced glycolysis due to inadequate energy supply through oxidative phosphorylation (Zong et al., 2018). However this increase in glycolytic activity happens in the initial phase of exposure, while a chronic exposure inhibits glycolysis due to negative effects on hexokinase, phosphofructokinase and pyruvate kinase caused by cadmium binding to the sulfhydryl (-SH) groups of the mentioned enzymes (Li et al., 2016; Sabir et al., 2019). Subsequently, cell energy production is likely obtained by proteins oxidation, since cadmium increases the activity of several enzymes involved in amino acids

catabolism, such as amino acid oxidase, glutamate dehydrogenase and xanthine oxidase (Sabir et al., 2019).

To better understand the role of cadmium in the mechanisms of neurodegeneration, in the present work we have evaluated the mitochondrial status and the energy metabolism of SH-SY5Y neuronal cells treated with 10 µM and 20 µM $CdCl_2$ for 24 hours, by measuring the oxygen consumption rate and the extracellular acidification rate through Seahorse technology. In addition, due to the recognized role of lipid peroxidation as an important factor in the development of neurodegenerative disorders (Peña-Bautista et al., 2019), we have analysed the oxidative status in SH-SY5Y cells under the same cadmium treatment conditions. Our results show a decrease of mitochondria functionality, together with an enhanced glycolysis, following cadmium treatment, suggesting a shift to anaerobiosis due to mitochondrial damage; this is confirmed by a greater glycolytic ATP production in cadmium treated cells. Moreover, regarding the evaluation of mitochondrial fuel oxidation, cadmium treatment led to an increase in glutamine dependency, suggesting the use of proteins for energy production.

3.2 Materials and methods

3.2.1 Mammalian cell culture

SH-SY5Y (ATCC® HTB-2266™) human neuroblastoma cell line was grown in F12:EMEM (1:1) medium supplemented with heat-inactivated 10% FBS, 2 mM L-glutamine, 100 U/mL penicillin, 100 µg/mL streptomycin and maintained at 37 °C in a humidified 5% CO_2 incubator. ATCC validated cell line by short tandem repeat profiles that are generated by simultaneous amplification of multiple short tandem repeat loci and amelogenin (for gender identification). All the reagents for cell culture were supplied by EuroClone (Pero, Milan, Italy).

3.2.2 Cell viability assay

Cell viability was investigated using *in vitro* toxicology assay kit MTT-based, according to manufacturer's protocols (Merck KGaA, Darmstadt, Germany).

In order to evaluate cadmium toxicity, cells were seeded in 96-well micro-titer plates at a density of 1×10^4 cells/well and after 24 hours were treated with different $CdCl_2$

concentrations (0-200 μM). After 24 hours at 37 °C, the medium was replaced with a complete medium without phenol red and 10 μL of a 5 mg/mL MTT (3-(4,5-dimethylthiazol-2)-2,5-diphenyltetrazolium bromide) solution was added to each well. After a further incubation for 4 hours, upon formed formazan crystals solubilization with 10% Triton-X-100 in acidic isopropanol (0.1 N HCl), absorbance was measured at 570 nm using a micro plate reader. Viabilities were expressed as a percentage of the untreated controls. Each experiment was performed in three replicate wells for each metal concentration and results are presented as the mean of at least three independent experiments.

3.2.3 Oxygen consumption rate and extra-cellular acidification rate measurements

Oxygen consumption rate (OCR) and extra-cellular acidification rate (ECAR) were investigated using Agilent Seahorse XFe96 Analyzer on SH-SY5Y cell line treated with cadmium.

The cells were seeded in Agilent Seahorse 96-well XF cell culture microplates at a density of 4×10^4 cells per well in 180 μL of growth medium and were allowed to adhere for 24 h in a 37 °C humidified incubator with 5% CO_2. Subsequently the seeded cells were treated with $CdCl_2$ 10 μM or 20 μM for 24 hours. In addition, before running the assay, the Seahorse XF Sensor Cartridge was hydrated and calibrated with 200 μL of Seahorse XF Calibrant Solution in a non-CO_2 37 °C incubator in order to remove CO_2 from the media that would otherwise interfere with measurements that are pH sensitive.

After the 24 hours of cadmium treatment, for Agilent Seahorse XF Cell Energy Phenotype Test Kit, Agilent Seahorse XF ATP Rate Assay Kit, Agilent Seahorse XF Cell Mito Stress Test Kit and Agilent Seahorse XF Mito Fuel Flex Test Kit the growth medium was replaced with 180 μL/well of Seahorse XF Base Medium containing 1 mM pyruvate, 2 mM L-glutamine and 10 mM glucose; while for Agilent Seahorse XF Glycolysis Stress Test Kit the medium substitution was made with XF Base Medium containing 2 mM L-glutamine and with XF Base Medium containing 1 mM pyruvate, 2 mM L-glutamine, 10 mM glucose and 5 mM Hepes for Agilent Seahorse XF Glycolytic Rate Assay Kit. Subsequently the plate was incubated into a 37 °C non-

CO_2 incubator for 1 hour, before starting the experimental procedure, and the compounds were loaded into injector ports of sensor cartridge.

For Agilent Seahorse XF Cell Energy Phenotype Test Kit a pre-warmed combined mixture of oligomycin and FCCP (carbonyl cyanide-4-(trifluoromethoxy)phenylhydrazone) was loaded into injector port A to reach working concentration of 1 μM and 2 μM respectively. OCR and ECAR were detected under basal conditions followed by the addition of the compounds to measure baseline phenotype, stressed phenotype and metabolic potential.

The OCR and ECAR detected during Agilent Seahorse XF Glycolysis Stress Test Kit allowed to measure the glycolytic function in cells (glycolysis, glycolytic capacity, glycolytic reserve and non-glycolytic acidification) through the sequential additions of pre-warmed glucose, oligomycin and 2-deoxy-D-glucose (2-DG) into injector ports A, B and C to reach final concentration of 10 mM, 1 μM and 50 mM, respectively.

Regarding Agilent Seahorse XF Glycolytic Rate Assay Kit, pre-warmed combination of rotenone and antimycin A at working concentration of 0.5 μM and 2-DG at 50 mM were loaded into injector ports A and B respectively. OCR and ECAR were detected under basal conditions followed by the sequential addition of the compounds in order to measure basal glycolysis, basal proton efflux rate, compensatory glycolysis and post 2-DG acidification.

Agilent Seahorse XF ATP Rate Assay Kit measures the total amount of ATP produced in living cells, distinguishing between the fractions of ATP derived from mitochondrial oxidative phosphorylation and glycolysis, through the detection of OCR and ECAR under basal conditions followed by the sequential addition of pre-warmed working concentration of 1.5 μM oligomycin in injector port A and of 1 μM rotenone and antimycin A into injector port B.

For Agilent Seahorse XF Cell Mito Stress Test Kit pre-warmed oligomycin, FCCP, rotenone and antimycin A were loaded into injector ports A, B and C of sensor cartridge at a final working concentration of 1 μM, 2 μM and 0.5 μM, respectively. OCR and ECAR were detected under basal conditions followed by the sequential addition of the compounds and non-mitochondrial respiration, maximal respiration, proton leak, ATP respiration, respiratory capacity and coupling efficiency can be evaluated. Using the Agilent Seahorse XF Mito Fuel Flex Test Kit the mitochondrial

fuel usage in living cells has been determined and, through OCR measuring, the dependency, capacity and flexibility of cells to oxidize glucose, glutamine and long-chain fatty acids can be calculated. Pre-warmed working concentration of 3 μM BPTES, 2 μM UK5099 or 4 μM etomoxir were loaded into injector port A and compounds mixture of 2 μM UK5099 and 4 μM etomoxir, 3 μM BPTES and 4 μM etomoxir or 3 μM BPTES and 2 μM UK5099 into injector port B in order to determine glutamine, glucose and long-chain fatty acid dependency, respectively. On the contrary fuels capacity is measured by the addition into injector port A of 2 μM UK5099 and 4 μM etomoxir, 3 μM BPTES and 4 μM etomoxir or 3 μM BPTES and 2 μM UK5099 working concentration, followed by injection in port B of 3 μM BPTES, 2 μM UK5099 or 4 μM etomoxir working concentration for glutamine, glucose and long-chain fatty acid, respectively.

All the kits and reagents were purchased by Agilent Technologies (Santa Clara, CA, USA).

3.2.4 Lipid peroxidation assay

The extent of lipid peroxidation was determined by the levels of malondialdehyde (MDA) measured using the thiobarbituric acid reactive substances assay (Buege and Aust, 1978). SH-SY5Y cells were seeded at 1×10^6 cells/100 mm dish and, on the following day, were treated with either 10 μM or 20 μM $CdCl_2$. Twenty-four hours after the treatment, the cells were harvested by trypsinization, washed with PBS (10 mM K_2HPO_4, 150 mM NaCl, pH 7.2) and the resulting pellet was resuspended in 500 μL PBS. Cell lysis was obtained through sonication (15 sec at 10% amplitude 3 times) and protein content was determined by Bradford assay, using BSA for the calibration curve (Bradford, 1976). Subsequently 1 mL of a 15% TCA (trichloroacetic acid), 0.375% TBA (2-thiobarbituric acid) and 0.25 M HCl solution was added to the lysates, followed by a 15 minutes incubation at 95 °C. Subsequently, samples were centrifuged at 10,000 × g for 10 min, supernatants were collected and the absorbance at 530 nm was measured. Additionally, a background sample made by only PBS was treated in the same way. Lipid peroxidation level was expressed as nmol of MDA/mg protein using a molar extinction coefficient of 1.56×10^5 M^{-1} cm^{-1}. Results were

reported as a percentage compared to untreated control and results are presented as the mean of at least three independent experiments.
All the chemicals were supplied by Merck KGaA, Darmstadt, Germany.

3.2.5 Glutathione detection

For the measurement of total glutathione (GSH tot), oxidized glutathione (GSSG) and reduced glutathione (GSH) content in cells treated with $CdCl_2$ for 24 hours, SH-SY5Y cells were seeded in 96-well micro-titer plates at a density of 2×10^4 cells/well. The day after seeding, the cells were exposed to either 10 µM or 20 µM $CdCl_2$ for 24 hours, with cells not treated with $CdCl_2$ representing the control.
At the end of the treatment, the cells were lysed in 100 µL/well of 1% SSA (Sulfosalicylic acid) and scraped to ensure complete lysis. The assays of total glutathione and GSSG were performed in a reaction mix containing 100 µM DTNB (5,5′-dithiobis(2-nitrobenzoic acid)), 200 µM NADPH and 0.46 U/mL glutathione reductase added to the GSH-buffer (100 mM Na_2HPO_4, 100 mM NaH_2PO_4, 1 mM EDTA, pH 7.5).
To measure total glutathione, 50 µL of each cell lysate were transferred into a new 96-well plate and 50 µL of MilliQ water were added. Then, 100 µL of reaction mixture were added to each well and absorbance at 405 nm was measured immediately after, as well as after 20 and 30 minutes using a micro plate reader. Additionally, a calibration curve was prepared (0-10 µM GSH) and treated like the samples.
For GSSG evaluation the 50 µL/well left were treated with 1 µL of 2-vinylpyridine solution (27 µL 2-vinylpyridine in 98 µL ethanol) for 1 hour at RT in order to block the SH-groups. Then 50 µL of MilliQ water and 100 µL of reaction mixture were added to each well and absorbance at 405 nm was measured immediately after, as well as after 20 and 30 minutes using a micro plate reader. Additionally, a calibration curve was prepared (0-10 µM GSSG) and treated like the samples.
The values of absorbance were compared to standard curves and converted into molarity of total glutathione and GSSG: GSH (GSH tot − GSSG) was calculated. Total glutathione was expressed as a percentage of the control; while GSSG and GSH were expressed as a percentage of total glutathione for each condition. Each

experiment was performed in three replicate wells for each metal concentration and results are presented as the mean of at least three independent experiments.
All the chemicals were supplied by Merck KGaA, Darmstadt, Germany.

3.2.6 Glutathione S-transferase and glutathione reductase enzyme activity assays

In order to evaluate the effect of cadmium on glutathione S-transferase (GST) and glutathione reductase (GR) activities, SH-SY5Y cells were seeded at 2×10^6 cells/100 mm dish and, 24 hours later, exposed to either 10 μM or 20 μM $CdCl_2$ for 24 hours. Cells not treated with $CdCl_2$ represented the control. Subsequently, control and cadmium treated cells were rinsed with ice-cold PBS (10 mM K_2HPO_4, 150 mM NaCl, pH 7.2) and lysed in 50 mM Tris/HCl, pH 7.4, 150 mM NaCl, 5 mM EDTA, 10% glycerol, 1% NP40 buffer, containing protease inhibitors and 1 mM PMSF. After lysis on ice, homogenates were obtained by passing the cells 5 times through a blunt 20-gauge needle fitted to a syringe and then centrifuging at 15,000 × g at 4 °C for 30 min. The resulting supernatant was used to measure GST activity according to Habig et al. (Habig et al., 1974) and GR activity according to Wang (Wang et al., 2001). Enzyme activities were expressed in international units and referred to protein concentration, quantified by Bradford assay, using BSA for the calibration curve (Bradford, 1976). All assays were performed in triplicate at 30 °C.
All chemicals were purchased by Merck KGaA, Darmstadt, Germany.

3.2.7 Statistical analysis

All the experiments were carried out in triplicate. The samples were compared to their reference controls and the data were tested by Dunnett multiple comparison procedure. Results were considered statistically significant at $p < 0.05$.

3.3 Results

3.3.1 Exposure to $CdCl_2$ affects neural cells viability

In order to determine $CdCl_2$ doses to be used in the analysis of oxidative stress and in Seahorse experiments, the effect of this metal was first evaluated on SH-SY5Y cells viability.

As reported in Figure 1, neuronal cells treated with $CdCl_2$ for 24 hours showed a dose-dependent reduction in their viability: while doses lower than 50 µM mildly affected the cell viability, with a 67% residual viability at 20 µM $CdCl_2$, higher concentrations strongly reduced viability, with only 13% residual viability at 200 µM; therefore, 10 µM and 20 µM $CdCl_2$ concentrations were used for our further experiments.

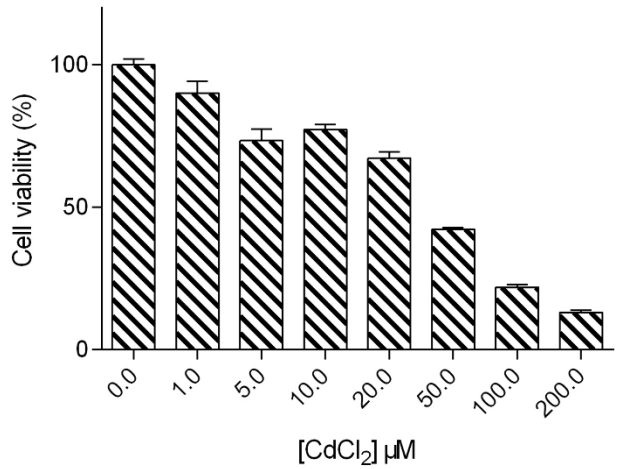

Figure 1. SH-SY5Y viability in the presence of cadmium.

Cell survival was determined by MTT assay, after a 24-hour incubation in the presence of different $CdCl_2$ concentrations (0–200 µM). Data are shown as means ± standard error (SEM).

3.3.2 Evaluation of SH-SY5Y energy phenotype shows that cadmium treated cells increase basal glycolysis

In order to investigate if cadmium could cause a different response in cells when stressor compounds are administered, the energy metabolism of SH-SY5Y cells treated for 24 hours with either 10 µM or 20 µM $CdCl_2$ was analysed using the Agilent Seahorse XF Cell Energy Phenotype Test Kit.

Under basal conditions, the OCR level, measuring mitochondrial respiration rate in living cells, showed no difference among the samples (Fig. 2A and C); while the ECAR rate, which represents a measure of glycolysis, was found higher in cadmium treated cells (Fig. 2B and D). A simultaneous injection of oligomycin, an ATP

synthase inhibitor, and FCCP, an uncoupling agent, determined an increase in both OCR and ECAR; however, while OCR level increased to the same extent in all the conditions studied (Fig. 2A and C), ECAR increase was higher for cadmium-treated cells than for control cells (Fig. 2B and D).

The percentage increase of stressed parameters over baseline ones is the metabolic potential, which is defined as the cells' ability to meet an energy demand via respiration and glycolysis. SH-SY5Y cells treated with cadmium showed the same metabolic potential of control cells for OCR, while showing a decreased metabolic potential for ECAR. In fact, as seen in Figure 2E, the latter showed a dose-dependent reduction following 24 hours Cd treatment, although statistically significant only at 20 μM $CdCl_2$.

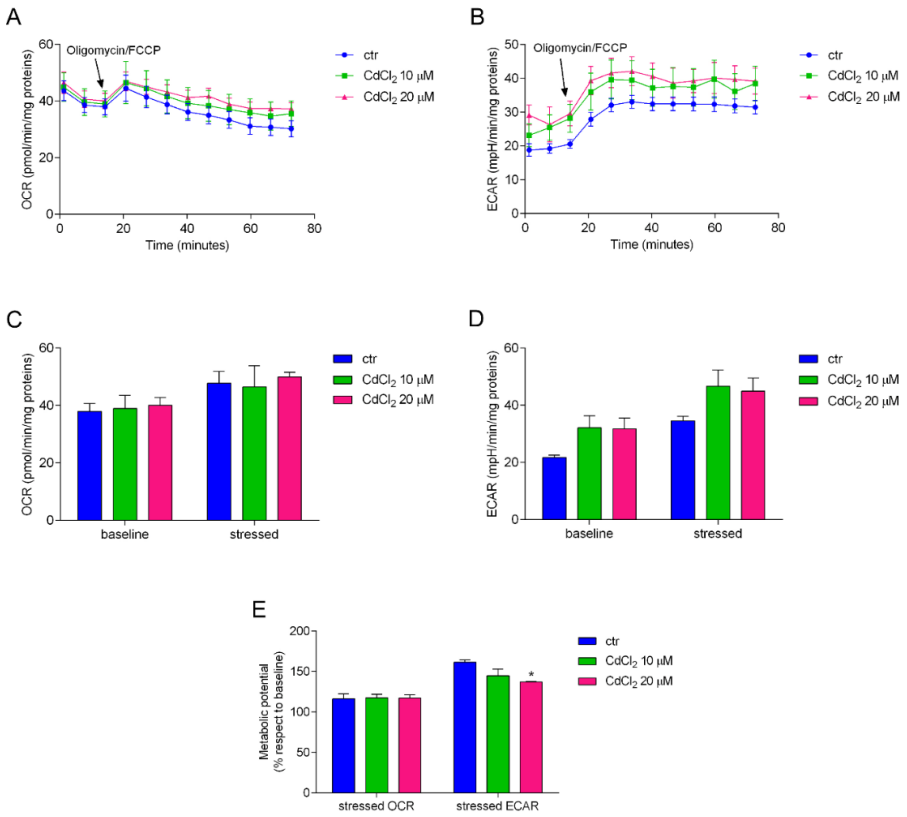

Fig. 2. Cell energy phenotype after 24-hour exposure to either 10 µM or 20 µM $CdCl_2$.

OCR (A) and ECAR (B) traces, expressed as pmol O_2/min/mg proteins and mpH/min/mg proteins respectively, in control and $CdCl_2$-treated cells. The arrows indicate the time of simultaneous addition of oligomycin/FCCP. The OCR and ECAR profiles are representative of three independent experiments. Analysis of baseline and stressed level of mitochondrial respiration (C) and glycolysis (D) and metabolic potential (E). Bars indicate the mean ± SEM obtained in three independent experiments. Statistically significant: * $p < 0.05$

3.3.3 $CdCl_2$ administration increases both glycolytic capacity and glycolytic reserve

The results obtained in the cell energy phenotype analysis led us to hypothesize an increased glycolysis level in cadmium-treated cells. In order to investigate the

glycolytic functions, the glycolytic rate and the compensatory glycolysis Agilent Seahorse XF Glycolysis Stress Test Kit and Agilent Seahorse XF Glycolytic Rate Assay Kit were used.

The ECAR profile, reported in Figure 3A, determined after treatment with cadmium, showed a dose-dependent increase in protons extrusion both at the basal level and after the injection of a saturating concentration of glucose; the administration of oligomycin and hexokinase inhibitor 2-deoxyglucose (2-DG) permitted, through modulation of ECAR, the analysis of glycolytic parameters. Extracellular acidification was found higher after cadmium administration. In particular, treatment with 20 µM $CdCl_2$ caused a significant increase in non-glycolytic acidification, as well as in glycolysis and glycolytic capacity; while following the 10 µM dose, the pattern was more similar to that of control cells, with the exception of the glycolytic capacity, which was found higher than that of control cells. Regarding the glycolytic reserve, we observed the same increase in both cadmium-treated samples (Fig. 3B).

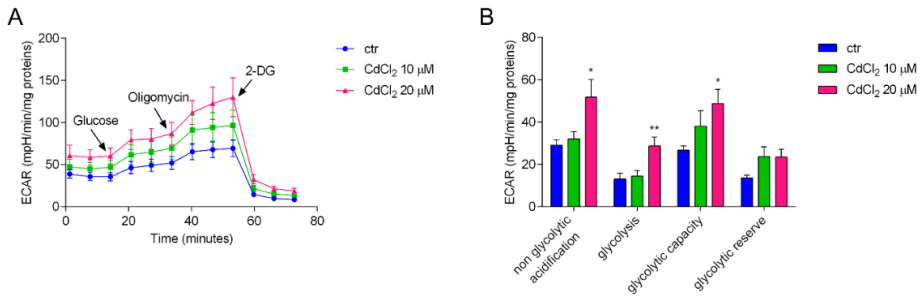

Figure 3. Glycolytic functions analysis in cadmium treated cells.

A) Representative ECAR profile of control and $CdCl_2$-treated cells of three independent experiments, expressed as mpH/min/mg proteins. The arrows indicate the time of addition of glucose, oligomycin and 2-DG. B) Analysis of different glycolytic parameters. Bars indicate the mean ± SEM obtained in three independent experiments. Statistically significant: * $p < 0.05$, ** $p < 0.01$

The cells possess the ability to switch from glycolysis to oxidative phosphorylation in response to environmental changes for energy production; this adaptation can be investigated using the Glycolytic Rate Assay. We measured the basal glycolytic rate

and the compensatory glycolysis following mitochondrial inhibition in SH-SY5Y cells previously treated with either 10 µM or 20 µM of $CdCl_2$ for 24 hours (Fig. 4). The proton efflux rate (PER) is sustained by both mitochondrial respiration and glycolysis in all conditions. The injection of rotenone and antimycin A, responsible for mitochondrial complex I and complex III inhibition, triggered a higher compensatory glycolysis in cadmium-treated cells, probably due to higher glycolytic capacity and reserve. When 2-DG was added, the PER was minimized, but the rate of acidification measured was still higher in treated cells compared to control cells (Fig. 4A).

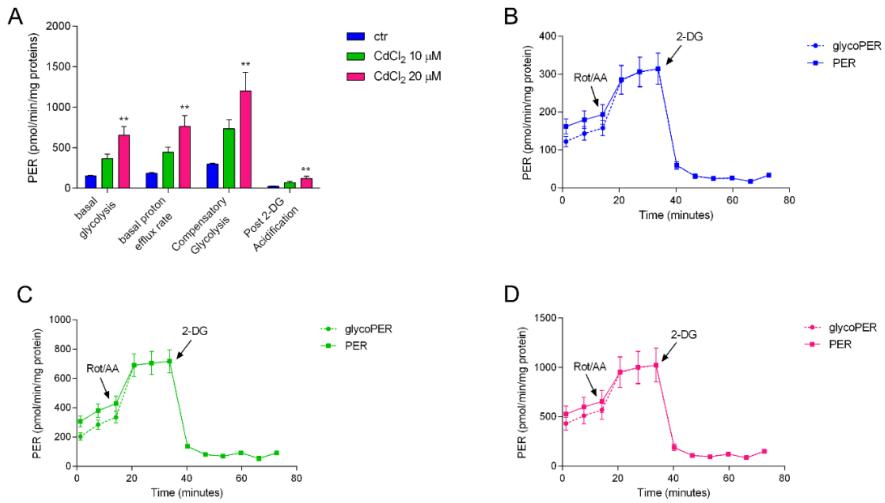

Figure 4. Evaluation of basal and compensatory glycolysis after cadmium treatment in neuronal cells.

Analysis of basal and compensatory glycolytic levels in control and cadmium treated cells (A). Bars indicate the mean ± SEM obtained in three independent experiments. Representative PER and glycoPER profiles of control cells (B) and 10 µM $CdCl_2$ (C) or 20 µM $CdCl_2$ (D) treated cells of three independent experiments; results are expressed as pmol/min/mg proteins. The arrows indicate the time of rotenone/antimycin A and 2-DG addition. Statistically significant: ** $p < 0.01$

3.3.4 $CdCl_2$ administration induces a higher ATP production rate through glycolysis

The increase in glycolytic rate, following $CdCl_2$ administration, suggested that cadmium could also act on total ATP production. The Seahorse ATP Rate Assay allows to calculate ATP production in living cells, distinguishing between the fraction of ATP produced by oxidative phosphorylation and the one produced by glycolysis.

$CdCl_2$ administration was found to increase the total ATP production rate (Fig. 5A). Moreover, cells treated with 10 µM $CdCl_2$ displayed a significantly higher glycolytic ATP level (Fig. 5E); on the other hand, cells treated with 20 µM $CdCl_2$ showed a decrease in ATP derived from oxidative phosphorylation, as well as an increase in glycolytic ATP (Fig. 5C and E).

Given the ATP production rate, it is also possible to calculate the relative contributions of glycolysis and oxidative phosphorylation to ATP production (Fig. 5B). Treatment with $CdCl_2$ caused a dose-dependent reduction in oxidative phosphorylation (Fig. 5D) and a specular dose-dependent increase in glycolysis, suggesting that most of the energy demand is supplied by glycolysis (Fig. 5F).

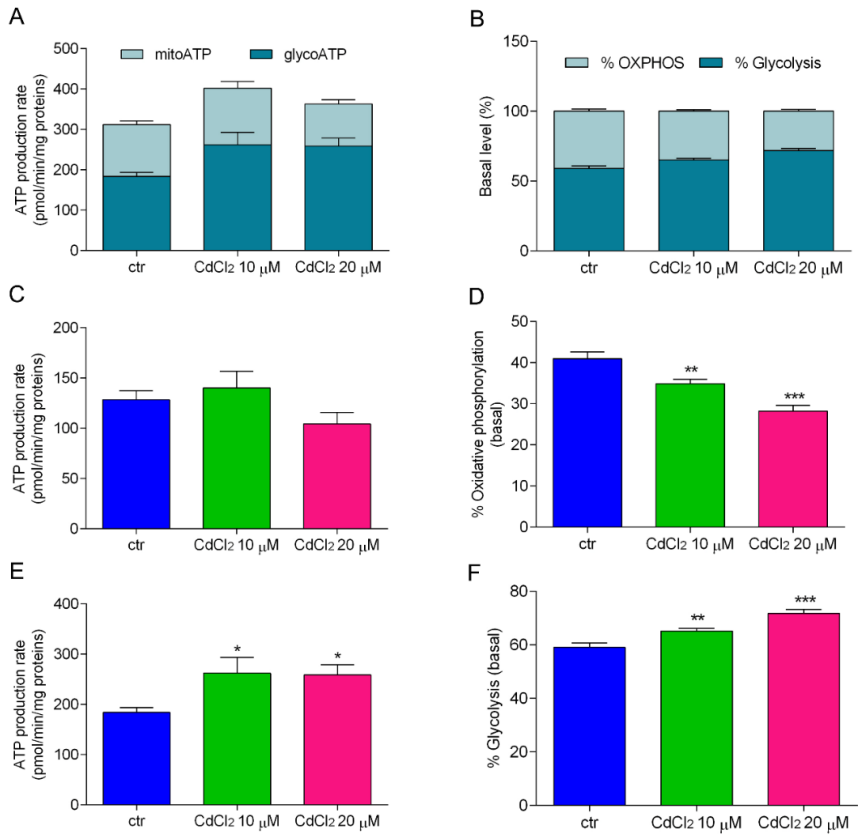

Figure 5. ATP production in cadmium treated cells.

Total (A), mitochondrial (C) and glycolytic (E) ATP production rate in neuronal cells treated for 24 hours with $CdCl_2$ (10 µM and 20 µM). Basal percentage level (B) of oxidative phosphorylation (D) and glycolysis (F). Bars indicate the mean ± SEM obtained in three independent experiments. Statistically significant: * $p < 0.05$, ** $p < 0.01$, *** $p < 0.001$

3.3.5 $CdCl_2$ administration leads to a decrease in mitochondrial respiration

The investigation of ATP production after treatment with $CdCl_2$ showed a decrease in oxidative phosphorylation that led us to investigate mitochondrial functions through the Mito Stress Test.

As shown in Figure 6, the presence of 20 µM $CdCl_2$ reduced the oxygen consumption basal rate. The injection of the ATP synthase inhibitor oligomycin allowed to determine the mitochondrial ATP production rate, which was found significantly

lower in 20 µM $CdCl_2$ treated cells (Fig. 6B). Following oligomycin addition, we also observed a decrease in OCR rate and an increase in ECAR level (Fig. 6A and C). Subsequently, OCR level increased after FCCP injection, allowing the evaluation of the maximal respiration rate, as well as the spare respiratory capacity. $CdCl_2$ administration caused a significant reduction in the maximal respiration rate at 20 µM $CdCl_2$, while the spare respiratory capacity significantly increased in treated cells at both $CdCl_2$ concentrations. Rotenone and antimycin A injection inhibited mitochondrial oxygen consumption leading to a sharp decrease in OCR level; however, the oxygen consumption not linked to mitochondria was found to be the same for all the conditions tested (Fig 6A and B). Finally, the coupling efficiency did not show any difference among the samples (Fig. 6D).

Taken together these results indicate a lower mitochondrial efficiency in respiration and energy production, following treatment with $CdCl_2$.

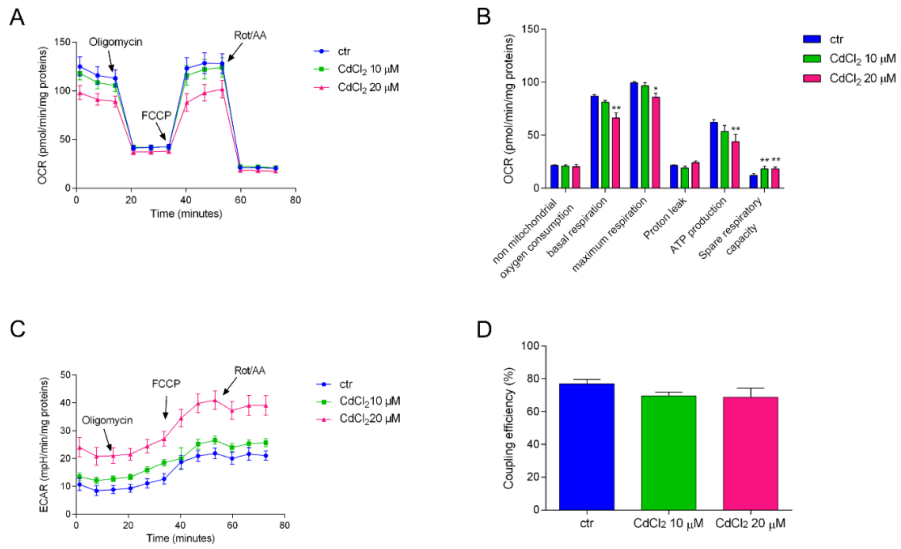

Figure 6. Mitochondrial functionality in SH-SY5Y cells treated with 10 µM and 20 µM $CdCl_2$.

OCR (A) and ECAR (C) traces, expressed as pmol O_2/min/mg proteins and mpH/min/mg proteins respectively, in control and cadmium treated cells. The arrows indicate the time of addition of oligomycin, FCCP and rotenone/antimycin A. Analysis of key mitochondrial parameters (B) and coupling efficiency (D). Bars indicate the mean ± SEM obtained in three independent experiments. Statistically significant: * $p < 0.05$, ** $p < 0.01$

3.3.6 Mitochondrial fuel oxidation pattern changes when neuronal cells are treated with cadmium

The Mito Fuel Flex test is used to investigate fuels oxidation by mitochondria in order to maintain OCR basal level. We analysed the oxidation of glucose, long-chain fatty acids and glutamine after 24 hours treatment with $CdCl_2$ at the concentrations of 10 µM and 20 µM (Fig. 7).

Analysing the dependency, i.e. the cells' reliance on a particular fuel pathway to maintain baseline respiration, we saw that, for all the conditions studied, half of the total dependency was linked to glucose oxidation: in control cells, the other half dependency was nearly equally distributed between glutamine and fatty acids, while, following treatment with $CdCl_2$, glutamine dependency increased and fatty acids

dependency decreased (Fig. 7B, D, F). In fact, Figure 8C and E show that the fatty acids dependency decreased in a dose-dependent way, while glutamine dependency was significantly higher in cadmium treated cells.

The evaluation of fuel capacity, i.e. the ability possessed by mitochondria to oxidize a fuel when other fuel pathways are inhibited, allows to calculate the fuel flexibility, which is the ability of the cells to increase oxidation of a particular fuel in order to compensate the inhibition of alternative fuel pathways. The fuel capacity linked to glucose oxidation was reduced at increasing $CdCl_2$ doses, leading to a significant reduction in fuel flexibility (Fig. 7A). Instead, the fuel flexibility of fatty acids remained constant due to the cadmium induced decrease in both dependency and capacity (Fig. 7C). Interestingly, glutamine flexibility was completely abolished in $CdCl_2$-treated cells, due to the increase in dependency and the lack of variation in capacity (Fig. 7E).

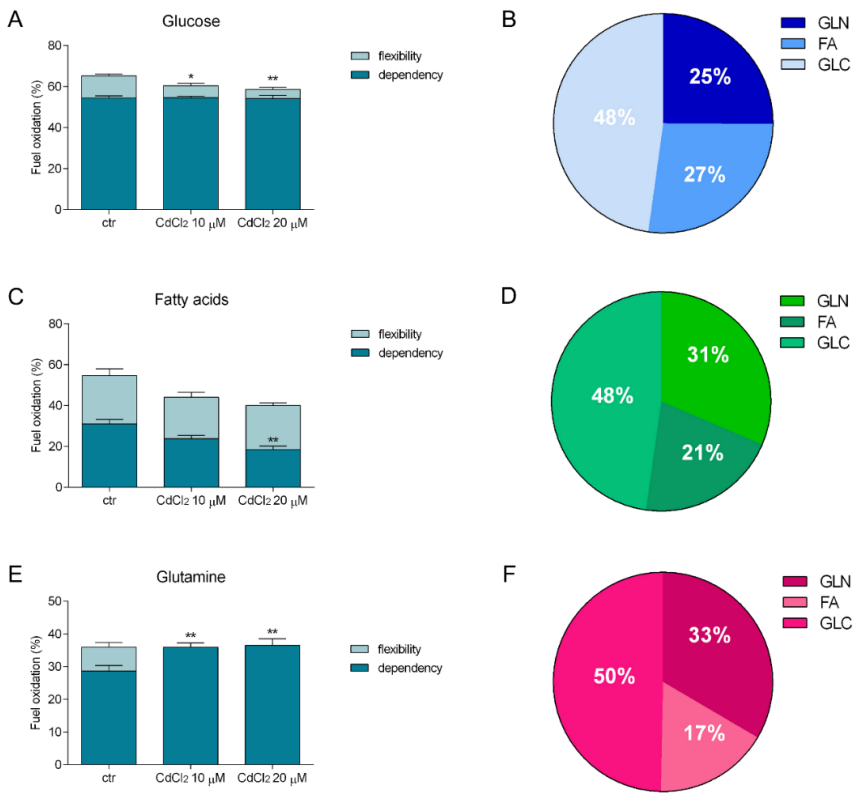

Figure 7. Evaluation of mitochondrial fuel oxidation in SH-SY5Y Cd-treated cells.

Glucose (A), long-chain fatty acids (C) and glutamine (E) mitochondrial fuel oxidation dependency and flexibility. Bars indicate the mean ± SEM obtained in three independent experiments. Pie charts of control cells (B), 10 µM $CdCl_2$ (D) and 20 µM $CdCl_2$ (F) fuel dependency. Statistically significant: * $p < 0.05$, ** $p < 0.01$

3.3.7 Cadmium exposure increases oxidative stress

One of the main mechanisms of cadmium toxicity is increasing oxidative stress, leading in turn to lipid peroxidation and to a decrease in antioxidant defences. In order to understand SH-SY5Y oxidative status, after 24 hours exposure to either 10 µM or 20 µM $CdCl_2$, lipid peroxidation and glutathione levels, as well as the activity of glutathione reductase (GR) and glutathione S-transferase (GST) were analysed.

Our data showed an increase in lipid peroxidation levels in cadmium treated cells, slightly higher at 10 µM $CdCl_2$ than at 20 µM $CdCl_2$ (Fig. 8A), as well as a significant increase in the total glutathione level (Fig. 8B). Moreover, we observed a nearly 2-fold increase in oxidized glutathione (GSSG) level, with a consequent decrease in the reduced, scavenging form (GSH), after incubation with $CdCl_2$ (Fig. 8C).

Enzyme assays performed on two enzymes involved in the glutathione metabolism, GST and GR, did not show any statistically significant variation (Fig. 8D).

Taken together these results showed an increase in oxidative stress level in cadmium treated cells, that could possibly affect energy metabolism.

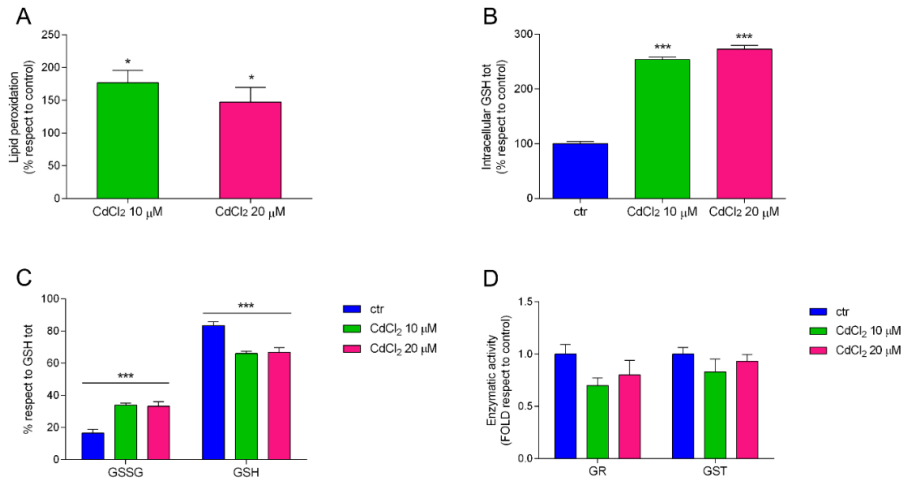

Fig. 8. Oxidative stress status after 10 µM and 20 µM $CdCl_2$ 24-hour administration. A) Lipid peroxidation level expressed as a percentage of the control. B-C) Total glutathione level (B) and GSSG and GSH (C) levels, expressed as percentages of total glutathione in cadmium treated and untreated cells. D) Glutathione reductase (GR) and glutathione S-transferase (GST) activities, expressed as folds respect to control. Data are shown as means ± standard error (SEM). Statistically significant: *$p<0.05$, ***$p<0.001$

3.4 Discussion

The metabolic analysis, performed through Seahorse, allowed to gain some insights into the metabolic rearrangements induced by cadmium, a toxic and widely diffused metal and a recognized carcinogen. Cadmium toxicity is mainly due to an increase in

oxidative stress, as well as to its ability to substitute zinc in hundreds of zinc-proteins (Satarug et al., 2018; Urani et al., 2015). Cadmium has been also associated to neurodegenerative diseases pathogenesis: oxidative stress has been demonstrated to play an essential role in ALS, as well as in Parkinson and Alzheimer disease, pathogenesis (Singh et al., 2019; Sultana et al., 2013). These data, along with our previous results (Forcella et al., 2020), prompted us to deeply investigate the effect of sublethal $CdCl_2$ concentrations on human neuroblastoma SH-SY5Y cultured cells, as possible mechanisms of induced neurodegeneration.

Seahorse analysis showed an increase in glycolytic basal level following cadmium administration, as shown by Glycolysis Stress Test and Glycolytic Rate Assay: this increase was found significant in the presence of 20 µM $CdCl_2$, although an increasing trend was already evident following 10 µM $CdCl_2$ administration. However, Cell Energy Phenotype analysis showed that cadmium administration reduced the ability to supply energy demand via glycolysis in the presence of stressor compounds, like the simultaneous administration of oligomycin and FCCP. Glycolytic capacity, the cell's ability to use glycolysis to its maximum capacity, was also increased upon $CdCl_2$ administration, while the glycolytic reserve, indicating how close the glycolytic function is to the cell theoretical maximum, was also increased, but to the same extent at both $CdCl_2$ concentrations. This could be due to the fact that basal glycolysis increased to higher levels after 20 µM $CdCl_2$ administration and/or to the fact that the theoretical maximum has been reached. Glycolysis Stress Test also showed a higher basal acidification level for cadmium treated cells, measured in the absence of glucose, which can be due to cadmium promoting amino acids breakdown to yield acetylCoA to fuel Krebs cycle; in fact, mitochondrial fuel oxidation pattern analysis showed that cadmium treated cells rely strongly on glutamine to maintain baseline respiration. The ECAR measured in this case would therefore be partly due to CO_2, explaining why the acidification level remained high, following glycolysis inhibition by 2-DG, in cadmium treated cells.

The fact that oligomycin alone was able to induce an increase in the glycolytic capacity of cadmium treated cells suggests that these cells rely more on glycolysis than on oxidative phosphorylation for ATP production. This is confirmed by Seahorse ATP Rate assay showing that, following cadmium administration, ATP is increasingly

produced by glycolysis, in a dose dependent way, while the relative contribution of oxidative phosphorylation to ATP production decreases. The analysis of PER and glycoPER showed that cadmium treated cells are endowed with a higher compensatory glycolysis, whose value becomes significant after administration of 20 µM $CdCl_2$, although an increase is evident also following 10 µM $CdCl_2$ administration. The ratio between PER and glycoPER confirms that the relative contribution of glycolysis to acidification increases with cadmium administration in a dose dependent way.

The switch to glycolysis for ATP production is also demonstrated by the Mito Stress Test, showing that cadmium administration leads to a decrease in basal respiration rate in a dose dependent way; this is mirrored by the lower increase, in cadmium treated cells, in maximum respiration, following the uncoupler FCCP addition. As previously observed in healthy murine C3H cells (Oldani et al., 2020), cadmium led to an increase in the spare respiratory capacity, which, for SH-SY5Y cells is similar for both $CdCl_2$ concentration, suggesting that the cell theoretical maximum had been reached. Although cadmium administration did not alter mitochondrial coupling efficiency, these data show that it interfered with mitochondrial respiration, leading to a decrease in mitochondrial ATP production, which was found significant only after 20 µM $CdCl_2$ administration, but could be detected also after 10 µM $CdCl_2$ administration. The higher ability of cadmium treated cells to compensate with glycolysis after mitochondrial respiration inhibition can be correlated to their higher glycolytic capacity and reserve.

The increase in glycolysis promoted by cadmium administration to SH-SY5Y cells is well in accordance with our previously reported data on C3H healthy fibroblast treated with cadmium (Oldani et al., 2020). This is likely at the basis of the malignant cell transformation induced by cadmium, a well-known carcinogen: however, our data show that cadmium is able to hyperactivate glycolysis also in cancer cells like SH-SY5Y cells. These cells already rely on glycolysis more than oxidative phosphorylation for ATP production, with more than 50% ATP produced by glycolysis, a much higher value compared with the 12% normally measured in healthy cells (Seyfried and Shelton, 2010); our measurements also show that basal glycolysis, measured as glycoPER, is much higher in SH-SY5Y cells (over 100

pmol/min/mgprotein) than in C3H cells (50 pmol/min/mgprotein), reflecting their cancer nature.

Besides increasing glutamine dependency of SH-SY5Y cells, cadmium administration induced other rearrangements in mitochondrial fuel oxidation pattern. Both control and cadmium-treated cells were found equally dependent on glucose as a fuel, reflecting the fact that they are all cancer cells; however, cadmium decreased cell capacity to use glucose as a fuel when both lipid and glutamine utilization pathways were blocked: as a consequence, fuel flexibility was also decreased. Lipid dependency was decreased by cadmium administration in a dose dependent way, as well as the cell capacity to use lipids as a fuel when other fuels pathways cannot be used; as a result of a decrease in both lipid dependency and capacity, flexibility remained constant. Finally, the increase in glutamine dependency, mentioned above, was not accompanied by any variation in glutamine capacity, showing that the cells cannot increase their ability to use glutamine as a fuel when other fuels pathways are blocked; as a result cadmium administration abolished flexibility. The increase in glutamine dependency was found similar at both $CdCl_2$ concentrations, suggesting that a maximum has been reached in glutamine supply. Moreover, this explains the decrease in lipid dependency, since glutamine enters Krebs cycle as α-ketoglutarate to yield citrate; the latter can be translocated into the cytosol where it is converted by citrate lyase into oxalacetate and acetylCoA, which is carboxylated to malonylCoA, producing fatty acids.

Increased glutamine consumption also involves increased glutamate production, which could be used for glutathione synthesis, together with glycine and cysteine produced from glycolytic intermediates; this could be a defensive mechanism against oxidative stress triggered by cadmium and could explain the increase in total glutathione observed in our experiments. However, the GSSG/GSH ratio is increased following cadmium administration and, although cell death is prevented, lipid peroxidation could be detected in cells treated with cadmium. Other cell defense mechanisms against oxidative stress play an important role, like metallothioneines, whose expression is induced in SH-SY5Y cells following cadmium treatment (Forcella et al., 2020); however, GSH is essential for neuronal cells and is normally

supplied also by microglia. Further work will address the role of GSH in the protection against cadmium toxicity in neuronal cells.

3.5 Conclusions

Overall, cadmium exposure caused alterations in the oxidative balance of human neuronal cells, that led to a rearrangement of the energy metabolism, with an increase in glycolysis and in glutamine dependency. This is probably linked to the observed higher total glutathione level, since glutamine can lead to a higher glutamate production, that could be used for glutathione synthesis, together with glycine and cysteine produced by glycolytic intermediates.

References

Al-Ghafari, A., Elmorsy, E., Fikry, E., Alrowaili, M., Carter, W.G., 2019. The heavy metals lead and cadmium are cytotoxic to human bone osteoblasts via induction of redox stress. PLoS One 14, e0225341. https://doi.org/10.1371/journal.pone.0225341

Bradford, M.M., 1976. A rapid and sensitive method for the quantitation of microgram quantities of protein utilizing the principle of protein-dye binding. Anal. Biochem. 72, 248–254. https://doi.org/10.1006/abio.1976.9999

Branca, J.J.V., Fiorillo, C., Carrino, D., Paternostro, F., Taddei, N., Gulisano, M., Pacini, A., Becatti, M., 2020. Cadmium-induced oxidative stress: Focus on the central nervous system. Antioxidants 9, 1–21. https://doi.org/10.3390/antiox9060492

Brand, M.D., 2016. Mitochondrial generation of superoxide and hydrogen peroxide as the source of mitochondrial redox signaling. Free Radic. Biol. Med. 100, 14–31. https://doi.org/10.1016/j.freeradbiomed.2016.04.001

Buege, J.A., Aust, S.D., 1978. Microsomal lipid peroxidation. Methods Enzymol. 52, 302–310. https://doi.org/10.1016/s0076-6879(78)52032-6

Cannino, G., Ferruggia, E., Luparello, C., Rinaldi, A.M., 2009. Cadmium and mitochondria. Mitochondrion 9, 377–384. https://doi.org/10.1016/j.mito.2009.08.009

Cuypers, A., Plusquin, M., Remans, T., Jozefczak, M., Keunen, E., Gielen, H., Opdenakker, K., Nair, A.R., Munters, E., Artois, T.J., Nawrot, T., Vangronsveld, J., Smeets, K., 2010. Cadmium stress: an oxidative challenge. Biometals an Int. J. role Met. ions Biol. Biochem. Med. 23, 927–940. https://doi.org/10.1007/s10534-010-9329-x

Forcella, M., Lau, P., Oldani, M., Melchioretto, P., Bogni, A., Gribaldo, L., Fusi, P., Urani, C., 2020. Neuronal specific and non-specific responses to cadmium possibly involved in neurodegeneration: A toxicogenomics study in a human neuronal cell model. Neurotoxicology 76, 162–173. https://doi.org/https://doi.org/10.1016/j.neuro.2019.11.002

Genchi, G., Sinicropi, M.S., Lauria, G., Carocci, A., Catalano, A., 2020. The Effects of Cadmium Toxicity. Int. J. Environ. Res. Public Health 17.

https://doi.org/10.3390/ijerph17113782

Habig, W.H., Pabst, M.J., Jakoby, W.B., 1974. Glutathione S-transferases. The first enzymatic step in mercapturic acid formation. J. Biol. Chem. 249, 7130–7139.

Li, L., Tian, X., Yu, X., Dong, S., 2016. Effects of Acute and Chronic Heavy Metal (Cu, Cd, and Zn) Exposure on Sea Cucumbers (*Apostichopus japonicus*). Biomed Res. Int. 2016, 4532697. https://doi.org/10.1155/2016/4532697

Mezynska, M., Brzóska, M.M., 2018. Environmental exposure to cadmium—a risk for health of the general population in industrialized countries and preventive strategies. Environ. Sci. Pollut. Res. 25, 3211–3232. https://doi.org/10.1007/s11356-017-0827-z

Nordberg, G.F., 2009. Historical perspectives on cadmium toxicology. Toxicol. Appl. Pharmacol. 238, 192–200. https://doi.org/10.1016/j.taap.2009.03.015

Oh, S.-H., Lim, S.-C., 2006. A rapid and transient ROS generation by cadmium triggers apoptosis via caspase-dependent pathway in HepG2 cells and this is inhibited through N-acetylcysteine-mediated catalase upregulation. Toxicol. Appl. Pharmacol. 212, 212–223. https://doi.org/10.1016/j.taap.2005.07.018

Oldani, M., Manzoni, M., Villa, A.M., Stefanini, F.M., Melchioretto, P., Monti, E., Forcella, M., Urani, C., Fusi, P., 2020. Cadmium elicits alterations in mitochondrial morphology and functionality in C3H10T1/2Cl8 mouse embryonic fibroblasts. Biochim. Biophys. Acta - Gen. Subj. 1864, 129568. https://doi.org/https://doi.org/10.1016/j.bbagen.2020.129568

Peña-Bautista, C., Vento, M., Baquero, M., Cháfer-Pericás, C., 2019. Lipid peroxidation in neurodegeneration. Clin. Chim. Acta 497, 178–188. https://doi.org/10.1016/j.cca.2019.07.037

Sabir, S., Akash, M.S.H., Fiayyaz, F., Saleem, U., Mehmood, M.H., Rehman, K., 2019. Role of cadmium and arsenic as endocrine disruptors in the metabolism of carbohydrates: Inserting the association into perspectives. Biomed. Pharmacother. 114, 108802. https://doi.org/10.1016/j.biopha.2019.108802

Sabolić, I., Breljak, D., Škarica, M., Herak-Kramberger, C.M., 2010. Role of metallothionein in cadmium traffic and toxicity in kidneys and other mammalian organs. BioMetals 23, 897–926. https://doi.org/10.1007/s10534-010-9351-z

Sarkar, A., Ravindran, G., Krishnamurthy, V., 2013. a Brief Review on the Effect of

Cadmium Toxicity: From Cellular To Organ Level. Int. J. Bio-Technology Res. 3, 2249–6858.

Satarug, S., Nishijo, M., Ujjin, P., Moore, M.R., 2018. Chronic exposure to low-level cadmium induced zinc-copper dysregulation. J. trace Elem. Med. Biol. organ Soc. Miner. Trace Elem. 46, 32–38. https://doi.org/10.1016/j.jtemb.2017.11.008

Seyfried, T.N., Shelton, L.M., 2010. Cancer as a metabolic disease. Nutr. Metab. (Lond). 7, 7. https://doi.org/10.1186/1743-7075-7-7

Singh, A., Kukreti, R., Saso, L., Kukreti, S., 2019. Oxidative Stress: A Key Modulator in Neurodegenerative Diseases. Molecules 24. https://doi.org/10.3390/molecules24081583

Sultana, R., Perluigi, M., Butterfield, D.A., 2013. Lipid peroxidation triggers neurodegeneration: A redox proteomics view into the Alzheimer disease brain. Free Radic. Biol. Med. 62, 157–169. https://doi.org/10.1016/j.freeradbiomed.2012.09.027

Thévenod, F., Fels, J., Lee, W.K., Zarbock, R., 2019. Channels, transporters and receptors for cadmium and cadmium complexes in eukaryotic cells: myths and facts. BioMetals 32, 469–489. https://doi.org/10.1007/s10534-019-00176-6

Tjälve, H., Henriksson, J., 1999. Uptake of metals in the brain via olfactory pathways. Neurotoxicology 20, 181–195.

Urani, C., Melchioretto, P., Bruschi, M., Fabbri, M., Sacco, M.G., Gribaldo, L., 2015. Impact of Cadmium on Intracellular Zinc Levels in HepG2 Cells: Quantitative Evaluations and Molecular Effects. Biomed Res Int 2015, 949514. https://doi.org/10.1155/2015/949514

Wang, B., Du, Y., 2013. Cadmium and its neurotoxic effects. Oxid. Med. Cell. Longev. 2013. https://doi.org/10.1155/2013/898034

Wang, Y., Oberley, L.W., Murhammer, D.W., 2001. Antioxidant defense systems of two lipidopteran insect cell lines. Free Radic. Biol. Med. 30, 1254–1262. https://doi.org/10.1016/s0891-5849(01)00520-2

Yang, Y., Estrada, E.Y., Thompson, J.F., Liu, W., Rosenberg, G.A., 2007. Matrix metalloproteinase-mediated disruption of tight junction proteins in cerebral vessels is reversed by synthetic matrix metalloproteinase inhibitor in focal

ischemia in rat. J. Cereb. blood flow Metab. Off. J. Int. Soc. Cereb. Blood Flow Metab. 27, 697–709. https://doi.org/10.1038/sj.jcbfm.9600375

Zhang, H., Reynolds, M., 2019. Cadmium exposure in living organisms: A short review. Sci. Total Environ. 678, 761–767. https://doi.org/10.1016/j.scitotenv.2019.04.395

Zheng, W., Perry, D.F., Nelson, D.L., Aposhian, H.V., 1991. Choroid plexus protects cerebrospinal fluid against toxic metals. FASEB J. 5, 2188–2193. https://doi.org/10.1096/fasebj.5.8.1850706

Zong, L., Xing, J., Liu, S., Liu, Z., Song, F., 2018. Cell metabolomics reveals the neurotoxicity mechanism of cadmium in PC12 cells. Ecotoxicol. Environ. Saf. 147, 26–33. https://doi.org/10.1016/j.ecoenv.2017.08.028

Chapter 4

The study of cadmium toxicity on LUHMES cell line showed the activation of Nrf2 signalling pathway and the protective role of GSH

This work was carried out at the University of Konstanz in Professor Marcel Leist' research group under the supervision of Professor Stefan Schildknecht

4.1 Introduction

The heavy metal cadmium (Cd) is a rare chemical element of non-biological function. It was discovered in 1817 by German chemist F. Strohmier, as an impurity of zinc carbonate, and from that day on cadmium compounds have been used in industry, as stabilizers in PVC products, colour pigment, in re-chargeable Ni–Cd batteries, as anticorrosion agent, and in agriculture as a pollutant in phosphate fertilizers, with about 22,000 tons produced yearly worldwide (IARC, 2012; Rani et al., 2014). This extensive use of cadmium by anthropogenic activities caused a widespread distribution of this element in the environment and the absence of a biodegradation mechanism led the scientific community to investigate the adverse effects of this metal. Several studies have been performed since the middle of the 19th century, underlying cadmium toxicity on organisms and leading to the classification of cadmium as one of the main environmental and occupational chemical pollutants in industrialised countries (Mezynska and Brzóska, 2018; Nordberg, 2009). Cadmium exposure can provoke damage to several organs, such as kidney, liver, lungs, brain, testes and heart. Moreover, it is a bio-accumulative element with an estimated half-life of 20-30 years in human.

Lungs and the gastrointestinal tract are the main entry pathways for cadmium in humans. Following its absorption through voltage gated calcium channels (VGCC), divalent metal transporter 1 (DMT1) and zinc transporters ZIP8 and ZIP14 in the lungs and/or intestine, cadmium primarily binds to albumin and other thiol-containing reactive biomolecules in the plasma, as well as on red blood cell membranes, making the blood stream responsible for its transport inside the organism (Genchi et al., 2020; Thévenod et al., 2019). Despite the fact that this xenobiotic mainly accumulates in the liver and kidneys and that under physiological conditions it cannot reach the blood brain barrier (BBB), cadmium neurotoxicity has been reported (Méndez-Armenta and Ríos, 2007; Wang and Du, 2013).

There are two routes for cadmium entrance into the central nervous system (CNS): BBB and the olfactory nerves. Acute cadmium exposure is blocked by the BBB; however a chronic exposure weakens the cellular antioxidant defences with a consequent increase in the level of reactive oxygen species (ROS), that activate matrix metalloproteinase responsible for BBB tight junctions disruption leading to increase

in permeability (Branca et al., 2020; Yang et al., 2007). An *in vivo* study on adult rats showed how a small amount of cadmium reaches the brain, due to selective permeability of BBB, while it might diffuse across the barrier with the help of a vehicle such as ethanol (Pal et al., 1993). Regarding the second route, the metal can be transported along the primary olfactory neurons and reach the termination in the olfactory bulbs bypassing the intact BBB (Tjälve and Henriksson, 1999). Kumar and colleagues suggested that the effect of cadmium in brain is region-specific and most pronounced in the olfactory bulb, since they observed a decrease in membrane fluidity, phosphatidylcholine and phosphatidylethanolamine content, as well as an increase in intracellular calcium level in olfactory bulb of rats after cadmium exposure (Kumar et al., 1996).

Once inside the CNS, cadmium enters the cerebrospinal fluid (CSF), through which it can reach a specific part of the CNS, and accumulates in the BBB, in the CSF and in the choroid plexus (CP), showing a weak integrity of the blood-cerebrospinal fluid barrier, despite the presence of several efflux mechanisms responsible for traffic's control in and out the brain (Karri et al., 2016; Yokel, 2006). Even in the nervous system, cadmium ions inside cells bind metallothioneins (MTs), forming Cd-MT as the first detoxification mechanism. However not only a small amount of cadmium is not bound by MTs, but also the metal accumulation reduces the pool of free MTs, leading to free cadmium ions in the cytosol exerting their toxicity.

One important mechanism by which cadmium toxicity takes place is represented by oxidative stress. Despite the fact that this metal is unable to directly generate ROS; cadmium exposure resulted in an increase in ROS production, through displacement of redox-active metals in proteins and weakening of antioxidant defence mechanisms (Casalino et al., 1997; Cuypers et al., 2010; Dudley and Klaassen, 1984; Nair et al., 2013; Rani et al., 2014). Due to its high affinity for sulfhydryl groups (-SH), cadmium binds glutathione (GSH) causing the depletion of the GSH pools and the alteration of the cellular redox balance with consequent increase in oxidative stress. Moreover, cadmium affects the enzymatic activities of antioxidant enzymes involved in GSH metabolism, such as glutathione peroxidase (GPx) and glutathione reductase (GR) (Nair et al., 2013). Cadmium atoms also combine with selenium ones and they are

excreted via the bile system, causing a depletion in the amount of selenium from the body, which leads to less selenium for GPx formation (Rani et al., 2014).

The aim of this work is the study of cadmium neurotoxicity on a differentiated neuronal model represented by Lund human mesencephalic (LUHMES) neuronal cell line. This cell line has been originated in 2005 at Lund University (Lund, Sweden) as a subclone of the tetracycline-controlled, v-*myc*-overexpressing human mesencephalon-derived cell line MESC2.10 (Lotharius et al., 2005, Lotharius et al., 2002). The transformation of committed neural precursor cells with *myc* oncogenes ensures both immortalization and continuous proliferation, with neuronal differentiation obtained through inactivation of the oncogene after exposure to neurotrophic factors or tetracycline-controlled gene expression (Scholz et al., 2011). LUHMES cells possess a high conversion rate to post-mitotic neurons (>99%) after a quick and relative synchronized differentiation, making this cell line an interesting model system for several applications, such as the study of processes involved in neurodegenerative diseases as well as neurodevelopmental studies and the evaluation of environmental neurotoxicity (Scholz et al., 2011).

Metal administration caused a dose-dependent reduction in LUHMES viability, and in GSH and ATP content; moreover, cadmium treatment induced the activation of Nuclear factor erythroid 2-related factor 2 (Nrf2), and its adversity could be rescued by GSH addition. Finally, cadmium effect on cell viability was investigated in a co-culture model of LUHMES and BV2 (murine microglia cell line) and in the presence of astrocyte-conditioned medium, showing not only a protective effect by glia, but also the importance of more complex cell line models.

4.2 Materials and methods

4.2.1 Cell cultures

LUHMES cells were cultured as described by Scholtz et al. (Scholz et al., 2011) in 50 µg/ml poly-L-ornithine/1 µg/ml fibronectin pre-coated flask and multi-well plates. Proliferating LUHMES cells were grown in proliferation medium, composed of advanced DMEM/F12 supplemented with 2 mM L-glutamine, 1x N2 supplement and 40 µg/mL FGF, at 37°C in a humidified atmosphere with 5% CO_2 and were splitted at an approximately 80% confluence. For differentiation 8 million cells were seeded

in a pre-coated T175 flask in proliferation medium and after 24h the medium was replaced by differentiation medium, consisting of advanced DMEM/F12 supplemented with 2 mM L-glutamine, 1 mM dibutyryl 3′,5′-cyclic adenosine monophosphate (cAMP), 2 ng/mL recombinant human glial cell-derived neurotrophic factor (GDNF) and 2,25 μM tetracycline. Differentiated LUHMES cells were seeded on day 2 at 3×10^5 cells/cm^2 and treated on day 6.

Mouse microglia cell line BV-2 was grown in DMEM/F-12 medium containing 10% FBS, 4 mM L-glutamine, 100 U/mL penicillin, 100 μg/mL streptomycin and maintained at 37 °C in a humidified 5% CO_2 incubator. BV-2 monoculture or in co-culture with LUHMES cells were seeded on day 5 of LUHMES cells differentiation at a confluence of 3×10^4 cells/cm^2 giving a BV-2 cells confluence equal to 10% of LUHMES cells. Conditioned medium (CM) was obtained from BV-2 cells seeded with a confluence of 3×10^4 cells/cm^2 in a 6 wells plate. After the incubation, the medium was centrifuged, to remove cell debris. Then, the CM was transferred to LUHMES cells on day 6.

Human astrocytes, differentiated from human stem cells H9 (Palm et al. 2015), were grown in DMEM/F12, 2 mM L-glutamine, 0.5x N2, 0.5x B27 and 1% FBS in 37°C incubator with 5% CO_2. CM was obtained from human astrocytes seeded with a confluence of 3×10^4 cells/cm^2 in a 6 wells plate. After the incubation, the medium was centrifuged and cell debris. Then, the CM was transferred to LUHMES cells and LUHMES-BV2 co-culture on day 6.

All the reagents were supplied by Sigma Aldrich (Merck KGaA, Darmstadt, Germany).

4.2.2 Viability assay

Cell viability was determined through resazurin reduction and LDH assay. Briefly, a resazurin solution was added to the cell medium to obtain a final concentration of 10 μg/mL. After a 60 min incubation at 37°C, the fluorescence signal was measured at an excitation wavelength of 530 nm, using a 590-nm long-pass filter to record the emission. Viabilities were expressed as a percentage of the untreated controls. Each experiment was performed in three replicate wells for each metal concentration, and the results are presented as the mean of at least three independent experiments.

LDH activity was detected in both the supernatant and cell homogenate. The medium was transferred into a separate plate and stored at 4°C; while the cells were lysed in 100 µL in a 0.1% Triton X-100/PBS (10 mM K_2HPO_4, 150 mM NaCl, pH 7.2) solution overnight at 4°C under shaking. Subsequently, 20 µL of each samples were added to 180 µL of reaction buffer containing 100 µM NADH and 600 µM sodium pyruvate in potassium-phosphate buffer (KPP-buffer, pH 7.4). Absorption at 340 nm was measured at 37 °C in 1 min intervals over a period of 15 min. The slope of the absorption intensity was calculated and the ratio of LDH supernatant/LDH total was calculated using the slopes of supernatant and homogenate. LDH release was expressed in percent.

All the reagents were supplied by Sigma Aldrich (Merck KGaA, Darmstadt, Germany).

4.2.3 GSH assay

For determination of GSH content, cells were lysed in 100 µL/well of 1% SSA and scratched to ensure complete lysis. Experimental determinations of GSH amount was performed in a reaction mix containing 100 µM DTNB (5,5′-Dithiobis(2-nitrobenzoic acid)), 200 µM NADPH and 0.46 U/mL glutathione reductase added to the GSH-buffer (100 mM Na_2HPO_4, 1 mM EDTA, pH 7.5). 40 µL of each cell lysate was transferred into a new 96-well plate and 60 µL of MilliQ water were added. Additionally, a calibration curve was prepared (0-10 µM GSH) and treated like the samples. Then, 100 µL of reaction mix were added to each well and absorbance at 405 nm was measured immediately, as well as after 20 and 30 minutes using a micro plate reader. All values were converted into molarity of GSH and normalized to the percentage of untreated cells. Each experiment was performed in three replicate wells for each metal concentration, and the results are presented as the mean of at least three independent experiments.

All the reagents were supplied by Sigma Aldrich (Merck KGaA, Darmstadt, Germany).

4.2.4 ATP assay

For the detection of ATP level, a commercially available ATP assay reaction mixture CellTiter-Glo (Promega, Madison, WI, USA), containing luciferin and luciferase, was used. 50 μL of a 1:1 mixture of 0.5% Triton-X 100 and CellTiter-Glo solution was added to the cells grown in 96-well plates. After a 2 minutes RT incubation 100 μL of each sample were transferred to a black 96-well plate. Additionally, a calibration curve was prepared (0-10 μM ATP) and treated like the samples. Luminescence was measured, values were converted into molarity of ATP and normalized to the percentage of untreated cells. Each experiment was performed in three replicate wells for each metal concentration, and the results are presented as the mean of at least three independent experiments.

4.2.5 SDS-PAGE and Western Blotting

To examine the effect of cadmium on Nrf2 pathway, differentiated LUHMES were treated on day 6 with $CdCl_2$ 5μM for 24 h.

The cells were lysed in RIPA buffer containing 1 μM leupeptin, 2 μg/mL aprotinin, 1 μg/mL pepstatin, 1 mM PMSF (phenylmethylsulfonyl fluoride) and phosphatase inhibitors. Lysates were transferred into a NucleoSpin filter and centrifuged at 10,000 × g, for 1 min to remove all DNA and RNA. Flow-through was collected and proteins amount was quantified using a BCA protein assay (Smith et al., 1985).

SDS-PAGE and Western blotting were performed by standard procedures (Laemmli, 1970). Twenty micrograms of proteins were separated on 10-15% acrylamide/bis-acrylamide gels depending on the size of the target proteins and transferred onto a nitrocellulose membrane using iBlot 2 at 20V for 3-5 min. The membrane was subsequently blocked for 30 min in 5% (w/v) BSA in TBS and incubated overnight at 4 °C probed with the appropriate primary antibodies. The following primary antibodies were used: mouse anti-NF200 (dilution 1:1000) (N0142 Sigma-Aldrich, Merck, Darmstad, Germany), mouse anti-Nrf2 (dilution 1:1000) (sc518033 Santa Cruz Biotechnology, Dallas, TX, USA), rabbit anti-p21 (dilution 1:1000) (#29475, Cell Signaling Technology, Danvers, MA, USA), rabbit anti-Akt (dilution 1:1000) (#9272, Cell Signaling Technology, Danvers, MA, USA), rabbit anti-phospho-Akt (dilution 1:1000) (#9272S, Cell Signaling Technology, Danvers, MA, USA), rabbit

anti-phospho-GSK3β (dilution 1:1000) (#558P, Cell Signaling Technology, Danvers, MA, USA) and mouse anti-GAPDH (dilution 1:500) (ab9484, Abcam, Cambridge, UK). After three washing (10 min each) in TBS, 0.1% (v/v) Tween 20, the membrane was incubated for 1 h with anti-mouse IgG HRP-conjugated secondary antibodies diluted 1:10000 (AB_10015289, Jackson ImmunoResearch, Cambridge, UK) and anti-rabbit IgG HRP-conjugated secondary antibodies diluted 1:5000 (AB_2307391, Jackson ImmunoResearch, Cambridge, UK). After three washing (10 min each) in TBS, 0.1% (v/v) Tween 20, proteins were visualized using ECL detection system. Protein levels were quantified by densitometry of immunoblots using ImageJ software.

All the reagents were supplied by Sigma Aldrich (Merck KGaA, Darmstadt, Germany).

4.2.6 Real-time quantitative PCR analysis

In order to evaluate cadmium effect on antioxidant, Nrf2-controlled ARE genes, a RT-qPCR on differentiated LUHMES treated on day 6 with $CdCl_2$ 5 μM for 24 h was performed.

Total RNA was extracted from both control and treated cells using PureLink RNA Mini Kit (Thermo Fisher Scientific, Waltham, MA, USA) and quantified using NanoDrop 1000 Spectrophotometer (Thermo Fisher Scientific, Waltham, MA, USA). cDNA was generated using iScript™ Reverse Transcription Supermix (Bio-Rad, Hercules, CA, USA) for 5 min at 25 °C, 20 min at 46°C and the reverse-transcriptase was inactivated for 1 min at 95 °C. All RT-PCRs were based on the SsoFast EvaGreen detection system, were run in a CFX96 Cycler and analysed with Biorad iCycler software. A comparative threshold cycle (CT) method was used to analyze the RT PCR data. The amount of target genes, normalized to the endogenous reference of *PGK and RPL13A* rDNA *primers* (ΔCT) and relative to the calibrator of untreated CTR (ΔΔCT), was calculated by the equation $2^{-\Delta\Delta CT}$ as previously described (Livak and Schmittgen, 2001).

4.2.7 Statistical analysis

All the experiments were carried out in triplicate. The samples were compared to their reference controls and the data were tested by Student t-test. Results were considered statistically significant at $p < 0.05$.

4.3 Results

4.3.1 Cadmium exposure reduces LUHMES cells viability and ATP and GSH intracellular content

To assess cadmium toxicity on cell viability, differentiated LUHMES cells at day 6 were treated with different metal concentrations. Cell viability dramatically dropped at concentrations higher than 10 µM, as shown from the resazurin and LDH assay in Figure 1A. Moreover, the intracellular ATP content decreased in a dose-dependent way, while the GSH content showed an increase, reaching a double value respect to control at the concentrations of 1 µM and 5 µM, and a subsequent decrease in a dose-dependent way (Figure 1B).

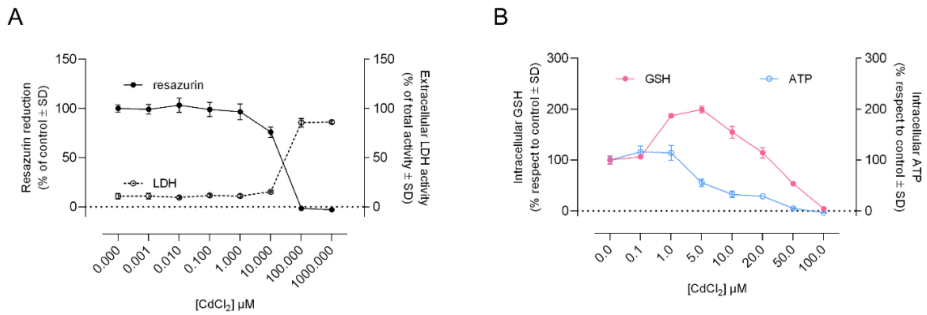

Figure 1. Cadmium effects on LUHMES cells viability.

LUHMES cells were treated on day 6 with $CdCl_2$ in a range of 0-1000 µM. After 24h the cells were analysed by resazurin assay and LDH assay (A), GSH and ATP assay (B). Data were reported as percentage normalized to the untreated cells. Data were reported as mean ± SD of at least three independent experiments.

4.3.2 Cadmium induces Nrf2 protein activation through p21 and P-Akt

Since cadmium can induce oxidative stress and Nrf2 represents a first line defence against oxidative metabolism alterations, we investigated both Nrf2 protein

expression level and mRNA level on day 6 LUHMES cells treated with 5 μM $CdCl_2$ for 24h. Cadmium treatment increased Nrf2 protein expression of about 2-fold compared to control, without altering its mRNA level, which remained constant, suggesting an activation through protein stabilization rather than an increase in transcription (Figure 2).

This enhanced protein level led us to perform further analysis on possible Nrf2-mediators. We decided to focus our attention on p21, which is able to contribute to basal and inducible antioxidant response through its binding to Nrf2 domains required for Keap1-mediated ubiquitination and degradation (Chen et al., 2009), and to GSK3β, which promotes Nrf2 degradation by decreasing its stability in a Keap1-indipendent way (Chowdhry et al., 2013). Moreover, the level of phosphorylated Akt was analysed as well, since not only GSK3β is negatively regulated by the PI3K-Akt axis, but this axis is also a positive Nrf2 regulator (Huang et al., 2015). Our results, reported in Figure 2A-B, showed not only a significant increase of about 10-fold in the expression level of p21, but also in phosphorylated, active Akt and in phosphorylated, inactive GSK3β, in the presence of 5 μM $CdCl_2$. The enhanced level of these proteins led us hypothesize that Nrf2 activation could be mediated by p21 and P-Akt.

Cadmium exposure led to an increase in Nrf2 protein level, which in turn can lead to an enhanced transcriptional activity of Nrf2-controlled genes. Among the over 200 antioxidant response element (ARE) genes controlled by this transcriptional factor, we focused our attention on the ones involved in the synthesis and metabolism of glutathione, as well as the genes coding for heme oxygenase and superoxide dismutase, due to cadmium indirect ability in oxidative stress induction. Cadmium 24h exposure triggered a significant increase of more than 10-fold in *GCLM* and of 150-fold in *HMOX1* transcripts, responsible for the coding of glutamate-cysteine ligase modifier subunit and heme oxygenase 1 respectively (Figure 2C). No differences were observed in the mRNA level of genes coding for glutathione S-transferases (*GSTT1* and *GSTM1*), glutamate-cysteine ligase catalytic subunit (*GCLC*), glutathione synthetase (*GSS*), glutathione reductase (*GSR*) and superoxide dismutases (*SOD1* and *SOD2*), that was found similar in untreated cells as shown in Figure 2C.

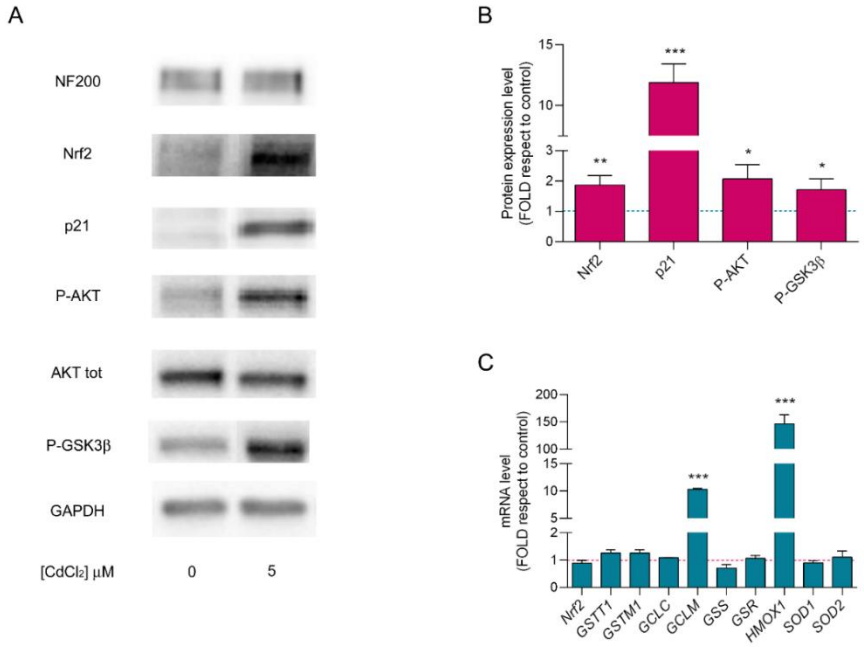

Figure 2. Analysis of Nrf2 activation pathway and Nrf2-controlled genes on cadmium treated LUHMES cells.

A) Representative Western blot analyses performed on differentiated LUHMES cells treated with 5 µM $CdCl_2$ on day 6 for 24 h. Protein extracts were separated on a 12% SDS-PAGE and probed with anti-NF200 (marker of differentiation), anti-Nrf2, anti-p21, anti-P-Akt, anti-Akt and anti P-GSK3β antibodies. GAPDH was used as a loading control. The experiments were performed in triplicate. B) Densitometric analysis was performed with ImageJ Software. Data are expressed by comparing the data obtained after Cd treatment with those of control cells and are presented as means ± SD. C) mRNA expression of *Nrf2*, *GSTT1*, *GSTM1*, *GCLC*, *GCLM*, *GSS*, *GSR*, *HMOX1*, *SOD1* and *SOD2* genes. The expression was monitored by RT-PCR and normalized to *PGK and RPL13A* rDNA *primers*. Expression profiles were determined using the $2^{-\Delta\Delta CT}$ method. Data are expressed by comparing the data obtained after cadmium treatment with control cells and are presented as means ± SD. Statistically significant: * $p < 0.05$, ** $p < 0.01$, *** $p < 0.001$

4.3.3 Glutathione rescues LUHMES cells loss of viability induced by cadmium

As the results obtained on cadmium-treated LUHMES cells showed alterations in glutathione metabolism, with a first high increase in glutathione content followed by a dose-dependent reduction and enhanced Nrf2 protein level with elevated *GCLM* transcription, we decided to investigate cell viability in the presence of both cadmium and reduced glutathione (GSH).

A pre-treatment with a range of GSH concentrations in the presence of fixed 20 µM $CdCl_2$ showed a rescue in cell viability in a dose-dependent manner after 24h, as shown by resazurin reduction and LDH assay in Figure 3A, suggesting a protective effect of GSH. Moreover, this protection was confirmed when LUHMES cells were pre-treated with 500 µM GSH and subsequently exposed to a range of cadmium concentrations: cell viability remained comparable to control with only a slight reduction (84% viability) at the highest dose (Figure 3B). In conclusion, we can assume that GSH exerts a protective function on LUHMES cells in the presence of cadmium, keeping the cells viable compared to the differentiated neurons exposed only to the toxicant (Figure 3C).

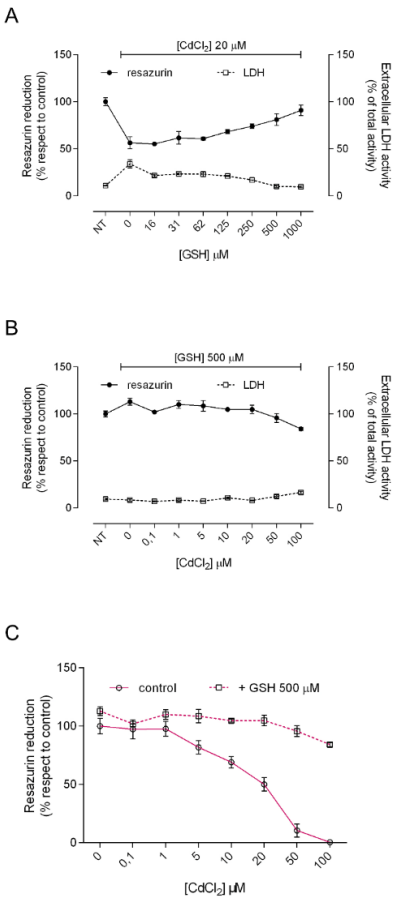

Figure 3. Protective role of GSH on LUHMES cells treated with cadmium.

A) LUHMES cells were pre-treated on day 6 with GSH (0-1000 µM) for 1h and then treated with 20 µM $CdCl_2$. After 24h, cell viability was evaluated by resazurin assay and LDH assay. Data were reported as percentage normalized to untreated (NT) cells. Data were reported as mean ± SD of at least three independent experiments. B) LUHMES cells were pre-treated on day 6 with 500 µM GSH for 1h and then treated with 0-100 µM $CdCl_2$. After 24h, cell viability was evaluated by resazurin assay and LDH assay. Data were reported as percentage normalized to untreated (NT) cells. Data were reported as means ± SD of at least three independent experiments. C) Comparative graph of LUHMES cells treated on day 6 with only 0-100 µM $CdCl_2$ (control) and LUHMES cells pre-treated on day 6 with 500 µM GSH for 1h and then treated with 0-100 µM $CdCl_2$ (+ GSH 500 µM).

4.3.4 Evaluation of cadmium toxicity on viability in a LUHMES-BV2 co-culture model and in astrocytes CM

Microglia are the resting macrophages of the CNS. They rapidly respond to brain injury and disease by altering their morphology and phenotype to adopt an activated state, which takes place upon exposure to different stimuli, including trauma to brain or spinal cord, ischemia, infection, air pollutants, neurotoxic agents and dysregulated cellular functions (Block and Hong, 2007; Davalos et al., 2005). In physiological conditions, microglia monitor the surrounding microenvironment, using their ramifications as sentinels; while in neuropathological conditions or in the presence of infectious agents, they rapidly activate, adopting an amoeboid phenotype characterized by a large cell body. Depending on the source of the signal, microglia give a specific response, which includes phagocytosis, increased migration, proliferation and release of bioactive molecules (Soulet and Rivest, 2008). Although, the activation of microglia has a neuroprotective function, its hyperactivation can cause neurotoxicity through the release of inflammatory cytokines and chemokines (Block and Hong, 2007).

In the CNS the most abundant glial cells are represented by astrocytes, essential in synapse formation and function, in ion and neurotransmitter concentrations, contributing to the integrity of BBB and to brain homeostasis and neuronal survival (Heithoff et al., 2021). Astrocytes are also in contact with different brain cells as well as the vasculature, thereby coupling neurons and other brain cells to blood supply through astrocytic end feet.

Since in the nervous system the glial cells play an important role in neurons' protection against injuries and toxicants, we evaluated cadmium toxicity on LUHMES cells viability in a co-culture with murine microglia BV2 cell line, as well as in astrocytes or BV2 CM.

LUHMES and BV2 cells showed quite a similar dose-dependent reduction in cell viability after a 24h treatment with cadmium; a dose-dependent reduction was seen also in the co-culture system, even if accompanied by a slight improvement of viability (Figure 4A-B). In the presence of cadmium, BV2 and LUHMES-BV2 cells intracellular total GSH content does not increase as in LUHMES cells, but remains

comparable to control until the dose of 10 µM, dropping dramatically at higher concentrations (Figure 4C). Regarding ATP, we observed a lower dose-dependent reduction in co-cultures compared to LUHMES cells, as seen in Figure 4D.

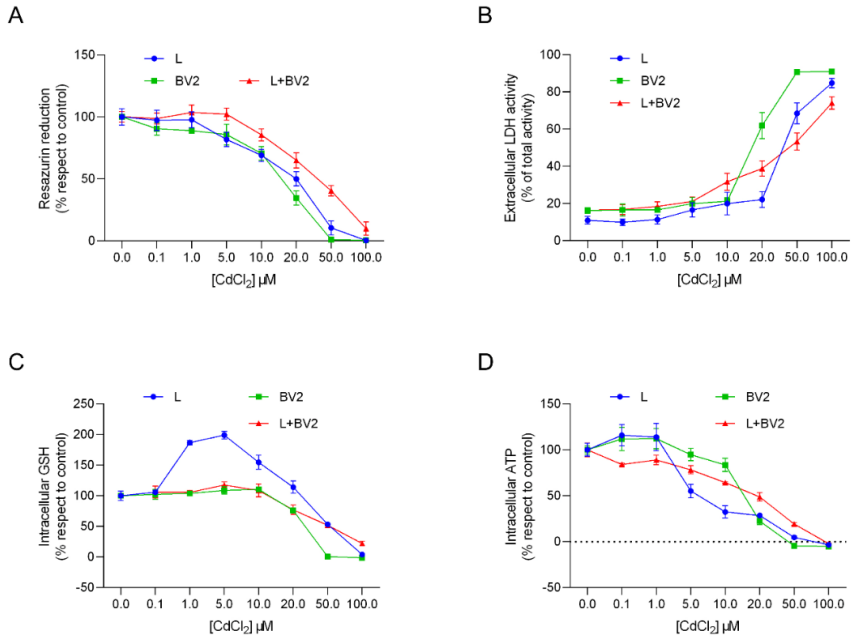

Figure 4. Cadmium effects on LUHMES-BV2 cells viability.
BV2 cells were added to LUHMES cells on day 5 and the treatment was performed on day 6 with $CdCl_2$ concentrations in a range of 0-100 µM. After 24h the cells were analysed by resazurin reduction (A), LDH assay (B), GSH assay (C) and ATP assay (D). Data were reported as percentage normalized to the untreated cells. Data were reported as mean ± SD of at least three independent experiments.

LUHMES cells viability in the presence of BV2 cells and astrocytes CM showed a resistance to cadmium toxicity, with a lower viability reduction than LUHMES cells alone. In particular, at the highest dose of 100 µM, $CdCl_2$ cells viability in astrocytes CM was about 50% of the initial value (Figure 5A-B). The total GSH content in both CMs remained constant and similar to the control at all the concentrations tested (Figure 5C); while the ATP level reduced in a dose-dependent way more dramatically in BV2 cells supplemented with CM than in the astrocytes (Figure 5D). The co-culture viability, together with total GSH and ATP content, in astrocytes CM was also

evaluated. As shown in Figure 5, LUHMES-BV2 co-cultured in astrocyte CM behaved in the same way as LUHMES cells in astrocyte CM, underlying the stronger protective role of astrocyte rather than microglia.

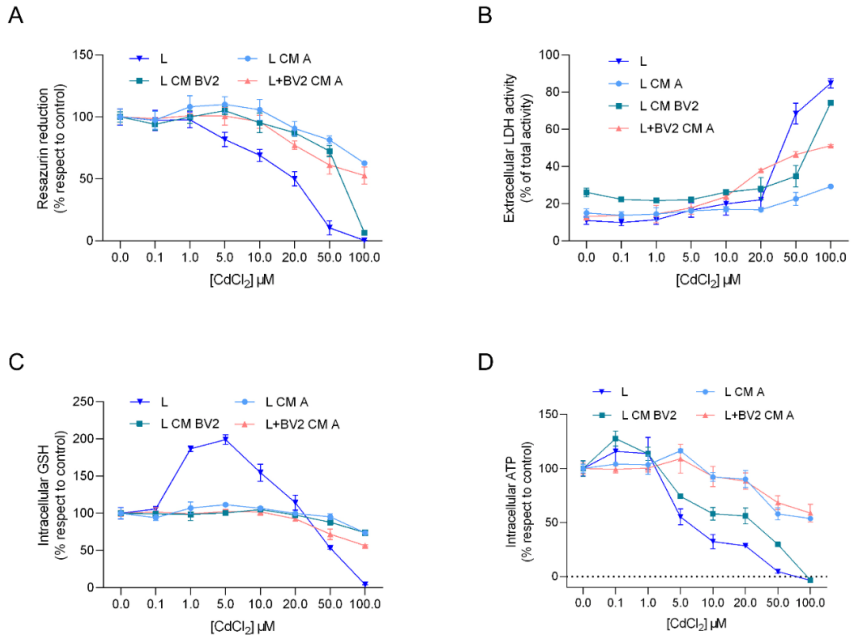

Figure 5. Viability of LUHMES cells in astrocyte and BV2 CM and of LUHMES-BV2 co-cultures in astrocyte CM after cadmium exposure.

BV2 cells were added to LUHMES cells on day 5 and the treatment was performed on day 6 in either BV2 or astrocytes CM with $CdCl_2$ concentrations in a range of 0-100 µM. After 24h the cells were analysed by resazurin reduction (A), LDH assay (B), GSH assay (C) and ATP assay (D). Data were reported as percentage normalized to the untreated cells. Data were reported as means ± SD of at least three independent experiments.

4.4 Discussion

The evaluation of cadmium neurotoxicity on differentiated neurons was carried out using LUHMES cell line as a model, due to its inducible, quick and relative synchronized differentiation (Scholz et al., 2011). As expected, metal administration caused a reduction of cell viability in a dose-dependent way, with a complete neurons'

death at the highest dose. Moreover, the analysis of ATP and GSH level, as indicators of energy metabolism and oxidative stress, underlined a cell altered homeostasis after cadmium exposure. In particular the dose-dependent decrease in ATP level indicates a reduced mitochondrial functionality, probably due to the electron transport chain disruption caused by cadmium binding to complex II and/or III, leading to ROS overproduction. This, in turn, would lead to a widespread impairment in oxidative balance, which is confirmed by the strong increase in GSH level at the lower $CdCl_2$ doses, reaching a peak at 5 µM, followed by a dramatical dose-dependent decrease. Since GSH is one of the major non enzymatic antioxidant defence mechanism and since high oxidative stress is one of the main mechanisms through which cadmium exerts its toxicity, we have focused our attention on Nrf2.

The transcriptional factor (TF) Nrf2 is an important player in cellular homeostasis maintenance. Under physiological conditions it is negatively regulated by Keap1, which binds Nrf2 leading to its ubiquitination and proteasomal degradation. However, upon stress conditions, Keap1 dissociates from Nrf2, which consequently accumulates in the cytosol and translocates to the nucleus where it binds to ARE genes activating them. The Nrf2 pathway acts as a complementary signal in enhancing the action of antioxidant systems against oxidative damage. Our results showed, upon 24h treatment with 5 µM $CdCl_2$, an enhanced Nrf2 protein level, but no variation in mRNA level, leading us to hypothesize that this metal administration caused alterations in oxidative balance with consequent cytosolic Nrf2-protein stabilization; this was confirmed by the expression level of p21 and phosphorylation levels of both GSK3β and Akt. The over 10-fold increase of p21 together with a nearly 2-fold increase in P-GSK3β and P-Akt suggest the disruption of Keap1-Nrf2 complexes. In fact, p21 and P-Akt are positive regulators of Nrf2 activation: p21 and Keap1 bind on the same domain on Nrf2, but with opposite functions; while P-Akt phosphorylates GSK3β inhibiting it and cancelling its negative effect on Nrf2 (Chen et al., 2009; Chowdhry et al., 2013). A further evidence of alteration in oxidative homeostasis leading to Nrf2 activation is given by the increased transcriptional levels of *GCLM* and *HMOX1*, coding for glutamate-cysteine ligase modified subunit and heme oxygenase 1 rispectively. These are two important proteins involved in oxidative stress metabolism, since glutamate-cysteine ligase reaction is the rate limiting step of GSH

synthesis, while heme oxygenase 1 is a stress inducible enzyme involved in ROS detoxification. Moreover, not only Nrf2 is activated after cadmium exposure, but its over-expression also exerts a protective role against cadmium toxicity, making the regulation of this TF a possible therapeutic approach (Al-Ghafari et al., 2019; Ashrafizadeh et al., 2020; Chen and Shaikh, 2009; Khan et al., 2019; Wang and Gallagher, 2013; Wu et al., 2012). Further analysis of Nrf2 activation and downstream effectors at different times after cadmium exposure and/or at different concentrations should be performed in order to better investigate its activation in the presence of this toxicant.

Since an acute, but especially a prolonged cadmium exposure, is responsible for the reduction of GSH pool, due to cadmium high affinity for -SH groups, we decided to investigate LUHMES cells viability when GSH was added to the cultures. In the presence of cadmium, a pre-treatment with GSH increased cell viability; in particular, 500 µM GSH restored LUHMES cells viability compared to control cells, even at the highest $CdCl_2$ doses at which in the absence of GSH the viability is completely null, suggesting a protective role of GSH on LUHMES cells viability. This could be due to either to a bigger pool of GSH that scavenge cadmium, or to a higher antioxidant defence potential; the evaluation of the GSH/GSSG ratio in both control and pre-treated cells, together with Nrf2 signalling pathway should be the following steps.

We have to take into account that the CNS is not only made by neurons, but the glial cells (astrocytes, microglia, oligodendrocytes) are of vital importance for brain architecture and functions. Therefore, for a more appropriate approach to the study of cadmium neurotoxicity we evaluated LUHMES cells viability in a co-culture system with BV2, a murine microglial cell line, and in astrocyte or microglia CM. Our results showed an increased LUHMES cells viability in astrocytes and BV2 CM, while LUHMES-BV2 co-culture alone behaved quite similarly to LUHMES cells. ATP levels are increased both in the co-culture and in the presence of CM, but what is really interesting is the disappearance of GSH initial peak when cells are treated with CM, leading us to hypothesize a possible external GSH uptake. This could be another important role of GSH and the evaluation of Nrf2 in LUHMES cells treated with either astrocytes or BV2 CM could be an interesting approach. Moreover, these data show

the protective effects of glial cells and the importance of more complex experimental model for the study of cadmium neurotoxicity.

References

Al-Ghafari, A., Elmorsy, E., Fikry, E., Alrowaili, M., Carter, W.G., 2019. The heavy metals lead and cadmium are cytotoxic to human bone osteoblasts via induction of redox stress. PLoS One 14, e0225341. https://doi.org/10.1371/journal.pone.0225341

Ashrafizadeh, M., Ahmadi, Z., Farkhondeh, T., Samarghandian, S., 2020. Back to Nucleus: Combating with Cadmium Toxicity Using Nrf2 Signaling Pathway as a Promising Therapeutic Target. Biol. Trace Elem. Res. 197, 52–62. https://doi.org/10.1007/s12011-019-01980-4

Block, M.L., Hong, J.-S., 2007. Chronic microglial activation and progressive dopaminergic neurotoxicity. Biochem. Soc. Trans. 35, 1127–1132. https://doi.org/10.1042/BST0351127

Branca, J.J.V., Fiorillo, C., Carrino, D., Paternostro, F., Taddei, N., Gulisano, M., Pacini, A., Becatti, M., 2020. Cadmium-induced oxidative stress: Focus on the central nervous system. Antioxidants 9, 1–21. https://doi.org/10.3390/antiox9060492

Casalino, E., Sblano, C., Landriscina, C., 1997. Enzyme activity alteration by cadmium administration to rats: the possibility of iron involvement in lipid peroxidation. Arch. Biochem. Biophys. 346, 171–179. https://doi.org/10.1006/abbi.1997.0197

Chen, J., Shaikh, Z.A., 2009. Activation of Nrf2 by cadmium and its role in protection against cadmium-induced apoptosis in rat kidney cells. Toxicol. Appl. Pharmacol. 241, 81–89. https://doi.org/10.1016/j.taap.2009.07.038

Chen, W., Sun, Z., Wang, X.-J., Jiang, T., Huang, Z., Fang, D., Zhang, D.D., 2009. Direct interaction between Nrf2 and p21(Cip1/WAF1) upregulates the Nrf2-mediated antioxidant response. Mol. Cell 34, 663–673. https://doi.org/10.1016/j.molcel.2009.04.029

Chowdhry, S., Zhang, Y., McMahon, M., Sutherland, C., Cuadrado, A., Hayes, J.D., 2013. Nrf2 is controlled by two distinct β-TrCP recognition motifs in its Neh6 domain, one of which can be modulated by GSK-3 activity. Oncogene 32, 3765–3781. https://doi.org/10.1038/onc.2012.388

Cuypers, A., Plusquin, M., Remans, T., Jozefczak, M., Keunen, E., Gielen, H.,

Opdenakker, K., Nair, A.R., Munters, E., Artois, T.J., Nawrot, T., Vangronsveld, J., Smeets, K., 2010. Cadmium stress: an oxidative challenge. Biometals an Int. J. role Met. ions Biol. Biochem. Med. 23, 927–940. https://doi.org/10.1007/s10534-010-9329-x

Davalos, D., Grutzendler, J., Yang, G., Kim, J. V, Zuo, Y., Jung, S., Littman, D.R., Dustin, M.L., Gan, W.-B., 2005. ATP mediates rapid microglial response to local brain injury in vivo. Nat. Neurosci. 8, 752–758. https://doi.org/10.1038/nn1472

Dudley, R.E., Klaassen, C.D., 1984. Changes in hepatic glutathione concentration modify cadmium-induced hepatotoxicity. Toxicol. Appl. Pharmacol. 72, 530–538. https://doi.org/10.1016/0041-008x(84)90130-3

Genchi, G., Sinicropi, M.S., Lauria, G., Carocci, A., Catalano, A., 2020. The Effects of Cadmium Toxicity. Int. J. Environ. Res. Public Health 17. https://doi.org/10.3390/ijerph17113782

Heithoff, B.P., George, K.K., Phares, A.N., Zuidhoek, I.A., Munoz-Ballester, C., Robel, S., 2021. Astrocytes are necessary for blood-brain barrier maintenance in the adult mouse brain. Glia 69, 436–472. https://doi.org/10.1002/glia.23908

Huang, Y., Li, W., Su, Z. yuan, Kong, A.N.T., 2015. The complexity of the Nrf2 pathway: Beyond the antioxidant response. J. Nutr. Biochem. 26, 1401–1413. https://doi.org/10.1016/j.jnutbio.2015.08.001

IARC, 2012. TOXICOLOGICAL PROFILE FOR CADMIUM. U.S. Dep. Heal. Hum. Serv. Public Heal. Serv. Agency ToxicSubstances Dis. Regist.

Karri, V., Schuhmacher, M., Kumar, V., 2016. Heavy metals (Pb, Cd, As and MeHg) as risk factors for cognitive dysfunction: A general review of metal mixture mechanism in brain. Environ. Toxicol. Pharmacol. 48, 203–213. https://doi.org/10.1016/j.etap.2016.09.016

Khan, A., Ikram, M., Muhammad, T., Park, J., Kim, M.O., 2019. Caffeine Modulates Cadmium-Induced Oxidative Stress, Neuroinflammation, and Cognitive Impairments by Regulating Nrf-2/HO-1 In Vivo and In Vitro. J. Clin. Med. 8, 680. https://doi.org/10.3390/jcm8050680

Kumar, R., Agarwal, A.K., Seth, P.K., 1996. Oxidative stress-mediated neurotoxicity of cadmium. Toxicol. Lett. 89, 65–69. https://doi.org/10.1016/s0378-

4274(96)03780-0

Laemmli, U.K., 1970. Cleavage of structural proteins during the assembly of the head of bacteriophage T4. Nature 227, 680–685. https://doi.org/10.1038/227680a0

Livak, K.J., Schmittgen, T.D., 2001. Analysis of relative gene expression data using real-time quantitative PCR and the 2(-Delta Delta C(T)) Method. Methods 25, 402–408. https://doi.org/10.1006/meth.2001.1262

Lotharius, J., Barg, S., Wiekop, P., Lundberg, C., Raymon, H.K., Brundin, P., 2002. Effect of mutant α-synuclein on dopamine homeostasis in a new human mesencephalic cell line. J. Biol. Chem. 277, 38884–38894. https://doi.org/10.1074/jbc.M205518200

Lotharius, J., Falsig, J., van Beek, J., Payne, S., Dringen, R., Brundin, P., Leist, M., 2005. Progressive degeneration of human mesencephalic neuron-derived cells triggered by dopamine-dependent oxidative stress is dependent on the mixed-lineage kinase pathway. J. Neurosci. 25, 6329–6342. https://doi.org/10.1523/JNEUROSCI.1746-05.2005

Méndez-Armenta, M., Ríos, C., 2007. Cadmium neurotoxicity. Environ. Toxicol. Pharmacol. 23, 350–358. https://doi.org/10.1016/j.etap.2006.11.009

Mezynska, M., Brzóska, M.M., 2018. Environmental exposure to cadmium—a risk for health of the general population in industrialized countries and preventive strategies. Environ. Sci. Pollut. Res. 25, 3211–3232. https://doi.org/10.1007/s11356-017-0827-z

Nair, A.R., DeGheselle, O., Smeets, K., Van Kerkhove, E., Cuypers, A., 2013. Cadmium-induced pathologies: Where is the oxidative balance lost (or not)? Int. J. Mol. Sci. 14, 6116–6143. https://doi.org/10.3390/ijms14036116

Nordberg, G.F., 2009. Historical perspectives on cadmium toxicology. Toxicol. Appl. Pharmacol. 238, 192–200. https://doi.org/10.1016/j.taap.2009.03.015

Pal, R., Nath, R., Gill, K.D., 1993. Influence of ethanol on cadmium accumulation and its impact on lipid peroxidation and membrane bound functional enzymes (Na+, K(+)-ATPase and acetylcholinesterase) in various regions of adult rat brain. Neurochem. Int. 23, 451–458. https://doi.org/10.1016/0197-0186(93)90129-s

Rani, A., Kumar, A., Lal, A., Pant, M., 2014. Cellular mechanisms of cadmium-

induced toxicity: A review. Int. J. Environ. Health Res. 24, 378–399. https://doi.org/10.1080/09603123.2013.835032

Scholz, D., Pöltl, D., Genewsky, A., Weng, M., Waldmann, T., Schildknecht, S., Leist, M., 2011. Rapid, complete and large-scale generation of post-mitotic neurons from the human LUHMES cell line. J. Neurochem. 119, 957–971. https://doi.org/10.1111/j.1471-4159.2011.07255.x

Smith, P.K., Krohn, R.I., Hermanson, G.T., Mallia, A.K., Gartner, F.H., Provenzano, M.D., Fujimoto, E.K., Goeke, N.M., Olson, B.J., Klenk, D.C., 1985. Measurement of protein using bicinchoninic acid. Anal. Biochem. 150, 76–85. https://doi.org/10.1016/0003-2697(85)90442-7

Soulet, D., Rivest, S., 2008. Microglia. Curr. Biol. 18, R506-8. https://doi.org/10.1016/j.cub.2008.04.047

Thévenod, F., Fels, J., Lee, W.K., Zarbock, R., 2019. Channels, transporters and receptors for cadmium and cadmium complexes in eukaryotic cells: myths and facts. BioMetals 32, 469–489. https://doi.org/10.1007/s10534-019-00176-6

Tjälve, H., Henriksson, J., 1999. Uptake of metals in the brain via olfactory pathways. Neurotoxicology 20, 181–195.

Wang, B., Du, Y., 2013. Cadmium and its neurotoxic effects. Oxid. Med. Cell. Longev. 2013. https://doi.org/10.1155/2013/898034

Wang, L., Gallagher, E.P., 2013. Role of Nrf2 antioxidant defense in mitigating cadmium-induced oxidative stress in the olfactory system of zebrafish. Toxicol. Appl. Pharmacol. 266, 177–186. https://doi.org/10.1016/j.taap.2012.11.010

Wu, K.C., Liu, J.J., Klaassen, C.D., 2012. Nrf2 activation prevents cadmium-induced acute liver injury. Toxicol. Appl. Pharmacol. 263, 14–20. https://doi.org/10.1016/j.taap.2012.05.017

Yang, Y., Estrada, E.Y., Thompson, J.F., Liu, W., Rosenberg, G.A., 2007. Matrix metalloproteinase-mediated disruption of tight junction proteins in cerebral vessels is reversed by synthetic matrix metalloproteinase inhibitor in focal ischemia in rat. J. Cereb. blood flow Metab. Off. J. Int. Soc. Cereb. Blood Flow Metab. 27, 697–709. https://doi.org/10.1038/sj.jcbfm.9600375

Yokel, R.A., 2006. Blood-brain barrier flux of aluminum, manganese, iron and other metals suspected to contribute to metal-induced neurodegeneration. J.

Alzheimers. Dis. 10, 223–253. https://doi.org/10.3233/jad-2006-102-309

Chapter 5

Superoxide dismutase 1 (SOD1) and cadmium: a three models approach to the comprehension of its neurotoxic effects

Federica Bovio, Barbara Sciandrone, Chiara Urani, Paola Fusi, Matilde Forcella and Maria Elena Regonesi

This chapter is an extract of the submitted and accepted paper in Neurotoxicology

Abstract

Cadmium (Cd) is a widespread toxic environmental contaminant, released by anthropogenic activities. It interferes with essential metal ions homeostasis and affects protein structures and functions by substituting zinc, copper and iron. In this study, the effect of cadmium on SOD1, a CuZn metalloenzyme catalyzing superoxide conversion into hydrogen peroxide, has been investigated in three different biological models. We first evaluated the effects of cadmium combined with copper and/or zinc on the recombinant GST-SOD1, expressed in *E. coli* BL21. The enzyme activity and expression were investigated in the presence of fixed copper and/or zinc doses with different cadmium concentrations, in the cellular medium. Cadmium caused a dose-dependent reduction in SOD1 activity, while the expression remains constant. Similar results were obtained in the cellular model represented by the human SH-SY5Y neuronal cell line. After cadmium treatment for 24 and 48 hours, SOD1 enzymatic activity decreased in a dose- and time-dependent way, while the protein expression remained constant. Finally, a 16 hours cadmium treatment caused a 25% reduction of CuZn-SOD activity without affecting the protein expression in the *Caenorhabditis elegans* model. Taken together our results show an inhibitory effect of cadmium on SOD1 enzymatic activity, without affecting the protein expression, in all the biological models used, suggesting that cadmium can displace zinc from the enzyme catalytic site.

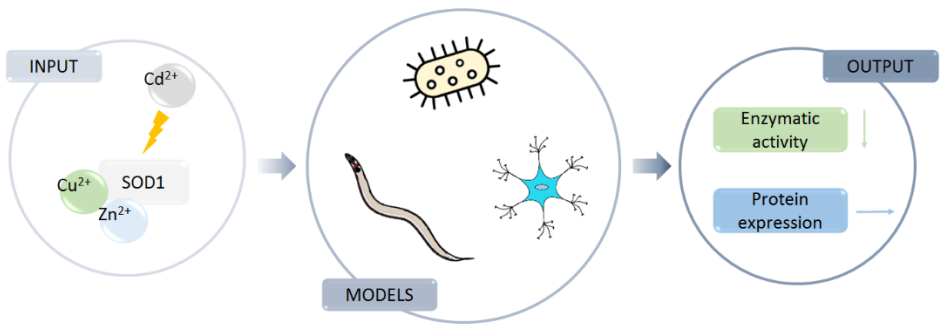

5.1 Introduction

Cadmium (Cd) is a toxic, rare heavy metal, naturally occurring with zinc. However, due to huge anthropogenic release into the environment (~22,000 tons/year) it has become a widespread contaminant. Being massively used in battery production, as well as alloys coatings, plating, and a stabilizer for plastics (IARC, 2012), exposure can occur occupationally; however, the general population can also be exposed environmentally, since cadmium is found in air, soil and water. Cadmium exposure for non-occupational reasons can primarily occur through contaminated food, air, drinking water, cosmetics and cigarette smoking (Bocca et al., 2014; Hartwig and Jahnke, 2017; Satarug and Moore, 2004). Moreover, although occupational exposure is decreasing, thanks to better regulations of cadmium exposure in the workplaces (Zhang and Reynolds, 2019), environmental contamination is steadily increasing, due to the bioaccumulative nature of this metal (IARC, 2012). Cadmium accumulates in the human body with a biological half-life of 26-30 years and is primarily taken up by the liver and kidney (e.g. 2 μg/g liver, and 70 μg/g kidney) (Mezynska and Brzoska, 2018; Rani et al., 2014). It can also penetrate into neurons *via* voltage-gated calcium channels (Usai et al., 1999) and has been shown to significantly affect the function of both peripheral (Miura et al., 2013) and central nervous system (Marchetti, 2014). Clinical symptoms include olfactory dysfunction, peripheral neuropathy, neurological disturbances, mental retardation, and learning disabilities, as well as motor activity impairment and behavioral alterations (Wang and Du, 2013).

Because of its similarity to zinc, cadmium easily enters the cells by molecular mimicry, *via* several transporters and receptors for essential metals such as Cu/Zn transporters, DMT1 (Divalent Metal Transporter 1), and Ca-channels. Inside the cell, cadmium toxicity is linked to its ability to bind thiol containing molecules such as GSH, and protein-Cys leading to displacement of redox-active metals and mitochondrial and metabolic dysfunction.

Cadmium therefore represents a serious hazard for human health, considering both toxicity and exposure frequency (ATDSR, 2019). Epidemiological and experimental studies have linked cadmium exposure to lung cancer and other cancers (Joseph et al., 2001; Waalkes, 2000), however, many data show that cadmium is also a neurotoxin (Garza-Lombó et al., 2018; Wang and Du, 2013). Although there is still much to be

elucidated, cadmium neurotoxicity has been related to different neurodegenerative diseases, such as Alzheimer's disease, Parkinson disease (Chin-Chan et al., 2015), multiple sclerosis and amyotrophic lateral sclerosis (Bar-Sela et al., 2001; Branca et al., 2018; Sheykhansari et al., 2018).

Amyotrophic lateral sclerosis (ALS) is a progressive and invariably fatal neurodegenerative disease: less than 10% of all ALS cases are familial (fALS), and among these 20% are related to SOD1 mutations (Huai and Zhang, 2019). The etiology of sporadic forms (sALS), representing over 90% of all cases, is still unknown, although many genetic and environmental factors have been suggested to play a role (Ingre et al., 2015; Wang et al., 2017). Among these factors are heavy metals, like copper, aluminium, arsenic, cobalt, zinc and cadmium, all of which have been found at elevated concentrations in ALS patients (Roos et al., 2013). In particular, cadmium has been shown to enter olfactory neurons, from where it can easily reach the brain bypassing the blood brain barrier, especially in younger individuals (Wang and Du, 2013). It is noteworthy that cigarette smoking, one of the most important routes for cadmium uptake, is the only factor correlated to negative survival in ALS patients (Calvo et al., 2016).

Although SOD1 mutations are responsible for many ALS familial forms, wild-type SOD1 (WT-SOD1) has also been implicated in ALS pathogenesis (Pansarasa et al., 2018). Gruzman et al., 2007 suggested the involvement of altered WT-SOD1 in sALS pathogenesis, showing that a single crosslinked protein species of SOD1 is common in both fALS and sALS. Ezzi et al., 2007 also demonstrated that oxidized WT-SOD1 can gain many of the toxic properties of ALS-linked mutant SOD1. Moreover, the presence of aggregated, misfolded SOD1 in the nuclei of glial cells of the spinal cord from ALS patients, with and without SOD1 mutations, was also demonstrated (Forsberg et al., 2010). Human SOD1 maturation includes the coordination of copper and zinc ions, as well as disulfide bond formation between Cys57 and Cys146. The formation of the disulfide bond, which is facilitated by the copper chaperone for SOD1 (CCS), is a rare event for cytosolic proteins that are surrounded by a reducing environment (Banci et al., 2012). These post-translational modifications (PTM) are essential for the production of a stabilized native conformation and the subsequent functional homodimer formation (Ding and Dokholyan, 2008). Because of its affinity

for thiols, cadmium can easily interfere with SOD1 folding by binding cysteines, as well as by substituting to zinc. In fact, it has been shown that in SOD1 G93A transgenic mice, mutant SOD1 inhibits the fast retrograde transport that is facilitated by the dynein-dynactin complex, even during ALS presymptomatic stages (Bilsland et al., 2010). On the other hand, cadmium has been shown to affect axonal transport, causing microtubule disassembly, inhibition of microtubule formation, and kinesin- and dynein-dependent motility (Böhm, 2014; Méndez-Armenta and Ríos, 2007). This metal can also interfere with the release of neurotransmitters and cause oxidative stress, mitochondrial damage and induction of apoptosis (Choong et al., 2014; Maret and Moulis, 2013). Previous investigations of cadmium ability to displace either zinc or copper, or both, from human SOD1 (hSOD1) have led to contradicting results (Huang et al., 2006; Kofod et al., 1991; Luchinat et al., 2014; Polykretis et al., 2019; Wang et al., 2015). Therefore, due to the primary function of SOD1, and the emerging role of environmental factors in the pathogenesis of ALS, we investigated cadmium neurotoxicity on SOD1 activity and expression in three different biological models: recombinant *E. coli* cells overexpressing human superoxide dismutase 1 (hSOD1), SH-SY5Y human neuroblastoma cells, and *Caenorhabditis elegans*. *E. coli* is the most widely used microorganism for overexpressing recombinant proteins; we chose to express human SOD1 as a Glutathione-S- transferase (GST) fusion protein, which allows easy purification through affinity chromatography and tag removal. SH-SY5Y human neuroblastoma cells are a widely used model for *in vitro* studies on neurotoxicity and neurodegenerative diseases (Cheung et al., 2009; Rossi et al., 2015), while *C. elegans* is an organism largely used as a model in different research fields, including metal toxicology (Du et al., 2019; Moyson et al., 2018; Soares et al., 2017; Srivastava et al., 2016), neurotoxicology (Chia et al., 2020) and ALS (Therrien and Parker, 2014; Van Damme et al., 2017). *E. coli* has an endogenous CuZn-SOD, while human neuronal cells possess three different SODs, like all animals: a cytosolic CuZn-SOD (SOD1), a mitochondrial isoform containing manganese in its catalytic site (SOD2) and an extracellular CuZn enzyme (SOD3) (Miller, 2012). *C. elegans* has five SOD isoforms, two of which are expressed in the cytosol and are homologous to the human CuZn-SOD1 (sod-1 and sod-5). The sod-1 isoform is the primary CuZn-SOD expressed in actively growing worms, whereas the sod-5 isoform is expressed in a

particular larval growing phase named dauer (Jensen and Culotta, 2005; Wang and Kim, 2003), in which nematodes enter when there are depletion of nutrients or harsh environmental conditions (Hu, 2007).

Our results show that cadmium administration leads to a decrease in CuZn-SOD1 activity in all models, without affecting the protein expression and suggest that Cd ions can displace zinc from the enzyme catalytic site.

5.2 Materials and methods

5.2.1 Human SOD1 cloning and bacterial strains

Human superoxide dismutase 1 (hSOD1) cDNA sequence was purchased from Addgene (Watertown, MA, USA) and was amplified using the following specific primers: forward primer (5' CCGGAATTCATGGCGACGAAG 3') with an EcoRI site (underlined), reverse primer (5' CGCTCGAGTTATTGGGCGATC 3') with a XhoI site (underlined). PCR product was digested using EcoRI and XhoI restriction enzymes (New England Biolabs, Ipswich, MA, USA) and cloned into previously digested EcoRI/XhoI plasmid pGEX-6P-1 (GE Healthcare, Chicago, IL, USA). The obtained pGEX-6P-1/hSOD1 recombinant plasmid was verified by automated sequencing (Bio-Fab research, Pomezia, Italy), using commercially available vector oligonucleotide primers. *Escherichia coli* strain DH5α (Invitrogen UK Ltd. Paisley, England) was used for DNA manipulation, for storing and propagating plasmids, whereas *E. coli* BL21 (DE3) (Invitrogen UK Ltd. Paisley, England) was used as expression strain. These strains were transformed with pGEX-6P-1/hSOD1 plasmid and recombinant hSOD1 was expressed as GST-fusion protein.

5.2.2 Recombinant protein expression optimization

In order to optimize time and temperature conditions for recombinant protein expression, the *E. coli* BL21 harboring pGEX-6P-1/hSOD1 plasmid was grown at 37°C and, once optical density at 600 nm (OD_{600}) has reached 0.6, the induction was carried out with IPTG 200 μM at 20°C, 30°C and 37°C for 3 hours and overnight.

Collected samples were centrifuged at 6,000 × g for 15 min at 4°C. The cell pellet obtained from 200 mL of bacterial culture was resuspended in PBS (10 mM K_2HPO_4, 150 mM NaCl, pH 7.2 containing 1 μM leupeptin, 2 μg/mL aprotinin, 1 μg/mL

pepstatin and 1 mM PMSF) with a ratio of 50 µL PBS per 1 mL of culture. Then the suspension was lysed by sonication (30 sec at 10 % amplitude for 3 times) and centrifuged at 13,000 × g for 20 min at 4°C.

Soluble fraction protein concentration was determined by the Bradford method, using BSA for the calibration curve (Bradford, 1976). SDS-PAGE and Blue-Coomassie staining were carried out by standard procedures (Laemmli, 1970). Protein soluble samples (15 µg) and cellular pellets were separated on a 12% SDS-PAGE gel and stained with Blue-Coomassie reagent overnight at 4°C or transferred onto a nitrocellulose membrane (Millipore, Burlington, MA, USA). Subsequently the membrane was blocked for 30 min in 1% (w/v) dried milk in PBS and immunodecorated overnight at 4°C with mouse anti-human SOD1 antibody (1:1,000 dilution) (NBP1-47443, Novus Biologicals, Centennial, CO, USA). After extensive washing in PBS with 0.3% (v/v) Tween20, the membrane was incubated for 1 hour with goat anti-mouse horseradish peroxidase conjugated IgG (1:10,000 dilution) (#7076, Cell Signaling Technology, Danvers, MA, USA). After a final wash in PBS, 0.3% (v/v) Tween20, detection of antibody binding was carried out with ECL detection system (EuroClone, Pero, Milan, Italy), according to the manufacturer's instructions.

All chemicals were purchased from Merck KGaA, Darmstadt, Germany.

5.2.3 E. coli BL21 growth curves, hSOD1 expression and activity analysis in the presence of different metals mixtures

Growth curves of *E. coli* BL21 transformed strain were assessed in the presence of copper, zinc or cadmium metals added to bacterial growth medium. Overnight cultured bacteria were inoculated at OD_{600} = 0.1 into fresh LB medium supplemented with ampicillin (100 µg/mL) and different concentrations of Cu_2SO_4 (0-1000 µM), $ZnCl_2$ (0-100 µM) or $CdCl_2$ (0-500 µM) and growth rate was monitored by measuring OD_{600} every 60 min over a total time of 6 hours.

Subsequently the metals influence on hSOD1 expression and activity was carried out either at inoculation or induction. In the first case the overnight cultured bacteria were inoculated into fresh LB medium directly in the presence of Cu_2SO_4, $ZnCl_2$ or $CdCl_2$. Regarding the induction condition, overnight cultured bacteria were inoculated into

fresh LB medium and copper, zinc or cadmium ions were added once OD_{600} of 0.6 was reached. In both cases protein induction was performed at OD_{600} = 0.6 with IPTG 200 μM and bacterial cultures grew at 30°C for 3 hours. Bacteria samples with no metals added represented the control.

The effect of combination of different metals mixtures (Cu_2SO_4 and $CdCl_2$, or $ZnCl_2$ and $CdCl_2$, or Cu_2SO_4, $ZnCl_2$ and $CdCl_2$) on hSOD1 was investigated by selecting Cu_2SO_4 and $ZnCl_2$ concentrations in which the enzyme activity was highest and then different concentrations of $CdCl_2$ (0-500 μM) were added. The combination of the metals was added in the LB medium at either inoculation or induction as described above. Bacteria samples without $CdCl_2$ represented the control.

Aliquots of cell suspensions were collected after 3 hours from the induction and processed (see *2.2*) to assay hSOD1 activity (see *2.4*) and recombinant protein expression levels through SDS-PAGE. Protein soluble samples (15 μg) were separated on a 12% SDS-PAGE gel and stained with Blue-Coomassie reagent overnight at 4°C. Densitometry analysis of GST-SOD1 normalized against the total loaded proteins was performed using ImageJ software (National Institute of Health, USA).

All chemicals were purchased from Merck KGaA, Darmstadt, Germany.

5.2.4 SOD1 activity assay

Recombinant hSOD1 catalytic activity was measured using an indirect method described by Vance et al., 1972. This technique is based upon the ability of the enzyme to compete with ferricytochrome *c* for superoxide anions generated by the aerobic xanthine oxidase system, causing an inhibition in the reduction of ferricytochrome *c*. Briefly, a solution of 0.01 mM ferricytochrome *c*, 0.1 mM EDTA, and 0.01 mM xanthine was incubated with different volumes of soluble protein samples, containing the hSOD1 recombinant protein. Ferricytochrome *c* was dissolved in 10 mM Hepes-Tris pH 7.5 and xanthine in 1 mM NaOH. All reactions were performed in 1 mL of total volume at room temperature. Reactions were initiated with the addition of xanthine oxidase at a final concentration of 0.0061 U/mL: this amount of xanthine oxidase has a rate of ferricytochrome *c* reduction corresponding to an increase of 0.025 absorbance per min at 550 nm, as suggested by Vance et al., 1972.

Under these conditions, 1 unit of SOD1 is the amount of enzyme able to yield a 50% decrease in the rate of ferricytochrome *c* reduction. The enzymatic activity was calculated using the following formula:

$$U/mg = \frac{[(\Delta E/min\ unhibited - \Delta E/min\ sample)/1/2\Delta E/min\ unhibited] \times V_t}{\varepsilon \times d \times V_c \times mg/ml}$$

Where E is the absorbance at 550 nm, V_t is the total reaction volume, V_c is the volume of sample use for the assay and ε is the ferricytochrome c molar extinction coefficient of 27.7 $mM^{-1}cm^{-1}$.

The uninhibited sample represents the rate of ferricytochrome *c* reduction and it contains all the reaction reagents except the recombinant protein.

All chemicals were purchased from Merck KGaA, Darmstadt, Germany.

5.2.5 Mammalian cell culture

SH-SY5Y (ATCC® HTB-2266™) human neuroblastoma cell line was grown in F12:EMEM (1:1) medium supplemented with heat-inactivated 10% FBS, 2 mM L-glutamine, 100 U/mL penicillin, 100 µg/ml streptomycin and maintained at 37°C in a humidified 5% CO_2 incubator. ATCC validated cell line by short tandem repeat profiles that are generated by simultaneous amplification of multiple short tandem repeat loci and amelogenin (for gender identification). All the reagents for cell culture were supplied by EuroClone (Pero, Milan, Italy).

5.2.6 Neuronal cell viability assay

Cell viability was investigated using *in vitro* toxicology assay kit MTT-based, according to manufacturer's protocols (Merck KGaA, Darmstadt, Germany).

In order to evaluate cadmium toxicity, cells were seeded in 96-well micro-titer plates at a density of 1×10^4 cells/well and after 24 hours were treated with different $CdCl_2$ concentrations (0, 0.01, 0.1, 1, 10, 100,1000 µM). After 48 hours at 37°C, the medium was replaced with a complete medium without phenol red and 10 µl of a 5 mg/mL MTT (3-(4,5-dimethylthiazol-2)-2,5-diphenyltetrazolium bromide) solution was added to each well. After a further incubation for 4 hours, the formed formazan crystals were solubilized with 10% Triton-X-100 in acidic isopropanol (0.1 N HCl)

and the absorbance at 570 nm was measured using a micro plate reader. Viabilities were expressed as a percentage of the untreated controls. The 50% growth inhibition (IC50) was determined from dose-response curves. Each experiment was performed in three replicate wells for each metal concentration and results are presented as the mean of at least three independent experiments.

5.2.7 SDS-PAGE and Western blotting of SOD1 from SH-SY5Y human neuroblastoma cells

To evaluate the effect of cadmium on SOD1 activity and expression, SH-SY5Y cells were seeded at 2×10^6 cells/100 mm dish and treated with the metal for 24-48 hours at the final concentrations of 10 μM and 20 μM. Cells not treated with $CdCl_2$ represented the control.

The cells were then rinsed with ice-cold PBS and lysed in 10 mM potassium phosphate, 0.6 M sorbitol containing 1 μM leupeptin, 2 μg/mL aprotinin, 1 μg/mL pepstatin and 1 mM PMSF. Sorbitol was added to lysis buffer in order to avoid the release of mitochondrial SOD (Jensen and Culotta, 2005). After lysis on ice, homogenates were obtained by passing 5 times through a blunt 20-gauge needle fitted to a syringe and then by sonicating (10 sec at 10% amplitude 2 times). Then, a centrifugation was performed at 14,000 × g for 10 min at 4°C and supernatants were used to assay SOD1 activity (see *2.4*) and expression. Protein content was quantified by Bradford method (Bradford, 1976). To evaluate the SOD1 expression levels, 25 μg of protein samples were analyzed by Western blot analysis. This was performed by resolving protein soluble samples on 15% acrylamide gel and then blotted onto a nitrocellulose membrane (Millipore, Burlington, MA, USA). The membrane was subsequently blocked and incubated overnight at 4°C with mouse anti-human SOD1 antibody (1:1,000 dilution) (NBP1-47443, Novus Biologicals, Centennial, CO, USA) and rabbit anti-human α-tubulin (1:1,000 dilution) (#2144, Cell Signaling Technology, Danvers, MA, USA), used as a loading control. After washing, membrane was incubated for 1 hour with goat anti-mouse or anti-rabbit horseradish peroxidase conjugated IgG (1:10,000 dilution) (#7076, #7074, Cell Signaling Technology, Danvers, MA, USA). The antibody detection was carried out with ECL detection system (EuroClone, Pero, Milan, Italy), according to the manufacturer's

instructions. Protein levels were quantified by densitometry of immunoblots using ImageJ software (National Institute of Health, USA). All chemicals were purchased from Merck KGaA, Darmstadt, Germany.

5.2.8 C. elegans strain maintenance and handing procedures

The Bristol N2 wild type strain (University of Minnesota, MN, USA) was used for this work. Worms were cultured at 20°C in small plates with 3 mL of solid nematode growth medium (NGM: 50 mM NaCl, 2.5 g/L peptone, 17 g/L agar; 1 mM $CaCl_2$, 1 mM $MgSO_4$, 5 mg/mL cholesterol in ethanol) and seeded with live OP50 *E. coli* as food source, according to the standard procedure (Brenner, 1974).

To avoid the possibility that the treatments with $CdCl_2$ could directly affect *E. coli* and thus indirectly the nematodes (Liao et al., 2011), all experiments were performed with heat-killed *E. coli* according to Gruber et al., 2007.

All chemicals were purchased from Merck KGaA, Darmstadt, Germany.

5.2.9 C. elegans acute toxicity assay

An acute toxicity assay was performed to assess cadmium effect on *C. elegans* viability and to determine the concentration for further experiments. Three-days-old adult gravid nematodes were transferred onto freshly OP50-seeded NGM plates for 12 hours to lay eggs. After removing adult worms from the plates, newly laid eggs were grown and after 3 days the synchronized worms were used for carrying out the experiments. 60 synchronized adult worms were placed onto 3 mL NGM plates supplemented with different concentrations of $CdCl_2$, which was given to worms as food source through OP50 absorption (H??ss et al., 2011) and prepared as follows. All $CdCl_2$ (0, 4, 8, 12, 16 g/L) concentrations were prepared in distilled water and was used to resuspend 0.3 OD_{600} of OP50. Absorption was carried out overnight at 4°C in shaking conditions; thereafter the bacteria were pelleted, at 7000 × g, for 15 min at 4°C, resuspended in LBLS medium (10 g/L peptone, 5 g/L yeast extract and 5 g/L NaCl) and killed for 150 minutes at 65°C in a water-bath. Two hundred of OP50 with cadmium absorbed solution was plated onto the NGM agar. Survived worms were recorded daily and transferred for 5 days onto a new fresh plate. Worms were counted as dead if they did not respond to gentle stimulation with platinum transfer pick. At

least 60 worms were used for each treatment and three independent experiments were performed.

All chemicals were purchased from Merck KGaA, Darmstadt, Germany.

5.2.10 C. elegans protein extraction and quantification

For SOD1 enzymatic assay, 70-days-old adult gravid nematodes were allowed to lay eggs for 7 hours onto 10 cm freshly OP50-seeded NGM. Subsequently the adult worms were removed, and newly laid eggs were left to grow. One-day synchronized adult worms were collected in S-buffer (0.1 M NaCl, 0.05 M K_2HPO_4, 0.05 M KH_2PO_4, pH 6), washed for removing OP50 residues, counted and seeded in equal number onto 10 cm plates containing 20 mL of NGM supplemented with 4 g/L and 8 g/L of $CdCl_2$ OP50 absorbed (see *2.9*) for 16 hours. The control (0 g/L) and treated nematode (about 3000 worms each) were collected separately in S-buffer, washed 3 times and then resuspended in 200 µL of lysis buffer (10 mM potassium phosphate, 0.6 M sorbitol, 1 µM leupeptidin, 2 µg/mL aprotinin, 1 µg/mL pepstatin and 1 mM PMSF). Lysate was obtained by sonication (1 min at 20% amplitude in ice-water bath, followed by 10 sec at 10% amplitude for 4 times). Finally, a centrifugation was performed at 13000 × g for 10 min at 4°C and supernatants were used to assay SOD1 activity.

For Western blot analysis, 3-days-old adult gravid nematodes were allowed to lay eggs for 16 hours onto 10 cm freshly OP50-seeded NGM. After adult worms removal, newly laid eggs were left to grow. One-day synchronized adult worms were collected in S-buffer and about 1000 worms were seeded onto 10 cm plates containing 20 mL of NGM supplemented with 4 g/L and 8 g/L of $CdCl_2$ OP50 absorbed (see *2.9*) for 16 hours. Cd treated and not treated worms were collected in PBS 1X and washed two times at 6000 x g for 1 min at 4°C. Then nematodes were resuspended in 200 µL of lysis buffer (PBS 1X, glycerol 10%, β-mercaptoethanol 1 mM, PMSF 2 mM) and incubated at -80°C for 15 min. Subsequently worms were sonicated (2 min at 20% amplitude in ice-water bath, followed by 10 sec at 10% amplitude for 4 times) and centrifugated at 13000 x g for 10 min at 4°C. The supernatants were used to assay SOD1 expression by Western blot, using tubulin as loading control (20 µg). SOD1 antibody (1: 1,000 dilution) (sc-17767) was supplied by Santa Cruz Biotechnology

(Dallas, TX, USA) and α-tubulin antibody (1: 2,000 dilution) (T6199) was supplied by Merck KGaA (Darmstadt, Germany).

Protein content were quantified by Bradford method (Bradford, 1976). For each treatment three independent experiments were performed.

All chemicals were purchased from Merck KGaA, Darmstadt, Germany.

5.2.11 Statistical analysis

All the experiments were carried out in biological triplicates. The samples were compared to their reference controls and the data were tested by Dunnett multiple comparison procedure. Results were considered statistically significant at $p < 0.05$.

5.3 Results

5.3.1 Recombinant hSOD1 expression optimization

Human wild-type superoxide dismutase 1 (hSOD1) was expressed in-frame with the GST tag coding sequence.

The optimal expression condition, yielding a high-level of soluble hSOD1-GST, was reached by inducing with 200 µM IPTG, for 3 hours at 30°C (Figure 1). Overnight induction at all temperatures tested, as well as induction at 37°C for 3 hours, led to a higher expression of the protein in inclusion bodies, whereas induction at 20°C led to a lower yield in protein expression (data not shown).

The apparent molecular mass of monomeric recombinant hSOD1 fused with GST was found about 42 kDa, in accordance with hSOD1 and GST moiety molecular masses of 15.8 kDa (Ahl et al., 2004) and 27 kDa, respectively.

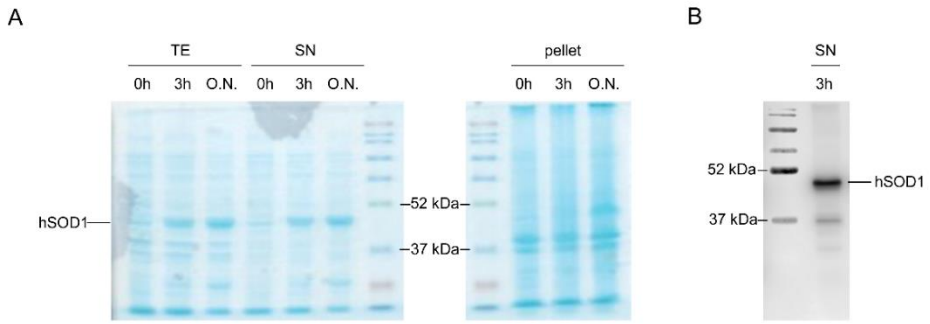

Figure 1. hSOD1 expression evaluation through SDS-PAGE analysis and Western blot.

Bacterial growth was performed at 37°C and, when OD_{600} reached 0.6, induction was carried out with 200 µM IPTG, at 30°C, at three different times (0h, 3h and ON). (A) Representative SDS-PAGE analysis performed on soluble protein samples (15 µg) and pellets prepared from *E. coli* BL21 strain transformed with recombinant pGEX-6P-1/hSOD1 plasmid and stained with Coomassie blue. TE: total extract, SN: supernatant; ON: overnight. (B) Representative Western blot performed on soluble protein samples (15 µg) from *E. coli* BL21 pGEX-6P-1/hSOD1 after 3 hours of induction at 30°C.

5.3.2 Single metals administration effects on E. coli BL21 growth and recombinant hSOD1 activity

In order to evaluate the possible toxic effect of cadmium on hSOD1 activity and expression, we first investigated the toxicity of this metal on *E. coli* cells, analyzing the growth curve of *E. coli* BL21 expressing hSOD1 by adding different concentrations of $CdCl_2$ (0, 50, 100, 250, 500 µM) directly in the LB medium at inoculation (see Materials and Methods). No significant differences were observed at all concentrations tested (Supplementary Figure 1A).

Moreover, cadmium addition to the medium, either at inoculation or just before induction, did not affect hSOD1 activity (Figure 2A).

Since the amounts of Cu_2SO_4 and $ZnCl_2$ could be limiting in *E. coli* cells, due to SOD1 overexpression, we also tested the effect of these metal ions addition. BL21 cells expressing recombinant hSOD1 were grown in the presence of different

concentrations of Cu_2SO_4 or $ZnCl_2$ showing that these metals did not affect bacterial growth (Supplementary Figure 1B, C). Copper addition led to a dose-dependent increase in hSOD1 activity, with a maximum activity at 500 μM Cu_2SO_4, followed by a decrease at higher Cu_2SO_4 concentrations (Figure 2C).

Administration of 15 μM $ZnCl_2$ led to a decrease in hSOD1 activity, when the metal was added both at the inoculation and after induction. However, higher concentrations did not significantly change hSOD1 activity, which remained comparable to the control (Figure 2E).

Single metals addition did not cause any alteration in recombinant protein expression (Figure 2B, D, F and Supplementary Figure 2).

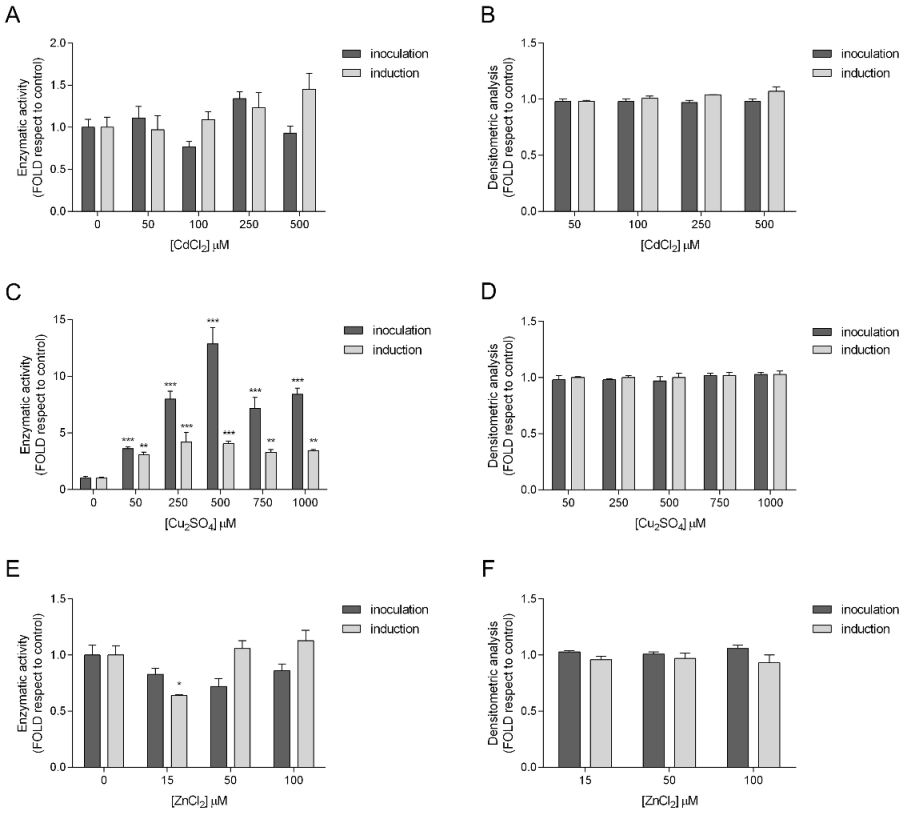

Figure 2. Evaluation of $CdCl_2$, Cu_2SO_4 and $ZnCl_2$ effect on recombinant hSOD1 activity and expression.

Enzymatic activity of hSOD1 after *E. coli* exposure to different concentrations of $CdCl_2$ (A), Cu_2SO_4 (C) and $ZnCl_2$ (E) (reported on the x-axis): y-axis represents SOD1 specific activity, as folds respect to control. Densitometric analysis, performed with ImageJ software, of recombinant hSOD1 expression after *E. coli* exposure to different concentrations of $CdCl_2$ (B), Cu_2SO_4 (D) and $ZnCl_2$ (F) (reported on the x-axis).
All data were normalized to the control. Data represent mean ± standard error (SE) of three independent experiments. *p<0.05, **p<0.01, ***p<0.001.

5.3.3 Metal mixture effects on recombinant GST-SOD1

The effect of different $CdCl_2$ concentrations (0, 50, 100, 250, 500 µM) on hSOD1 expressed in *E. coli* was investigated in the presence of fixed, optimal Cu_2SO_4 or $ZnCl_2$ concentrations (500 µM and 50 µM respectively).

The simultaneous addition of both $CdCl_2$ and Cu_2SO_4 led to a dose-dependent reduction in hSOD1 enzymatic activity, with a decrease of 50% in the presence of 500 μM $CdCl_2$. On the other hand, the presence of both $CdCl_2$ and $ZnCl_2$ did not affect hSOD1 activity, which remained comparable to the control (Figure 3A, C).

Finally, we tested the addition of different $CdCl_2$ concentrations (0, 50, 100, 250, 500 μM) in the presence of both 500 μM Cu_2SO_4 and 50 μM $ZnCl_2$. The presence of all three metals led to a decrease in hSOD1 activity in a dose-dependent way, which was more evident when the metals were added at the inoculation (Figure 3E). It is worth noting that the decrease measured in the presence of only 500 μM Cu_2SO_4 was much higher (Figure 3A), suggesting a protective role for $ZnCl_2$.

No $CdCl_2$ effect was detected on hSOD1 expression levels in any of the conditions tested (Figure 2B, D, E and Supplementary Figure 3).

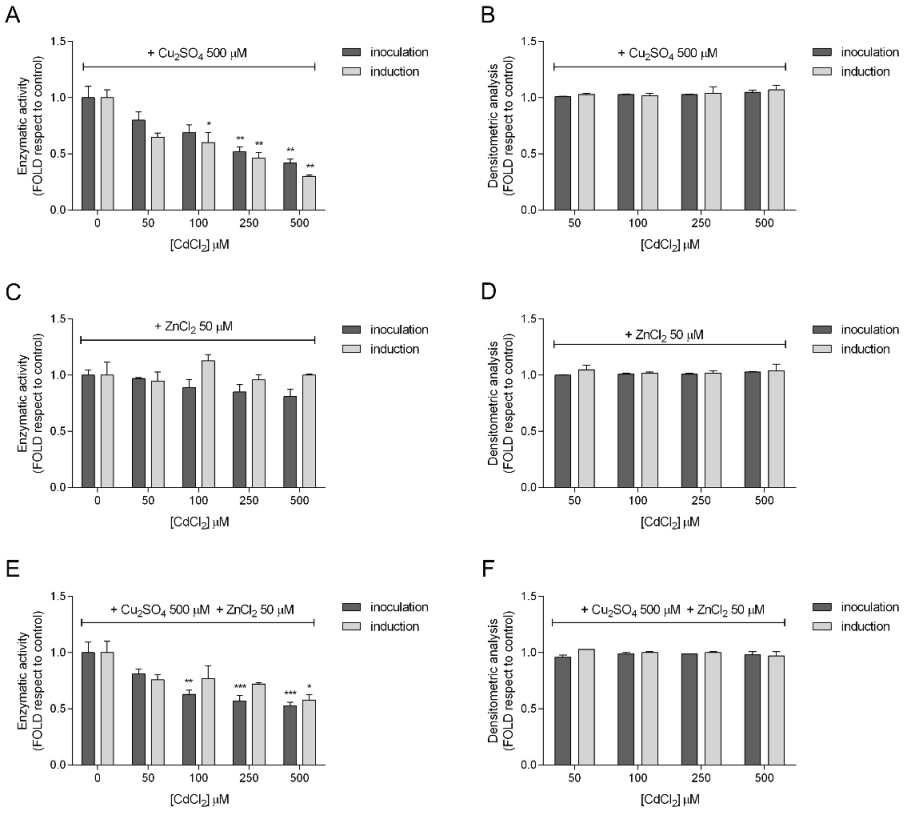

Figure 3. Evaluation of $CdCl_2$ effects on recombinant hSOD1 in *E. coli* cells treated with either Cu_2SO_4 and/or $ZnCl_2$.

Enzymatic activity of hSOD1 after *E. coli* exposure to different $CdCl_2$ concentrations (0-500 µM), in the presence of either 500 µM Cu_2SO_4 (A) or 50 µM $ZnCl_2$ (C) or both 500 µM Cu_2SO_4 and 50 µM $ZnCl_2$ (E). Y-axis represents specific activity folds. Densitometric analysis, performed with ImageJ software, of recombinant hSOD1 after *E. coli* exposure to different $CdCl_2$ concentrations (0-500 µM), in the presence of either 500 µM Cu_2SO_4 (B) or 50 µM $ZnCl_2$ (D) or both 500 µM Cu_2SO_4 and 50 µM $ZnCl_2$ (F).

The controls (0 µM $CdCl_2$) were used to normalize data that represent mean ± standard error (SE) of three independent experiments. *p<0.05, **p<0.01, ***p<0.001.

5.3.4 Cadmium effect on endogenous SOD1 in SH-SY5Y cell line

The investigation of cadmium neurotoxicity on SOD1 was further carried out on the SH-SY5Y human neuroblastoma cell line as an *in vitro* model.

To assess optimal, non-cytotoxic $CdCl_2$ concentration to be used in SH-SY5Y cell line, we initially evaluated the half maximal inhibiting concentration (IC50), after a 48-hours cadmium treatment. As shown in Figure 4A, cadmium treatment induced a high cell mortality, with an IC50 of 26.676 ± 3.498 μM. We therefore decided to investigate endogenous SOD1 activity and expression following 10 and 20 μM $CdCl_2$ administration for 24 and 48 hours.

A 24-hours treatment did not cause any effect on the catalytic activity of the enzyme, while we obtained a reduction of about 50% in SOD1 activity after 48 hours of $CdCl_2$ administration at both concentrations (Figure 4B). Moreover, even in this model the protein expression levels remained constant at all the conditions studied, as shown in Western blot and densitometric analysis reported in Figure 4 C-D.

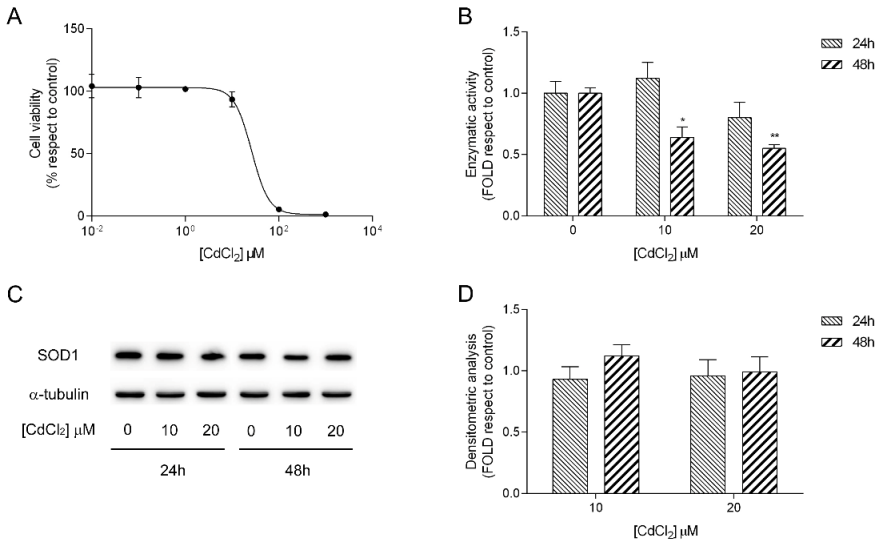

Figure 4. Evaluation of $CdCl_2$ effect on endogenous SOD1 in SH-SY5Y cell line. (A) Dose-response curves of human SH-SY5Y cell lines to $CdCl_2$. Cell survival was determined by MTT assay in the presence of different $CdCl_2$ doses (0-1000 µM) for 48 hours. Nonlinear Regression of experimental data was obtained using a Four Parameter Logistic Curve f1 = min + (max-min)/(1 + (x/EC50)^(-Hillslope)). (B) SOD1 activity after SH-SY5Y exposure to either 10 or 20 µM $CdCl_2$ for 24 and 48 hours. The different $CdCl_2$ concentrations are reported on the x-axis. Y-axis represents the fold of specific activity. Data were normalized to the control and represent mean ± E.S. of three independent experiments. (C) Representative Western blot analyses of SOD1 in SH-SY5Y cells soluble extracts (25 µg) treated with $CdCl_2$. α-Tubulin was used as a loading control. (D) Densitometric analysis was performed with ImageJ Software. Values are expressed by comparing the data obtained after $CdCl_2$ treatment with those of control. Values are presented as means ± standard error (SE) of three independent experiments. *$p<0.05$, **$p<0.01$.

5.3.5 SOD1 analysis in the presence of cadmium in the in vivo Caenorhabditis elegans model

Cadmium effect on SOD1 was also evaluated in a whole model organism, the nematode *C. elegans*. At first, we performed an acute toxicity assay to assess the effect of cadmium treatment on the nematode viability and determine the concentration to use in the following experiments. Worms were treated for 5 days with different doses of $CdCl_2$ (0, 4, 8,12, 16 g/L), given as a food source through *E. coli* adsorption; dead and live nematodes were recorded everyday (Figure 5A). For all the conditions tested, mortality showed a peak between day 1 and day 2 and subsequently decreased until it reached 30% of the initial value for the lower doses and 60% for the higher ones. These results underline how cadmium administration caused a reduction in worm viability in a non-linear dose dependent way, with 4-8 g/L and 12-16 g/L concentrations behaving similarly.

Subsequently, we evaluated SOD1 activity and expression after a 16-hours treatment with cadmium, since a longer time of exposure caused an elevated mortality that could lead to non-optimal results.

The protein extraction performed in a sorbitol lysis buffer allowed the enzymatic assay only of cytosolic SOD1, discarding the mitochondrial superoxide dismutases, which were part of the insoluble fraction. In the presence of 4 and 8 g/L $CdCl_2$, SOD1 activity showed a reduction of about 25 % (Figure 5B), while there were no significant differences in protein levels with respect to the control at all the doses investigated, as confirmed by Western blot analysis reported in Figure 5C-D.

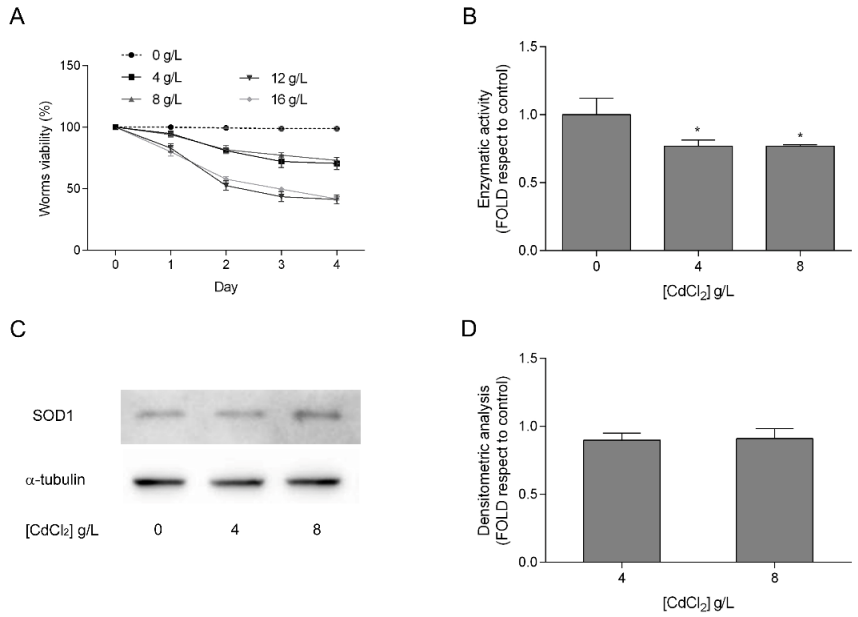

Figure 5. Evaluation of $CdCl_2$ effects on SOD1 in *C. elegans*.

(A) Acute cadmium toxicity test on *C. elegans*. For each concentration tested, worms viability was calculated as the percentage of live animals respect to the number of nematode on day 0. (B) SOD1 activity after 16 hours treatment with 0-4-8 g/L $CdCl_2$. Different $CdCl_2$ concentrations are reported on the x-axis; specific activity folds are reported on the y-axis. Data were normalized to the control and represent mean ± standard error (SE) of three independent experiments. (C) Representative Western blot analyses of SOD1 in nematode protein soluble extracts (20 µg) treated with $CdCl_2$. α-Tubulin was used as a loading control. (D) Densitometric analysis was performed with ImageJ Software. Values are expressed by comparing the data obtained after cadmium treatment with those obtained without cadmium administration. Values are presented as means ± standard error (SE) of three independent experiments. *$p<0.05$.

5.4 Discussion

Cadmium exerts serious toxic effects at multiple levels: it enters the cells through zinc transporters, causes copper and zinc dysregulation, and it can easily substitute zinc in a variety of zinc proteins (Satarug et al., 2018; Urani et al., 2015), including the cytosolic CuZn superoxide dismutase (SOD1). SOD1 is one of the most important

proteins involved in oxidative stress defense, especially in neuronal cells (Kaur et al., 2016). In this work we show, in three different experimental models, that cadmium can impair SOD1 activity, without affecting its expression level. Concentrations of $CdCl_2$ up to 500 µM were found not to be toxic for *E. coli* and did not cause a reduction in SOD1 enzymatic activity. This suggests that either copper or zinc are limiting during *E. coli* growth, as a consequence of the high expression levels of the recombinant protein. Absolute SOD1 specific activity measurements, yielding a value around 8.1 U/mg for cells grown in the presence of either copper alone or copper and zinc and a value of 2.8 U/mg for cells grown without copper, show that copper is the limiting metal in our conditions. Our data are in accordance with previous data obtained by Lin et al., 2018 showing that Cu^{2+}-binding sites saturation facilitates Zn^{2+} binding.

When administered together with optimal 500 µM Cu_2SO_4 concentration, cadmium led to a dose dependent decrease in SOD1 specific activity, starting at 50 µM $CdCl_2$. However, in the presence of an optimal $ZnCl_2$ concentration (50 µM), no decrease in SOD1 activity was measured at increasing $CdCl_2$ concentrations, suggesting that cadmium displaces zinc when copper is in excess and zinc is limiting. Due to their larger size, cadmium ions can be difficult to release once they have displaced zinc ions. Moreover, Crow et al., 1997 suggested that zinc is more likely to dissociate than copper, because SOD1 has an approximately 7000-fold lower affinity for zinc than it does for copper. More recently Huang et al., 2006 showed that cadmium can displace zinc, inducing a conformational change in SOD1 and decreasing its activity. Kofod et al., 1991, investigating yeast SOD1 structure by NMR, showed that cadmium binds to the Zn site with the same coordination, the Cu-Cd enzyme having a structure identical to the native enzyme, and that cadmium binding to the copper site occurs only if the zinc site is already occupied.

When both copper and zinc were administered to *E. coli* recombinant cells, a decrease in SOD1 specific activity was still detected, although to a minor extent with respect to the decrease observed in the absence of zinc; this could be due to a higher amount of SOD1 undergoing folding in *E. coli* in the presence of 500 µM copper, so that a 50 µM $ZnCl_2$ concentration becomes limiting. Adding the metals at induction or at inoculation produced the same result, suggesting that copper and zinc can be inserted

into SOD1 in both conditions. No additional amounts of copper and zinc were administered to neuronal cells and *C. elegans*, because SOD1 is not overexpressed in these two experimental models and thus the metals concentrations are not limiting.

SOD1 folding requires the insertion of copper and zinc ions into the catalytic site. Copper can be inserted either through the copper chaperone (CCS), as in yeast, or in an independent way requiring glutathione, as in *E. coli* and *C. elegans*; in humans both pathways can be used for copper insertion (Banci et al., 2012; Carroll et al., 2004; Leitch et al., 2009). On the other hand, zinc insertion mechanism during SOD1 folding has not yet been fully elucidated. Moreover, SOD1 is an aggregation-prone enzyme and amyloid fibers have been detected in patients of both familial and sporadic ALS (Kaur et al., 2016). SOD1 misfolding has since long been associated to ALS pathogenesis. Data obtained by de la Torre et al., 1996 and Ravikumar et al., 2000 already showed its activity to be reduced in Parkinson's disease and other neurodegenerative diseases. In fact, besides displacing zinc from proteins, cadmium has a high affinity for cysteines and could interfere with SOD1 folding, which requires the formation of a disulfide bridge between C57 and C146. This is well in accordance with previous data from showing that cadmium binds to the interface of the two SOD1 subunits leading to enzyme misfolding (Polykretis et al., 2019; Wang et al., 2015). These authors investigated cadmium replacement of copper and zinc in SOD1 through in-cell NMR in HEK393 cells, showing that Cd^{2+} does not replace Zn^{2+} but induces the formation of a disulfide bridge between C57 and C146. Premature Cys oxidation could prevent zinc binding, since only the native structured apoSOD1 can effectively bind zinc, as shown by Luchinat et al., 2014 through in-cell NMR. Moreover, cadmium binding to glutathione, which in *E. coli* is essential for SOD1 folding, could also impair folding leading to SOD1 aggregation.

A decrease in SOD1 specific activity was demonstrated by our results in SH-SY5Y cells treated with either 10 or 20 µM $CdCl_2$. These concentrations were chosen to mimic a real *in vivo* situation, since cadmium concentrations up to 20 µM have been reported in the human body, due to the metal extremely long half-life (Satarug and Moore, 2004). SOD1 expression level was found unaltered upon cadmium administration, in accordance with our previous toxicogenomic study (Forcella et al., 2020) showing that $CdCl_2$ addition to cultured SH-SY5Y cells did not change SOD1

expression level, while up-regulating metallothioneines and down-regulating genes related to neuronal functions. In accordance with our results, Huang et al., 2006 showed that cadmium induces metallothioneins expression and oxidative stress mediated apopotosis in N2A murine neuroblastoma cells.

The results were further confirmed in *Caenorhabditis elegans*, the multicellular model organism chosen for its easy laboratories handling (Kaletta and Hengartner, 2006), the similarity of biological traits within human physiology, anatomy, and metabolism (Kaletta and Hengartner, 2006) and its wide use for metal toxicity evaluation (Du et al., 2019; Moyson et al., 2018; Soares et al., 2017; Srivastava et al., 2016). Since it has been demonstrated that the main uptake route of cadmium for *C. elegans* is driven by food ingestion (H??ss et al., 2011), we performed the acute toxicity assay. We observed that the daily treatment caused a significant reduction in worm viability, although in a non-linear dose dependent way. The employment of a daily treatment allowed us not only to determine the cadmium lethal concentration but also to evaluate the effect of a long exposure at sub-lethal concentrations, not least to choose the optimal condition for the subsequent experiments. Noteworthy, also in *C. elegans* the cadmium treatment with 4 and 8 g/L for 16 hours induced a 25% reduction in SOD1 activity, without altering the protein level. In accordance with results obtained in neuronal cells, Cui and coauthors reported that cadmium treatment induced the expression of genes involved in metal detoxification, including *mtl-1*, *mtl-2* and the cadmium-specific response gene, *cdr-1*, underlining the important roles of these proteins in the defense against cadmium toxicity (Cui et al., 2007). However, a more recent paper demonstrated that the knockdown of the three genes did not increase cadmium hypersensitivity, suggesting that other factors may be involved in the response to cadmium (Hall et al., 2012; Winter et al., 2016).

On the whole, our data confirm the results of previous papers (Huang et al., 2006; Kofod et al., 1991; Romandini et al., 1992; Wang et al., 2015) showing that cadmium can substitute zinc leading to a reduction in SOD1 enzymatic activity. However, we cannot exclude that cadmium can react also with cysteines, as suggested by Polykretis et al., 2019, particularly during SOD1 folding. Our work also shows that cadmium can interfere with SOD1 activity when administered to a whole organism, like *C. elegans*, at sublethal doses for a short time; this confirms the risk associated to

cadmium contamination and suggests a role for cadmium in ALS pathogenesis. In the past years, other authors (Vinceti et al., 1997) failed to detect cadmium in the blood of sporadic ALS patients and found no evidence of association between ALS risk and toenails content of cadmium (Bergomi et al., 2002). However, it is well known that, once inside the body, cadmium enters the cells through a variety of transporters, the most relevant being Zn transporters in the lung and DMT1 in the intestine; it is therefore quickly removed from biological fluids and accumulates within cells and tissues by binding to different proteins.

5.5 Conclusions

Our results using three different model systems clearly demonstrate that cadmium leads to a loss of SOD1 enzymatic activity. The role of SOD1 mutations in fALS is already known and recognized. However, the mechanism(s) of metals are gaining attention as possible factors contributing to ALS (Tesauro et al., 2021). Cadmium, as a widespread environmental contaminant, has recognized effects on oxidative stress and metal dyshomeostasis, all factors contributing to neurodegenerative diseases. Our data show that cadmium can be harmful at low doses, mimicking environmental contamination. Thus, although insights into the contribution of both environmental and genetic (or genetic-like) factors are essential to the comprehension of ALS pathogenesis, understanding the environmental contribution is a critical aspect being the only component of the risk which can be modified. Our data confirm the importance of introducing effective measures to prevent environmental accumulation of cadmium, along with restoration and/or control of metal homeostasis in subjects at higher risk.

5.6 Supplementary figures

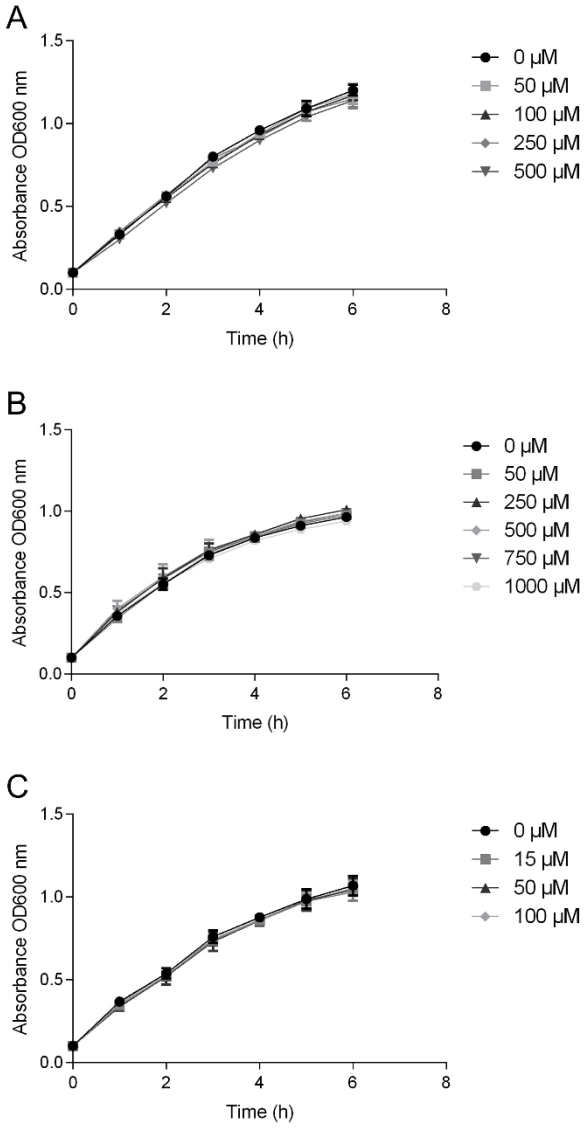

Figure S1. Evaluation of $CdCl_2$ effect on *E. coli* growth.

E. coli BL21 growth curve in the presence of different $CdCl_2$ doses (0-500 µM) (A), Cu_2SO_4 doses (0-1000 µM) (B) and $ZnCl_2$ doses (0-100 µM) (C) added to the inoculation.

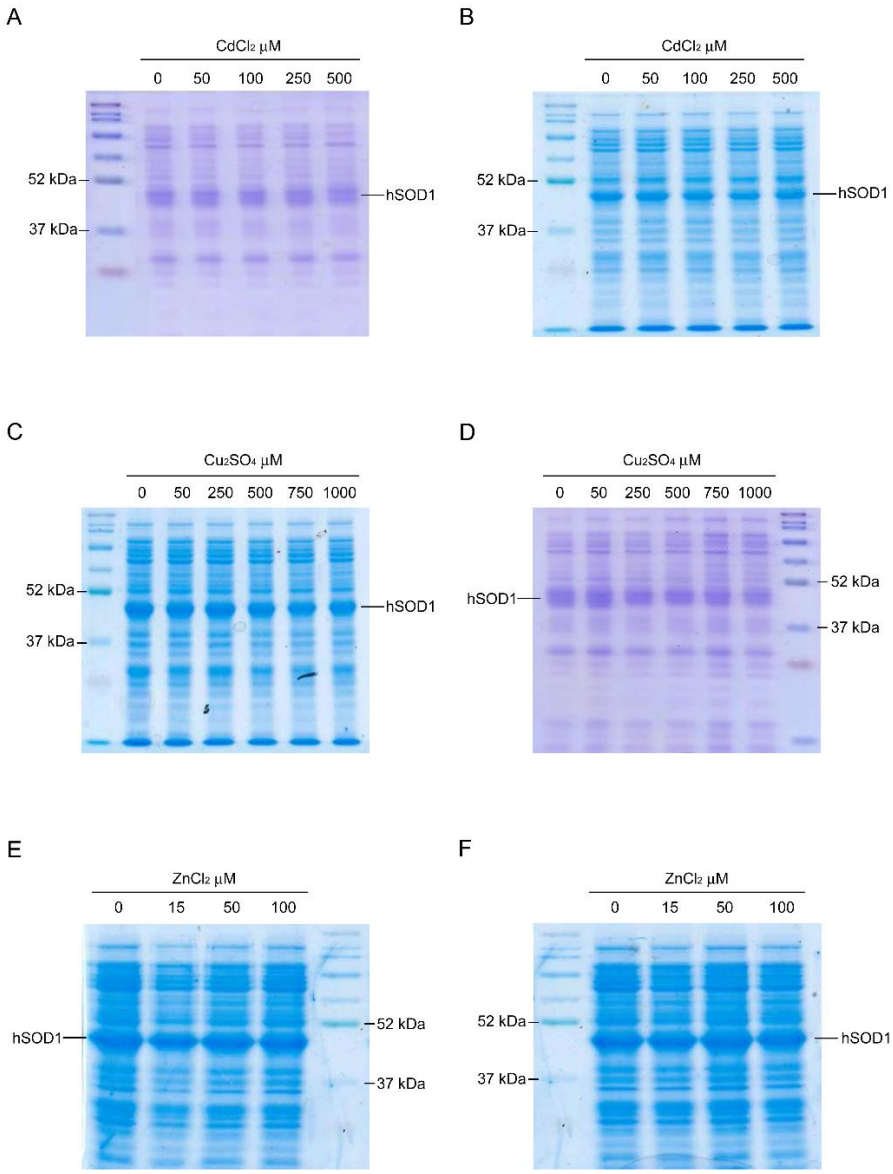

Figure S2. Evaluation of $CdCl_2$, Cu_2SO_4 and $ZnCl_2$ effect on recombinant hSOD1 expression.

Representative SDS-PAGE stained with Coomassie blue of soluble extracts (15 µg) prepared from recombinant *E. coli* exposed to different $CdCl_2$ concentrations at the time of inoculation (A) or induction (B), to different Cu_2SO_4 concentrations at the time of inoculation (C) or induction (D) and to different $ZnCl_2$ concentrations at the time of inoculation (E) or induction (F).

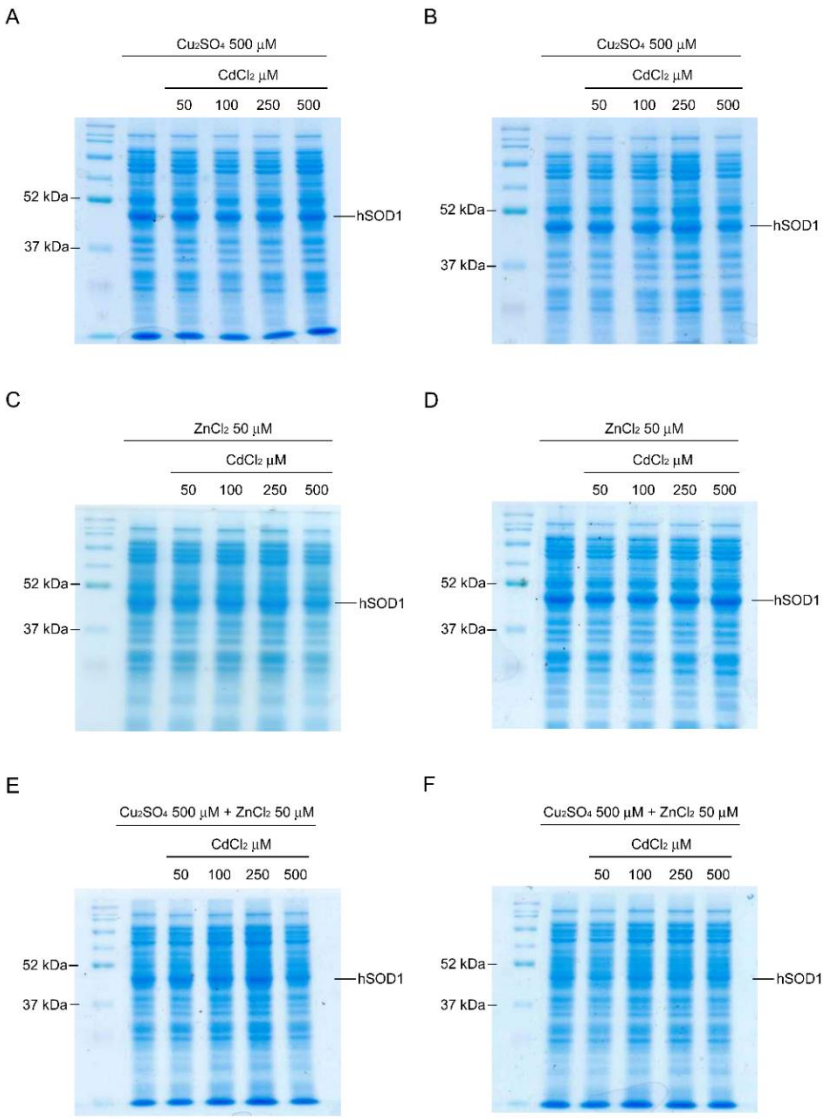

Figure S3. Evaluation of metal ions mixture effect on recombinant hSOD1 expression.

Representative SDS-PAGE stained with Coomassie blue of soluble extracts (15 µg) prepared from recombinant *E. coli* exposed to exposed to 500 µM Cu_2SO_4 and different $CdCl_2$ concentrations (0-500 µM) at the time of inoculation (A) or induction (B), to 50 µM $ZnCl_2$ and different $CdCl_2$ concentrations (0-500 µM) at the time of inoculation (C) or induction (D) and to fixed 500 µM Cu_2SO_4 and 50 µM $ZnCl_2$ together with different $CdCl_2$ concentrations (0-500 µM) at the time of inoculation (E) or induction (F).

References

Ahl, I.-M., Lindberg, M.J., Tibell, L.A.E., 2004. Coexpression of yeast copper chaperone (yCCS) and CuZn-superoxide dismutases in Escherichia coli yields protein with high copper contents. Protein Expr. Purif. 37, 311–319. https://doi.org/https://doi.org/10.1016/j.pep.2004.06.006

ATDSR, 2019. Support Document to the 2019 Substance Priority List (Candidates for Toxicological Profiles) Agency for Toxic Substances and Disease Registry Division of Toxicology and Human Health Sciences 1–12.

Banci, L., Bertini, I., Cantini, F., Kozyreva, T., Massagni, C., Palumaa, P., Rubino, J.T., Zovo, K., 2012. Human superoxide dismutase 1 (hSOD1) maturation through interaction with human copper chaperone for SOD1 (hCCS). Proc. Natl. Acad. Sci. U. S. A. 109, 13555–13560. https://doi.org/10.1073/pnas.1207493109

Bar-Sela, S., Reingold, S., Richter, E.D., 2001. Amyotrophic Lateral Sclerosis in a Battery-factory Worker Exposed to Cadmium. Int. J. Occup. Environ. Health 7, 109–112. https://doi.org/10.1179/107735201800339470

Bergomi, M., Vinceti, M., Nacci, G., Pietrini, V., Brätter, P., Alber, D., Ferrari, A., Vescovi, L., Guidetti, D., Sola, P., Malagu, S., Aramini, C., Vivoli, G., 2002. Environmental exposure to trace elements and risk of amyotrophic lateral sclerosis: A population-based case-control study. Environ. Res. 89, 116–123. https://doi.org/10.1006/enrs.2002.4361

Bilsland, L.G., Sahai, E., Kelly, G., Golding, M., Greensmith, L., Schiavo, G., 2010. Deficits in axonal transport precede ALS symptoms in vivo. Proc. Natl. Acad. Sci. U. S. A. 107, 20523–20528. https://doi.org/10.1073/pnas.1006869107

Bocca, B., Pino, A., Alimonti, A., Forte, G., 2014. Toxic metals contained in cosmetics: a status report. Regul Toxicol Pharmacol 68, 447–467. https://doi.org/10.1016/j.yrtph.2014.02.003

Böhm, K.J., 2014. Kinesin-dependent motility generation as target mechanism of cadmium intoxication. Toxicol. Lett. 224, 356–361. https://doi.org/https://doi.org/10.1016/j.toxlet.2013.11.004

Bradford, M.M., 1976. A rapid and sensitive method for the quantitation of microgram quantities of protein utilizing the principle of protein-dye binding. Anal.

Biochem. 72, 248–254. https://doi.org/10.1006/abio.1976.9999

Branca, J.J.V., Morucci, G., Pacini, A., 2018. Cadmium-induced neurotoxicity: still much ado. Neural Regen. Res. 13, 1879–1882. https://doi.org/10.4103/1673-5374.239434

Brenner, S., 1974. The genetics of Caenorhabditis elegans. Genetics 77, 71–94.

Calvo, A., Canosa, A., Bertuzzo, D., Cugnasco, P., Solero, L., Clerico, M., De Mercanti, S., Bersano, E., Cammarosano, S., Ilardi, A., Manera, U., Moglia, C., Marinou, K., Bottacchi, E., Pisano, F., Mora, G., Mazzini, L., Chiò, A., 2016. Influence of cigarette smoking on ALS outcome: a population-based study. J. Neurol. Neurosurg. Psychiatry 87, 1229–1233. https://doi.org/10.1136/jnnp-2016-313793

Carroll, M.C., Girouard, J.B., Ulloa, J.L., Subramaniam, J.R., Wong, P.C., Valentine, J.S., Culotta, V.C., 2004. Mechanisms for activating Cu- and Zn-containing superoxide dismutase in the absence of the CCS Cu chaperone. Proc. Natl. Acad. Sci. U. S. A. 101, 5964–5969. https://doi.org/10.1073/pnas.0308298101

Cheung, Y.-T., Lau, W.K.-W., Yu, M.-S., Lai, C.S.-W., Yeung, S.-C., So, K.-F., Chang, R.C.-C., 2009. Effects of all-trans-retinoic acid on human SH-SY5Y neuroblastoma as in vitro model in neurotoxicity research. Neurotoxicology 30, 127–135. https://doi.org/https://doi.org/10.1016/j.neuro.2008.11.001

Chia, S.J., Tan, E.-K., Chao, Y.-X., 2020. Historical Perspective: Models of Parkinson's Disease. Int. J. Mol. Sci. 21. https://doi.org/10.3390/ijms21072464

Chin-Chan, M., Navarro-Yepes, J., Quintanilla-Vega, B., 2015. Environmental pollutants as risk factors for neurodegenerative disorders: Alzheimer and Parkinson diseases. Front. Cell. Neurosci. 9, 124. https://doi.org/10.3389/fncel.2015.00124

Choong, G., Liu, Y., Templeton, D.M., 2014. Interplay of calcium and cadmium in mediating cadmium toxicity. Chem Biol Interact 211, 54–65. https://doi.org/10.1016/j.cbi.2014.01.007

Crow, J.P., Sampson, J.B., Zhuang, Y., Thompson, J.A., Beckman, J.S., 1997. Decreased zinc affinity of amyotrophic lateral sclerosis-associated superoxide dismutase mutants leads to enhanced catalysis of tyrosine nitration by peroxynitrite. J. Neurochem. 69, 1936–1944. https://doi.org/10.1046/j.1471-

4159.1997.69051936.x

Cui, Y., McBride, S.J., Boyd, W.A., Alper, S., Freedman, J.H., 2007. Toxicogenomic analysis of Caenorhabditis elegans reveals novel genes and pathways involved in the resistance to cadmium toxicity. Genome Biol. 8, R122. https://doi.org/10.1186/gb-2007-8-6-r122

de la Torre, M.R., Casado, A., López-Fernández, M.E., Carrascosa, D., Casado, M.C., Venarucci, D., Venarucci, V., 1996. Human aging brain disorders: role of antioxidant enzymes. Neurochem. Res. 21, 885–888. https://doi.org/10.1007/BF02532336

Ding, F., Dokholyan, N. V, 2008. Dynamical roles of metal ions and the disulfide bond in Cu, Zn superoxide dismutase folding and aggregation. Proc. Natl. Acad. Sci. U. S. A. 105, 19696–19701. https://doi.org/10.1073/pnas.0803266105

Du, Z., Yu, D., Du, X., Scott, P., Ren, J., Qu, X., 2019. Self-triggered click reaction in an Alzheimer{'}s disease model: in situ bifunctional drug synthesis catalyzed by neurotoxic copper accumulated in amyloid-β plaques. Chem. Sci. 10, 10343–10350. https://doi.org/10.1039/C9SC04387J

Ezzi, S.A., Urushitani, M., Julien, J.-P., 2007. Wild-type superoxide dismutase acquires binding and toxic properties of ALS-linked mutant forms through oxidation. J. Neurochem. 102, 170–178. https://doi.org/10.1111/j.1471-4159.2007.04531.x

Forcella, M., Lau, P., Oldani, M., Melchioretto, P., Bogni, A., Gribaldo, L., Fusi, P., Urani, C., 2020. Neuronal specific and non-specific responses to cadmium possibly involved in neurodegeneration: A toxicogenomics study in a human neuronal cell model. Neurotoxicology 76, 162–173. https://doi.org/https://doi.org/10.1016/j.neuro.2019.11.002

Forsberg, K., Jonsson, P.A., Andersen, P.M., Bergemalm, D., Graffmo, K.S., Hultdin, M., Jacobsson, J., Rosquist, R., Marklund, S.L., Brännström, T., 2010. Novel Antibodies Reveal Inclusions Containing Non-Native SOD1 in Sporadic ALS Patients. PLoS One 5, e11552.

Garza-Lombó, C., Posadas, Y., Quintanar, L., Gonsebatt, M.E., Franco, R., 2018. Neurotoxicity Linked to Dysfunctional Metal Ion Homeostasis and Xenobiotic Metal Exposure: Redox Signaling and Oxidative Stress. Antioxidants Redox

Signal. https://doi.org/10.1089/ars.2017.7272

Gruber, J., Tang, S.Y., Halliwell, B., 2007. Evidence for a trade-off between survival and fitness caused by resveratrol treatment of Caenorhabditis elegans. Ann. N. Y. Acad. Sci. 1100, 530–542. https://doi.org/10.1196/annals.1395.059

Gruzman, A., Wood, W.L., Alpert, E., Prasad, M.D., Miller, R.G., Rothstein, J.D., Bowser, R., Hamilton, R., Wood, T.D., Cleveland, D.W., Lingappa, V.R., Liu, J., 2007. Common molecular signature in SOD1 for both sporadic and familial amyotrophic lateral sclerosis. Proc. Natl. Acad. Sci. U. S. A. 104, 12524–12529. https://doi.org/10.1073/pnas.0705044104

H??ss, S., Schlottmann, K., Traunspurger, W., 2011. Toxicity of ingested cadmium to the nematode caenorhabditis elegans. Environ. Sci. Technol. 45, 10219–10225. https://doi.org/10.1021/es2027136

Hall, J., Haas, K.L., Freedman, J.H., 2012. Role of MTL-1, MTL-2, and CDR-1 in mediating cadmium sensitivity in Caenorhabditis elegans. Toxicol. Sci. 128, 418–426. https://doi.org/10.1093/toxsci/kfs166

Hartwig, A., Jahnke, G., 2017. [Metals and their compounds as contaminants in food : Arsenic, cadmium, lead and aluminum]. Bundesgesundheitsblatt. Gesundheitsforschung. Gesundheitsschutz 60, 715–721. https://doi.org/10.1007/s00103-017-2567-0

Hu, P.J., 2007. Dauer. WormBook 1–19. https://doi.org/10.1895/wormbook.1.144.1

Huai, J., Zhang, Z., 2019. Structural properties and interaction partners of familial ALS-associated SOD1 mutants. Front. Neurol. 10, 1–5. https://doi.org/10.3389/fneur.2019.00527

Huang, Y.H., Shih, C.M., Huang, C.J., Lin, C.M., Chou, C.M., Tsai, M.L., Liu, T.P., Chiu, J.F., Chen, C.T., 2006. Effects of cadmium on structure and enzymatic activity of Cu,Zn-SOD and oxidative status in neural cells. J. Cell. Biochem. 98, 577–589. https://doi.org/10.1002/jcb.20772

IARC, 2012. TOXICOLOGICAL PROFILE FOR CADMIUM. U.S. Dep. Heal. Hum. Serv. Public Heal. Serv. Agency ToxicSubstances Dis. Regist.

Ingre, C., Roos, P.M., Piehl, F., Kamel, F., Fang, F., 2015. Risk factors for amyotrophic lateral sclerosis. Clin. Epidemiol. 7, 181–193. https://doi.org/10.2147/CLEP.S37505

Jensen, L.T., Culotta, V.C., 2005. Activation of CuZn superoxide dismutases from Caenorhabditis elegans does not require the copper chaperone CCS. J. Biol. Chem. 280, 41373–41379. https://doi.org/10.1074/jbc.M509142200

Joseph, P., Muchnok, T.K., Klishis, M.L., Roberts, J.R., Antonini, J.M., Whong, W.Z., Ong, T., 2001. Cadmium-induced cell transformation and tumorigenesis are associated with transcriptional activation of c-fos, c-jun, and c-myc proto-oncogenes: role of cellular calcium and reactive oxygen species. Toxicol. Sci. 61, 295–303. https://doi.org/10.1093/toxsci/61.2.295

Kaletta, T., Hengartner, M.O., 2006. Finding function in novel targets: C. elegans as a model organism. Nat. Rev. Drug Discov. https://doi.org/10.1038/nrd2031

Kaur, S.J., McKeown, S.R., Rashid, S., 2016. Mutant SOD1 mediated pathogenesis of Amyotrophic Lateral Sclerosis. Gene 577, 109–118. https://doi.org/10.1016/j.gene.2015.11.049

Kofod, P., Bauer, R., Danielsen, E., Larsen, E., Bjerrum, M.J., 1991. 113Cd-NMR investigation of a cadmium-substituted copper, zinc-containing superoxide dismutase from yeast. Eur. J. Biochem. 198, 607–611. https://doi.org/https://doi.org/10.1111/j.1432-1033.1991.tb16057.x

Laemmli, U.K., 1970. Cleavage of structural proteins during the assembly of the head of bacteriophage T4. Nature 227, 680–685. https://doi.org/10.1038/227680a0

Leitch, J.M., Jensen, L.T., Bouldin, S.D., Outten, C.E., Hart, P.J., Culotta, V.C., 2009. Activation of Cu,Zn-superoxide dismutase in the absence of oxygen and the copper chaperone CCS. J. Biol. Chem. 284, 21863–21871. https://doi.org/10.1074/jbc.M109.000489

Liao, V.H.-C., Yu, C.-W., Chu, Y.-J., Li, W.-H., Hsieh, Y.-C., Wang, T.-T., 2011. Curcumin-mediated lifespan extension in Caenorhabditis elegans. Mech. Ageing Dev. 132, 480–487. https://doi.org/10.1016/j.mad.2011.07.008

Lin, F., Yan, D., Chen, Y., E, F.E., Shi, H., Han, B., Zhou, Y., 2018. Cloning, purification and enzymatic characterization of recombinant human superoxide dismutase 1 (hSOD1) expressed in Escherichia coli. Acta Biochim. Pol. 65, 235–240. https://doi.org/10.18388/abp.2017_2350

Luchinat, E., Barbieri, L., Rubino, J.T., Kozyreva, T., Cantini, F., Banci, L., 2014. In-cell NMR reveals potential precursor of toxic species from SOD1 fALS mutants.

Nat. Commun. 5. https://doi.org/10.1038/ncomms6502

Marchetti, C., 2014. Interaction of metal ions with neurotransmitter receptors and potential role in neurodiseases. Biometals an Int. J. role Met. ions Biol. Biochem. Med. 27, 1097–1113. https://doi.org/10.1007/s10534-014-9791-y

Maret, W., Moulis, J.-M., 2013. The bioinorganic chemistry of cadmium in the context of its toxicity. Met. Ions Life Sci. 11, 1–29. https://doi.org/10.1007/978-94-007-5179-8_1

Méndez-Armenta, M., Ríos, C., 2007. Cadmium neurotoxicity. Environ. Toxicol. Pharmacol. 23, 350–358. https://doi.org/10.1016/j.etap.2006.11.009

Mezynska, M., Brzoska, M.M., 2018. Environmental exposure to cadmium-a risk for health of the general population in industrialized countries and preventive strategies. Env. Sci Pollut Res Int 25, 3211–3232. https://doi.org/10.1007/s11356-017-0827-z

Miller, A.-F., 2012. Superoxide dismutases: ancient enzymes and new insights. FEBS Lett. 586, 585–595. https://doi.org/10.1016/j.febslet.2011.10.048

Miura, S., Takahashi, K., Imagawa, T., Uchida, K., Saito, S., Tominaga, M., Ohta, T., 2013. Involvement of TRPA1 activation in acute pain induced by cadmium in mice. Mol. Pain 9, 7. https://doi.org/10.1186/1744-8069-9-7

Moyson, S., Vissenberg, K., Fransen, E., Blust, R., Husson, S.J., 2018. Mixture effects of copper, cadmium, and zinc on mortality and behavior of Caenorhabditis elegans. Environ. Toxicol. Chem. 37, 145–159. https://doi.org/10.1002/etc.3937

Pansarasa, O., Bordoni, M., Diamanti, L., Sproviero, D., Gagliardi, S., Cereda, C., 2018. SOD1 in Amyotrophic Lateral Sclerosis: “Ambivalent” Behavior Connected to the Disease. Int. J. Mol. Sci. 19. https://doi.org/10.3390/ijms19051345

Polykretis, P., Cencetti, F., Donati, C., Luchinat, E., Banci, L., 2019. Cadmium effects on superoxide dismutase 1 in human cells revealed by NMR. Redox Biol. 21, 101102. https://doi.org/10.1016/j.redox.2019.101102

Rani, A., Kumar, A., Lal, A., Pant, M., 2014. Cellular mechanisms of cadmium-induced toxicity: A review. Int. J. Environ. Health Res. 24, 378–399. https://doi.org/10.1080/09603123.2013.835032

Ravikumar, A., Arun, P., Devi, K. V, Augustine, J., Kurup, P.A., 2000. Isoprenoid

pathway and free radical generation and damage in neuropsychiatric disorders. Indian J. Exp. Biol. 38, 438–446.

Romandini, P., Tallandini, L., Beltramini, M., Salvato, B., Manzano, M., De Bertoldi, M., Rocco, G.P., 1992. Effects of copper and cadmium on growth, superoxide dismutase and catalase activities in different yeast atrains. Comp. Biochem. Physiol. Part C Comp. Pharmacol. 103, 255–262. https://doi.org/https://doi.org/10.1016/0742-8413(92)90004-Q

Roos, P.M., Vesterberg, O., Syversen, T., Flaten, T.P., Nordberg, M., 2013. Metal concentrations in cerebrospinal fluid and blood plasma from patients with amyotrophic lateral sclerosis. Biol. Trace Elem. Res. 151, 159–170. https://doi.org/10.1007/s12011-012-9547-x

Rossi, S., Serrano, A., Gerbino, V., Giorgi, A., Di Francesco, L., Nencini, M., Bozzo, F., Schininà, M.E., Bagni, C., Cestra, G., Carrì, M.T., Achsel, T., Cozzolino, M., 2015. Nuclear accumulation of mRNAs underlies G4C2-repeat-induced translational repression in a cellular model of C9orf72 ALS. J. Cell Sci. 128, 1787 LP – 1799. https://doi.org/10.1242/jcs.165332

Satarug, S., Moore, M.R., 2004. Adverse health effects of chronic exposure to low-level cadmium in foodstuffs and cigarette smoke. Env. Heal. Perspect 112, 1099–1103. https://doi.org/10.1289/ehp.6751

Satarug, S., Nishijo, M., Ujjin, P., Moore, M.R., 2018. Chronic exposure to low-level cadmium induced zinc-copper dysregulation. J. trace Elem. Med. Biol. organ Soc. Miner. Trace Elem. 46, 32–38. https://doi.org/10.1016/j.jtemb.2017.11.008

Sheykhansari, S., Kozielski, K., Bill, J., Sitti, M., Gemmati, D., Zamboni, P., Singh, A.V., 2018. Redox metals homeostasis in multiple sclerosis and amyotrophic lateral sclerosis: A review review. Cell Death Dis. 9. https://doi.org/10.1038/s41419-018-0379-2

Soares, F.A., Fagundez, D.A., Avila, D.S., 2017. Neurodegeneration Induced by Metals in Caenorhabditis elegans. Adv. Neurobiol. 18, 355–383. https://doi.org/10.1007/978-3-319-60189-2_18

Srivastava, S., Pant, A., Trivedi, S., Pandey, R., 2016. Curcumin and β-caryophellene attenuate cadmium quantum dots induced oxidative stress and lethality in

Caenorhabditis elegans model system. Environ. Toxicol. Pharmacol. 42, 55–62. https://doi.org/10.1016/j.etap.2016.01.001

Tesauro, M., Bruschi, M., Filippini, T., D'Alfonso, S., Mazzini, L., Corrado, L., Consonni, M., Vinceti, M., Fusi, P., Urani, C., 2021. Metal(loid)s role in the pathogenesis of amyotrophic lateral sclerosis: Environmental, epidemiological, and genetic data. Environ. Res. 192, 110292. https://doi.org/https://doi.org/10.1016/j.envres.2020.110292

Therrien, M., Parker, J.A., 2014. Worming forward: Amyotrophic lateral sclerosis toxicity mechanisms and genetic interactions in Caenorhabditis elegans. Front. Genet. 5, 1–13. https://doi.org/10.3389/fgene.2014.00085

Urani, C., Melchioretto, P., Bruschi, M., Fabbri, M., Sacco, M.G., Gribaldo, L., 2015. Impact of Cadmium on Intracellular Zinc Levels in HepG2 Cells: Quantitative Evaluations and Molecular Effects. Biomed Res Int 2015, 949514. https://doi.org/10.1155/2015/949514

Usai, C., Barberis, A., Moccagatta, L., Marchetti, C., 1999. Pathways of cadmium influx in mammalian neurons. J. Neurochem. 72, 2154–2161. https://doi.org/10.1046/j.1471-4159.1999.0722154.x

Van Damme, P., Robberecht, W., Van Den Bosch, L., 2017. Modelling amyotrophic lateral sclerosis: progress and possibilities. Dis. Model. Mech. 10, 537–549. https://doi.org/10.1242/dmm.029058

Vance, P.G., Keele Jr., B.B., Rajagopalan, K. V, 1972. Superoxide dismutase from Streptococcus mutans. Isolation and characterization of two forms of the enzyme. J Biol Chem 247, 4782–4786.

Vinceti, M., Guidetti, D., Bergomi, M., Caselgrandi, E., Vivoli, R., Olmi, M., Rinaldi, L., Rovesti, S., Solimè, F., 1997. Lead, cadmium, and selenium in the blood of patients with sporadic amyotrophic lateral sclerosis. Ital. J. Neurol. Sci. 18, 87–92. https://doi.org/10.1007/BF01999568

Waalkes, M.P., 2000. Cadmium carcinogenesis in review. J. Inorg. Biochem. 79, 241–244. https://doi.org/10.1016/s0162-0134(00)00009-x

Wang, B., Du, Y., 2013. Cadmium and its neurotoxic effects. Oxid. Med. Cell. Longev. 2013. https://doi.org/10.1155/2013/898034

Wang, J., Kim, S.K., 2003. Global analysis of dauer gene expression in

Caenorhabditis elegans. Development 130, 1621–1634. https://doi.org/10.1242/dev.00363

Wang, J., Zhang, H., Zhang, T., Zhang, R., Liu, R., Chen, Y., 2015. Molecular mechanism on cadmium-induced activity changes of catalase and superoxide dismutase. Int. J. Biol. Macromol. 77, 59–67. https://doi.org/10.1016/j.ijbiomac.2015.02.037

Wang, M.-D., Little, J., Gomes, J., Cashman, N.R., Krewski, D., 2017. Identification of risk factors associated with onset and progression of amyotrophic lateral sclerosis using systematic review and meta-analysis. Neurotoxicology 61, 101–130. https://doi.org/https://doi.org/10.1016/j.neuro.2016.06.015

Winter, S.A., Dölling, R., Knopf, B., Mendelski, M.N., Schäfers, C., Paul, R.J., 2016. Detoxification and sensing mechanisms are of similar importance for Cd resistance in Caenorhabditis elegans. Heliyon 2, 1–23. https://doi.org/10.1016/j.heliyon.2016.e00183

Zhang, H., Reynolds, M., 2019. Cadmium exposure in living organisms: A short review. Sci. Total Environ. 678, 761–767. https://doi.org/10.1016/j.scitotenv.2019.04.395

Chapter 6

Discussion

The heavy metal cadmium is a widespread toxic pollutant, released into the environment mainly by anthropogenic activities. It has been classified as one of the main environmental and occupational chemical pollutants in industrialized countries, due to its extensive use in anthropogenic activities, to the absence of a biodegradation system and to its toxicity and accumulation in organisms, with an estimated half-life of 25-30 years in humans (Mezynska and Brzóska, 2018).

Human exposure can occur through different sources: occupationally for workers exposed to the metal or environmentally for the general population, since it is found in air, soil and water. Cadmium uptake can occur through inhalation of polluted air, cigarette smoking or ingestion of contaminated food and water. It mainly enters the human body through the respiratory and the gastrointestinal tract, accounting respectively for the 10-40% and 5-8% of the load, with the skin playing a minor role; it accumulates in liver and kidneys (Nordberg, 2009; Sabolić et al., 2010; Sarkar et al., 2013).

Brain is also a target of cadmium toxicity, since this toxicant may enter it either by increasing blood brain barrier permeability or through the olfactory nerves, affecting both peripheral and central nervous system (CNS) (Branca et al., 2020; Marchetti, 2014; Miura et al., 2013; Tjälve and Henriksson, 1999). Moreover, cadmium exposure has been related to impaired functions of the nervous system and to neurodegenerative diseases, like amyotrophic lateral sclerosis (ALS), a fatal motor neuron disease accounting for the 90-95% of sporadic cases (sALS) and the 5-10% of familial ones (fALS) (Branca et al., 2018). In the onset of this pathology genetic, environmental and lifestyle factors play an important role, with cigarette smoking being the only factor correlated to negative survival in ALS patients (Calvo et al., 2016). Moreover, ALS patients showed elevated heavy metals concentrations (Roos et al., 2013). 15-20% of fALS is related to mutations in superoxide dismutase 1 (SOD1) gene, that encodes for the homonym antioxidant protein responsible for superoxide anions dismutation. SOD1 is a homodimeric metalloenzyme of 32 kDa, mainly located in the cytoplasm, with each monomer binding one copper and one zinc ion and a disulfide intrasubunit bond. The zinc ion and the disulfide bond are involved in structure stability and correct folding, while the copper ion is responsible for the catalytic activity.

Inside the nervous system cadmium spreads its toxicity in several ways, such as interfering with essential metal ions homeostasis, depleting cell's antioxidant defence systems or damaging mitochondrial with a consequent alteration of energetic metabolism.

We initially investigated the energetic metabolism of human neural SH-SY5Y cells exposed to 10 µM or 20 µM $CdCl_2$. We have decided to use sub-lethal cadmium doses to mimick a real *in vivo* situation due to this metal widespread distribution and extremely long half-life; in fact, cadmium heavily accumulates in the organism (e.g. 2 µg/g liver, and 70 µg/g kidney) reaching its plateau in the kidney at 50 years of age and concentrations up to 20 µM have been reported in the human body (Forcella et al., 2020; Satarug and Moore, 2004). Moreover, depending on the composition of the diet and the quality of the consumed meals, the total amount of ingested cadmium in industrialized countries ranges from 10 µg to over 200 µg per day, considering an acceptable daily intake level of 0.1 µg kg^{-1} body weight per day for chronic exposure (Mezynska and Brzoska, 2018; Wang and Du, 2013).

SH-SY5Y cells treated with sub-lethal $CdCl_2$ concentrations showed an enhancement in glycolytic functions, although the metal administration caused a decrease in the ability to supply energy demand via glycolysis in the presence of stressor compounds, compared to control cells. Cadmium treatment induced an increase in basal and compensatory glycolysis, as well as in glycolytic capacity and glycolytic reserve, i.e. the cell's ability to use glycolysis to its maximum capacity, a measure of how close the glycolytic function is to the cell theoretical maximum. Moreover, upon cadmium addition, the evaluation of ATP production showed a higher rely on glycolysis rather than oxidative phosphorylation for energy production, although we did not observe any alteration in mitochondrial coupling efficiency in the presence of the toxicant. A closer investigation of mitochondrial functionality highlighted a reduction in basal respiration, maximum respiration and ATP production in the presence of $CdCl_2$ in a dose-dependent way, probably due to cadmium negative effects on complex II and complex III of the electron transport chain (ETC) (Brand, 2016). Overall, in the presence of cadmium we observed an enhanced glycolysis due to inadequate energy supply through oxidative phosphorylation, in accordance with previous work on mouse neuronal PC-12 cells, mouse C3H cell line and human osteoblasts treated with

sub-lethal cadmium concentrations (Al-Ghafari et al., 2019; Oldani et al., 2020; Zong et al., 2018).

The energy metabolism study also showed a higher basal extracellular acidification rate (ECAR) for cadmium treated cells, measured in the absence of glucose, which can be due to cadmium promoting amino acids breakdown to yield acetylCoA to fuel Krebs cycle, as suggested by Sabir and colleagues (Sabir et al., 2019). This hypothesis is supported by the mitochondrial fuel oxidation pattern analysis, showing that cadmium treated cells strongly rely on glutamine to maintain baseline respiration; therefore, the ECAR measured in this case would be partly due to CO_2, explaining why the acidification level remained high, following glycolysis inhibition, in cadmium treated cells. However, this increase in glutamine dependency was not accompanied by any variation in glutamine capacity, meaning that the cells cannot increase their ability to use glutamine as a fuel when other fuels pathways are blocked. Both $CdCl_2$ concentrations lead to a similar increase in glutamine dependency, suggesting that a maximum has been reached in glutamine supply. Moreover, this explains the decrease in lipid dependency in cadmium treated cells, since glutamine enters Krebs cycle as α-ketoglutarate to yield citrate; the latter can be translocated into the cytosol where it is converted by citrate lyase into oxalacetate and acetylCoA, which is carboxylated to malonylCoA, producing fatty acids.

An increase in glutamine consumption could be linked to a defensive mechanism against oxidative stress triggered by cadmium, since it can lead to a higher glutamate production, that could be used for glutathione synthesis, together with glycine and cysteine produced by glycolytic intermediates. This assumption could be an explanation of the increase in total glutathione observed in our experiments. However, the ratio GSSG/GSH is increased following cadmium administration and, although cell death is prevented, lipid peroxidation could be detected in cells treated with cadmium revealing an altered oxidative homeostasis, which was investigated in differentiated neurons, using differentiated LUHMES cells.

Upon cadmium exposure in differentiated LUHMES cells, we have observed a strong increase in GSH level at the lower $CdCl_2$ doses, reaching a maximum peak at 5 µM, followed by a dramatical dose-dependent decrease. This increase in GSH content at

lower metal doses could be a first scavenging response, due to cadmium high affinity for sulfhydryl groups (-SH).

In order to better understand this enhanced GSH content at cadmium lower doses, we have focused our attention on Nuclear factor erythroid 2-related factor 2 (Nrf2), an important player in cellular homeostasis maintenance. Under physiological conditions, Nrf2 is negatively regulated by Keap1, which dissociates in the presence of stress conditions, like an increase in reactive oxygen species (ROS). Free Nrf2 accumulates in the cytoplasm and subsequently translocates to the nucleus where it binds to antioxidant responsive element (ARE) genes activating them. Differentiated LUHMES treated with 5 μM $CdCl_2$ showed an increased Nrf2 protein level, leading us to hypothesize that cadmium induced oxidative balance alterations require the activation of complementary signalling pathway in enhancing the action of antioxidant systems against oxidative damage, like the Nrf2 one. However, we have observed an increase only in the protein expression level, while the mRNA transcript remains comparable to control, suggesting that Nrf2 is activated through protein stabilization. This stabilization was further confirmed by the enhanced p21 expression level and the increase in both GSK3β and Akt phosphorylation. In fact, p21 and P-Akt are positive regulators of Nrf2 activation as p21 and Keap1 bind on the same domain on Nrf2, but with opposite functions, while P-Akt phosphorylates GSK3β inhibiting it and cancelling its negative effect on Nrf2 (Chen et al., 2009; Chowdhry et al., 2013).

Another evidence of altered oxidative homeostasis causing Nrf2 activation is given by the increased transcriptional levels of *HMOX1* and *GCLM*. The first gene encodes for heme oxygenase 1, a stress inducible enzyme involved in ROS detoxification, while the second codes for glutamate-cysteine ligase modified subunit, a part of the glutamate-cysteine ligase, the enzyme catalyzing the rate limiting step in GSH synthesis. This increase in GCLM transcript could be an explanation for the higher GSH level found at $CdCl_2$ lowest doses, as an early response against cadmium toxicity. Moreover, the evaluation of GSH pre-treatment in the presence of the metal on LUHMES viability underlined the protective role exerted by GSH, since it restored cells viability even at the highest $CdCl_2$ doses, that could be inactivated either through a bigger pool of cadmium scavenging GSH, or by a higher antioxidant defence

potential. A protective role on LUHMES cells viability is also played by astrocytes and microglia conditioned medium (CM), which prevents cell death even at the highest metal concentrations. Regarding GSH, in CM its level remained quite similar to the control till 50 µM $CdCl_2$ and its initial peak observed in LUHMES cells at the lowest $CdCl_2$ doses was not present, leading us to suggest a possible external GSH uptake.

Our results showed an altered oxidative metabolism after cadmium administration, in accordance with this metal ability to indirectly increase oxidative stress, despite its inability in direct ROS generation. One of the mechanisms for cadmium induced oxidative stress is the weakening of antioxidant enzymes, like SOD1; previously investigations of cadmium ability to displace either zinc or copper, or both, led to contradicting results (Huang et al., 2006; Kofod et al., 1991; Luchinat et al., 2014; Polykretis et al., 2019; Wang et al., 2015). During SOD1 maturation the coordination of copper and zinc ions, as well as a disulfide bond formation between Cys57 and Cys146, are not only required, but also necessary for the production of a stabilized native conformation and the subsequent functional homodimer formation (Ding and Dokholyan, 2008). Although zinc insertion mechanism during SOD1 folding has not yet been fully elucidated, it is known that copper can be inserted either through the copper chaperone (CCS), as in yeast, or in an independent way requiring GSH, as in *Escherichia coli* and *Caenorhabditis elegans*, while in humans it can take place using both pathways (Banci et al., 2012; Carroll et al., 2004; Leitch et al., 2009).

Cadmium dysregulation of copper and zinc homeostasis and its substitution to zinc in a variety of zinc proteins, led as to suggest a possible involvement of cadmium negative effect on SOD1 linked to ALS, in accordance with SOD1 being most important in oxidative stress defense in neuronal cells and its mutations being responsible for 20% of fALS and 3% sALS (Kaur et al., 2016; Satarug et al., 2018; Urani et al., 2015).

Our results, obtained in three different experimental models, clearly demonstrate the inactivating effect of cadmium on SOD1 activity, not affecting its expression level. In the first model, represented by the human SOD1 expressed as a recombinant protein in *E. coli*, $CdCl_2$ concentrations up to 500 µM apparently did not cause any decrease in SOD1 activity. However, having a high expression levels of the recombinant

protein, either copper or zinc could be limiting during *E. coli* growth; in fact, the mean of absolute SOD1 specific activity was 8.1 U/mg for cells grown in the presence of either copper alone or copper and zinc and a value of 2.8 U/mg for cells grown without copper, showing that copper is the limiting metal in our conditions, in accordance with Lin and colleagues (Lin et al., 2018).

When administered together with optimal 500 µM Cu_2SO_4 concentration, cadmium led to a dose dependent decrease in SOD1 specific activity, starting at 50 µM $CdCl_2$, not seen in the presence of an optimal $ZnCl_2$ concentration (50 µM). When both copper and zinc were administered, a decrease in SOD1 specific activity was still detected, although to a minor extent respect to the decrease observed in the absence of zinc. Taken together these results suggest that cadmium displaces zinc when copper is in excess and zinc is limiting. Due to its larger size, cadmium ions can be difficult to release once they have displaced zinc ions and also zinc is more likely to dissociate than copper, because SOD1 has an approximately 7000-fold lower affinity for zinc than it does for copper (Crow et al., 1997). Moreover, cadmium can displace zinc, inducing a conformational change in SOD1 and decreasing its activity (Huang et al., 2006).

Another explanation could be that cadmium can increase SOD1 aggregation, since the amount of purified protein obtained from cells grown without cadmium was found to be one third of the amount obtained from the same number of cells grown in the presence of cadmium. In fact, besides displacing zinc from proteins, cadmium has a high affinity for cysteines and could interfere with SOD1 folding, which requires the formation of a disulfide bridge between Cys57 and Cys146, as shown by Polykretis and colleagues (Polykretis et al., 2019). Moreover, cadmium binding to GSH, which in *E. coli* is essential for SOD1 folding, could also impair folding leading to SOD1 aggregation.

Identical results were obtained also in the other two experimental models, the human neuroblastoma SH-SY5Y cell line and the nematode *C. elegans*. Not only SH-SY5Y cells treated with either 10 µM or 20 µM $CdCl_2$ showed a decrease in SOD1 specific activity, without alteration in SOD1 expression level, but a reduction in SOD1 activity was also further confirmed in *C. elegans*, in which a sub-lethal cadmium uptake

through food ingestion caused a 25% reduction of SOD1 activity without altering the protein level.

Overall, cadmium caused alterations in the oxidative balance, that led to a reduction in the activity of antioxidant enzymes, like SOD1, and to the activation of Nrf2 resulting in an increase in GSH production, as well as to a rearrangement of the energy metabolism. This plethora of adverse effect together with cadmium bio-accumulative attitude should be taken into account by the authority in order to have better cadmium regulations for long-term human safety.

References

Al-Ghafari, A., Elmorsy, E., Fikry, E., Alrowaili, M., Carter, W.G., 2019. The heavy metals lead and cadmium are cytotoxic to human bone osteoblasts via induction of redox stress. PLoS One 14, e0225341. https://doi.org/10.1371/journal.pone.0225341

Banci, L., Bertini, I., Cantini, F., Kozyreva, T., Massagni, C., Palumaa, P., Rubino, J.T., Zovo, K., 2012. Human superoxide dismutase 1 (hSOD1) maturation through interaction with human copper chaperone for SOD1 (hCCS). Proc. Natl. Acad. Sci. U. S. A. 109, 13555–13560. https://doi.org/10.1073/pnas.1207493109

Branca, J.J.V., Fiorillo, C., Carrino, D., Paternostro, F., Taddei, N., Gulisano, M., Pacini, A., Becatti, M., 2020. Cadmium-induced oxidative stress: Focus on the central nervous system. Antioxidants 9, 1–21. https://doi.org/10.3390/antiox9060492

Branca, J.J.V., Morucci, G., Pacini, A., 2018. Cadmium-induced neurotoxicity: still much ado. Neural Regen. Res. 13, 1879–1882. https://doi.org/10.4103/1673-5374.239434

Brand, M.D., 2016. Mitochondrial generation of superoxide and hydrogen peroxide as the source of mitochondrial redox signaling. Free Radic. Biol. Med. 100, 14–31. https://doi.org/10.1016/j.freeradbiomed.2016.04.001

Calvo, A., Canosa, A., Bertuzzo, D., Cugnasco, P., Solero, L., Clerico, M., De Mercanti, S., Bersano, E., Cammarosano, S., Ilardi, A., Manera, U., Moglia, C., Marinou, K., Bottacchi, E., Pisano, F., Mora, G., Mazzini, L., Chiò, A., 2016. Influence of cigarette smoking on ALS outcome: a population-based study. J. Neurol. Neurosurg. Psychiatry 87, 1229–1233. https://doi.org/10.1136/jnnp-2016-313793

Carroll, M.C., Girouard, J.B., Ulloa, J.L., Subramaniam, J.R., Wong, P.C., Valentine, J.S., Culotta, V.C., 2004. Mechanisms for activating Cu- and Zn-containing superoxide dismutase in the absence of the CCS Cu chaperone. Proc. Natl. Acad. Sci. U. S. A. 101, 5964–5969. https://doi.org/10.1073/pnas.0308298101

Chen, W., Sun, Z., Wang, X.-J., Jiang, T., Huang, Z., Fang, D., Zhang, D.D., 2009. Direct interaction between Nrf2 and p21(Cip1/WAF1) upregulates the Nrf2-

mediated antioxidant response. Mol. Cell 34, 663–673. https://doi.org/10.1016/j.molcel.2009.04.029

Chowdhry, S., Zhang, Y., McMahon, M., Sutherland, C., Cuadrado, A., Hayes, J.D., 2013. Nrf2 is controlled by two distinct β-TrCP recognition motifs in its Neh6 domain, one of which can be modulated by GSK-3 activity. Oncogene 32, 3765–3781. https://doi.org/10.1038/onc.2012.388

Crow, J.P., Sampson, J.B., Zhuang, Y., Thompson, J.A., Beckman, J.S., 1997. Decreased zinc affinity of amyotrophic lateral sclerosis-associated superoxide dismutase mutants leads to enhanced catalysis of tyrosine nitration by peroxynitrite. J. Neurochem. 69, 1936–1944. https://doi.org/10.1046/j.1471-4159.1997.69051936.x

Ding, F., Dokholyan, N. V, 2008. Dynamical roles of metal ions and the disulfide bond in Cu, Zn superoxide dismutase folding and aggregation. Proc. Natl. Acad. Sci. U. S. A. 105, 19696–19701. https://doi.org/10.1073/pnas.0803266105

Forcella, M., Lau, P., Oldani, M., Melchioretto, P., Bogni, A., Gribaldo, L., Fusi, P., Urani, C., 2020. Neuronal specific and non-specific responses to cadmium possibly involved in neurodegeneration: A toxicogenomics study in a human neuronal cell model. Neurotoxicology 76, 162–173. https://doi.org/https://doi.org/10.1016/j.neuro.2019.11.002

Huang, Y.H., Shih, C.M., Huang, C.J., Lin, C.M., Chou, C.M., Tsai, M.L., Liu, T.P., Chiu, J.F., Chen, C.T., 2006. Effects of cadmium on structure and enzymatic activity of Cu,Zn-SOD and oxidative status in neural cells. J. Cell. Biochem. 98, 577–589. https://doi.org/10.1002/jcb.20772

Kaur, S.J., McKeown, S.R., Rashid, S., 2016. Mutant SOD1 mediated pathogenesis of Amyotrophic Lateral Sclerosis. Gene 577, 109–118. https://doi.org/10.1016/j.gene.2015.11.049

Kofod, P., Bauer, R., Danielsen, E., Larsen, E., Bjerrum, M.J., 1991. 113Cd-NMR investigation of a cadmium-substituted copper, zinc-containing superoxide dismutase from yeast. Eur. J. Biochem. 198, 607–611. https://doi.org/https://doi.org/10.1111/j.1432-1033.1991.tb16057.x

Leitch, J.M., Jensen, L.T., Bouldin, S.D., Outten, C.E., Hart, P.J., Culotta, V.C., 2009. Activation of Cu,Zn-superoxide dismutase in the absence of oxygen and the

copper chaperone CCS. J. Biol. Chem. 284, 21863–21871. https://doi.org/10.1074/jbc.M109.000489

Lin, F., Yan, D., Chen, Y., E, F.E., Shi, H., Han, B., Zhou, Y., 2018. Cloning, purification and enzymatic characterization of recombinant human superoxide dismutase 1 (hSOD1) expressed in Escherichia coli. Acta Biochim. Pol. 65, 235–240. https://doi.org/10.18388/abp.2017_2350

Luchinat, E., Barbieri, L., Rubino, J.T., Kozyreva, T., Cantini, F., Banci, L., 2014. In-cell NMR reveals potential precursor of toxic species from SOD1 fALS mutants. Nat. Commun. 5. https://doi.org/10.1038/ncomms6502

Marchetti, C., 2014. Interaction of metal ions with neurotransmitter receptors and potential role in neurodiseases. Biometals an Int. J. role Met. ions Biol. Biochem. Med. 27, 1097–1113. https://doi.org/10.1007/s10534-014-9791-y

Mezynska, M., Brzoska, M.M., 2018. Environmental exposure to cadmium-a risk for health of the general population in industrialized countries and preventive strategies. Env. Sci Pollut Res Int 25, 3211–3232. https://doi.org/10.1007/s11356-017-0827-z

Mezynska, M., Brzóska, M.M., 2018. Environmental exposure to cadmium—a risk for health of the general population in industrialized countries and preventive strategies. Environ. Sci. Pollut. Res. 25, 3211–3232. https://doi.org/10.1007/s11356-017-0827-z

Miura, S., Takahashi, K., Imagawa, T., Uchida, K., Saito, S., Tominaga, M., Ohta, T., 2013. Involvement of TRPA1 activation in acute pain induced by cadmium in mice. Mol. Pain 9, 7. https://doi.org/10.1186/1744-8069-9-7

Nordberg, G.F., 2009. Historical perspectives on cadmium toxicology. Toxicol. Appl. Pharmacol. 238, 192–200. https://doi.org/10.1016/j.taap.2009.03.015

Oldani, M., Manzoni, M., Villa, A.M., Stefanini, F.M., Melchioretto, P., Monti, E., Forcella, M., Urani, C., Fusi, P., 2020. Cadmium elicits alterations in mitochondrial morphology and functionality in C3H10T1/2Cl8 mouse embryonic fibroblasts. Biochim. Biophys. Acta - Gen. Subj. 1864, 129568. https://doi.org/https://doi.org/10.1016/j.bbagen.2020.129568

Polykretis, P., Cencetti, F., Donati, C., Luchinat, E., Banci, L., 2019. Cadmium effects on superoxide dismutase 1 in human cells revealed by NMR. Redox Biol. 21,

101102. https://doi.org/10.1016/j.redox.2019.101102

Roos, P.M., Vesterberg, O., Syversen, T., Flaten, T.P., Nordberg, M., 2013. Metal concentrations in cerebrospinal fluid and blood plasma from patients with amyotrophic lateral sclerosis. Biol. Trace Elem. Res. 151, 159–170. https://doi.org/10.1007/s12011-012-9547-x

Sabir, S., Akash, M.S.H., Fiayyaz, F., Saleem, U., Mehmood, M.H., Rehman, K., 2019. Role of cadmium and arsenic as endocrine disruptors in the metabolism of carbohydrates: Inserting the association into perspectives. Biomed. Pharmacother. 114, 108802. https://doi.org/10.1016/j.biopha.2019.108802

Sabolić, I., Breljak, D., Škarica, M., Herak-Kramberger, C.M., 2010. Role of metallothionein in cadmium traffic and toxicity in kidneys and other mammalian organs. BioMetals 23, 897–926. https://doi.org/10.1007/s10534-010-9351-z

Sarkar, A., Ravindran, G., Krishnamurthy, V., 2013. a Brief Review on the Effect of Cadmium Toxicity: From Cellular To Organ Level. Int. J. Bio-Technology Res. 3, 2249–6858.

Satarug, S., Moore, M.R., 2004. Adverse health effects of chronic exposure to low-level cadmium in foodstuffs and cigarette smoke. Env. Heal. Perspect 112, 1099–1103. https://doi.org/10.1289/ehp.6751

Satarug, S., Nishijo, M., Ujjin, P., Moore, M.R., 2018. Chronic exposure to low-level cadmium induced zinc-copper dysregulation. J. trace Elem. Med. Biol. organ Soc. Miner. Trace Elem. 46, 32–38. https://doi.org/10.1016/j.jtemb.2017.11.008

Tjälve, H., Henriksson, J., 1999. Uptake of metals in the brain via olfactory pathways. Neurotoxicology 20, 181–195.

Urani, C., Melchioretto, P., Bruschi, M., Fabbri, M., Sacco, M.G., Gribaldo, L., 2015. Impact of Cadmium on Intracellular Zinc Levels in HepG2 Cells: Quantitative Evaluations and Molecular Effects. Biomed Res Int 2015, 949514. https://doi.org/10.1155/2015/949514

Wang, B., Du, Y., 2013. Cadmium and its neurotoxic effects. Oxid. Med. Cell. Longev. 2013. https://doi.org/10.1155/2013/898034

Wang, J., Zhang, H., Zhang, T., Zhang, R., Liu, R., Chen, Y., 2015. Molecular mechanism on cadmium-induced activity changes of catalase and superoxide

dismutase. Int. J. Biol. Macromol. 77, 59–67. https://doi.org/10.1016/j.ijbiomac.2015.02.037

Zong, L., Xing, J., Liu, S., Liu, Z., Song, F., 2018. Cell metabolomics reveals the neurotoxicity mechanism of cadmium in PC12 cells. Ecotoxicol. Environ. Saf. 147, 26–33. https://doi.org/10.1016/j.ecoenv.2017.08.028

Pubblications

De Giani A, Bovio F, Forcella M, Fusi P, Sello G, Di Gennaro P. Identification of a bacteriocin-like compound from Lactobacillus plantarum with antimicrobial activity and effects on normal and cancerogenic human intestinal cells. AMB Express. 2019 Jun 17;9(1):88. doi: 10.1186/s13568-019-0813-6. PMID: 31209580; PMCID: PMC6579796.

Bovio F, Epistolio S, Mozzi A, Monti E, Fusi P, Forcella M, Frattini M. Role of NEU3 Overexpression in the Prediction of Efficacy of EGFR-Targeted Therapies in Colon Cancer Cell Lines. Int J Mol Sci. 2020 Nov 20;21(22):8805. doi: 10.3390/ijms21228805. PMID: 33233823; PMCID: PMC7699864.

Acknowledgement

Questa volta non posso scamparla e quindi eccoci qui! Sono tante le persone da ringraziare, il cui sorriso e la cui presenza mi hanno accompagnata e sostenuta in questo viaggio.

Il primo grazie va a Paola, per avermi dato la possibilità di fare la tesi magistrale, prima, e il dottorato, poi, per avermi insegnato la passione per la ricerca, per le discussioni scientifiche, per tutti i consigli e i suggerimenti, per essere stata una guida e una certezza in questo percorso di crescita professionale e personale. Grazie anche per i momenti meno lavorativi e più ludici passati insieme: dalle abbuffate (soprattutto di dolci), al delirio del Meet me Tonight, alla spensieratezza delle feste di Natale!

Il secondo grazie non può non andare al pilastro del laboratorio 4010: Matilde. Grazie per avermi insegnato gran parte di ciò che so fare in un laboratorio, non solo il lavoro pratico, ma anche l'organizzazione degli esperimenti e la gestione dell'ambiente di lavoro. Grazie per avermi sopportato nelle pulizie drastiche e nei momenti più incasinati e frenetici! Durante il dottorato sei spesso stata una presenza silenziosa, ma sempre presente nel momento del bisogno, che mi ha accompagnata in modo materno nella mia crescita.

Metà del dottorato l'ho passato si a disperare sui vermetti, ma anche a ridere fino alle lacrime nel fantastico lab 4051! Siete stati il raggio di sole dopo la tempesta, il porto sicuro dove andare nel momento del bisogno.
Rego grazie! Grazie per tutto! Per avermi dato la possibilità di imparare a lavorare su *C. elegans*, per essermi stata accanto, specialmente nel mio periodo all'estero in piena pandemia le tue chiamate davano quel tocco di leggerezza in un momento non proprio semplicissimo. Grazie per tutto l'aiuto e il sostegno

dato, per le risate e le chiacchierate, per i pranzi e i compleanni, per esserci ed esserci stata.
Non posso non costruire un monumento per la mia Barb! Non c'è nulla di più bello del trovare una amica in una collega. Abbiamo sclerato come non mai, riso fino alle lacrime, mangiato biscotti (soprattutto ultimamente), condiviso pensieri e opinioni, ciacolato agli stereoscopi così tanto da fare invidia alle vecchiette di paese, organizzato dal nulla feste di Natale indimenticabili e costruito un'amicizia mattone dopo mattone. Sei stata una certezza in questo dottorato, sempre schietta e sincera. Grazie per tutto l'aiuto e per tutto il supporto! Ti voglio bene!
Grazie a Loredana per le risate e i consigli, per il tempo passato insieme e per l'avventura nei famosi 24 cfu. Sono felice di aver avuto la possibilità di conoscerti e di aver condiviso bei momenti con te!
E grazie anche a tutti i tesisti passati in questi anni. Grazie a Serena, Marta, Jacopo, Mele, Andrea, Linda e Roberta! Non sarebbe stata la stessa cosa senza di voi, avete sempre dato quel tocco di spensieratezza in più!

Parlando di tesisti non posso non ringraziare i miei: Maria, Antonio, Alice e Giovanni. Con voi ho iniziato ad imparare cosa significhi insegnare un lavoro e un metodo, cosa fare e cosa no, nella speranza di non aver fatto così schifo.
Grazie Maria per le belle chiacchierate e risate e per i tuoi fantastici dolci! Sei una persona riservata, ma che si è messa in gioco e che si è lasciata conoscere e coinvolgere. Grazie per essere stata paziente con me, perché sono consapevole di averti trascinata nel vortice del facciamo mille esperimenti alla settimana, ma non hai mai fatto un passo indietro. Grazie davvero!
Grazie ad Antonio, che più di tutti è stato vittima della mia frenesia! Sei arrivato nel periodo prima della partenza per Costanza e ti sei adattato immediatamente. Mai dimenticherò gli esperimenti sulle ROS con timer e orologi in mano.

E grazie anche ai miei due piccoli stagisti Alice e Giovanni. Anche voi non vi siete tirati indietro e mi avete seguita nella mia pazzia con entusiasmo, voglia di fare e forse incoscienza. Grazie per le risate e i bei momenti.

Non posso esimermi dal ringraziare la componente ambientale.
Un grazie speciale a Chiara, la cui presenza discreta mi ha accompagnata in questi tre anni. Grazie per l'occhio critico e per tutti i consigli lavorativi dati, per le discussioni scientifiche, per i suggerimenti e per i bei, anche se pochi, pranzi insieme. Il tuo aiuto ha contribuito alla mia crescita professionale, grazie di cuore.
Grazie al mitico Pasquale! Compagno di viaggio, di risate, di lavoro! Grazie per l'aiuto e il supporto e per i suggerimenti dati! La tua esperienza è un bagaglio prezioso per noi giovani leve!
Vorrei porre un ringraziamento e un caro ricordo al Prof Maurizio Bruschi. Ci siamo incontrati pochissime volte e sempre in riunione. I suoi commenti e le sue constatazioni sono sempre stati puntuali e pungenti. Sarebbe stato bello aver avuto più tempo.

Un grazie gigante va a Stefan, al Professor Leist e a tutto l'AG Leist. Grazie per avermi accolta nel vostro mondo e per quei fantastici mesi trascorsi insieme. Grazie per le risate, le chiacchierate e le tante torte condivise.

Grazia, la mia siciliana adorata. Ci siamo conosciute in laboratorio e giorno dopo giorno abbiamo visto nascere la nostra amicizia. Sei una delle persone più dolci e speciali che conosca. Abbiamo condiviso la qualunque in laboratorio, abbiamo fatto la coda per i Nutella Biscuits, abbiamo riso, ci siamo confidate e aiutate e ora stiamo solo aspettando che sia possibile stare di nuovo tutti insieme per poter costruire altri bei momenti e ricordi. La tua amicizia è stata una delle sorprese più belle di questo dottorato. Grazie per tutto!

Grazie alle Micro, il fantastico duo Alessandra e Jessica! Compagne di pranzi, sfoghi, risate e abbuffate. Con Ale ho avuto la possibilità di lavorare insieme e sono stati mesi troppo divertenti, tanto che avrei voluto fossero di più o che ci fosse la possibilità di lavorare ancora insieme, chissà forse ci stiamo riuscendo! Jessica invece è stata la tenerezza (quando non era arrabbiata per cause di forza maggiore) di questi anni. Grazie per i bei momenti passati insieme e per tutti i pranzi e i caffè condivisi.

Un grazie speciale va ai miei due angeli custodi Fabio e Andrea. La vostra presenza è stata un'ancora di salvezza.
Fabio grazie per esserci stato in questi anni, per i consigli dati, per tutte le volte che hai ascoltato i miei sfoghi e i miei dubbi. Per avermi fatto sorridere nei momenti tristi, per avermi spesso capita osservandomi in silenzio e per avermi spronata a rischiare. Grazie Andre per la pazienza che hai avuto nell'ascoltare i miei sfoghi (principalmente perché ti facevano ridere, ma te la perdono), per i momenti di confronto e per le risate. Siete due ragazzi fantastici, ma dai gusti calcistici discutibili! Vi voglio bene!

Non si può non ringraziare il gruppo Peri! Le fantastiche Valentina, Nicole, Michela e Jessica e i pazzi Alessio e Florent. In vostra compagnia ho spesso avuto le lacrime agli occhi dal tanto ridere! Grazie per tutti i bei momenti passati insieme!

Veronica, la mia ciccina. La tua tesi nel lab Fusi ci ha permesso di conoscerci meglio e di rafforzare la nostra amicizia. Grazie per avermi spronata a non mollare, a non arrendermi e a mostrare sempre il mio valore; per avermi sostenuta nei momenti peggiori, stando al mio fianco ed essendo la spalla su cui poter piangere. Grazie per tutto, per volermi bene così come sono, per sopportarmi e per essere una Amica!

Grazie a Ylenia e Stefano, due persone fantastiche. Grazie per avermi sostenuto in questa esperienza nonostante spesso l'abbiate ritenuta una pazzia. Grazie per essermi stati accanto!
Grazie anche a te Lollo! Compagni dalla triennale, i nostri momenti di sconforto nei corridoi sono stati il filo conduttore di questi tre anni, eppure siamo arrivati alla fine!

Il periodo a Costanza mi ha fatto conoscere due persone eccezionali, due ragazze semplici che quando si affezionano non ti mollano più. Non abbiamo proprio avuto un tempismo perfetto ritrovandoci bloccate in terra straniera nel mezzo di una pandemia, eppure ci siamo sostenute a vicenda senza mai perdere il sorriso sulle labbra. Grazie Maddalena e Arianna per quei bellissimi mesi, per tutti i pranzi e le cene condivise, per le gite, per i momenti seri e per quelli allegri, per le passeggiate, per le videochiamate, per l'affetto nei miei confronti. Non vedo l'ora di poterci riabbracciare di nuovo! Le mie schiscette!!!

Infine, un ringraziamento speciale alla mia famiglia, che non ha ancora capito esattamente cosa faccia ma che mi supporta e sopporta così come sono!